DISCLAIMER

This report was prepared as an account of work sponsored by an agency of the United States Government. Neither the United States Government nor any agency thereof, nor any of their employees, makes any warranty, express or implied, or assumes any legal liability or responsibility for the accuracy, completeness, or usefulness of any information, apparatus, product, or process disclosed, or represents that its use would not infringe privately owned rights. Reference herein to any specific commercial product, process, or service by trade name, trademark, manufacturer, or otherwise does not necessarily constitute or imply its endorsement, recommendation, or favoring by the United States Government or any agency thereof. The views and opinions of authors expressed herein do not necessarily state or reflect those of the United States Government or any agency thereof. Reference herein to any social initiative (including but not limited to Diversity, Equity, and Inclusion (DEI); Community Benefits Plans (CBP); Justice 40; etc.) is made by the Author independent of any current requirement by the United States Government and does not constitute or imply endorsement, recommendation, or support by the United States Government or any agency thereof.

SANDIA REPORT
SAND2026-20700
Printed May 2026

Sandia National Laboratories

Code Verification of Sandia Shock Physics Codes using the Sedov and Noh Problems

Brian Carnes
VVUQ
Sandia National Laboratories
P.O. Box 5800
Albuquerque, NM 87185-0828
bcarnes@sandia.gov

Prepared by
Sandia National Laboratories
Albuquerque, New Mexico 87185
Livermore, California 94550

Issued by Sandia National Laboratories, operated for the United States Department of Energy by National Technology & Engineering Solutions of Sandia, LLC.

Available to DOE and DOE contractors from

U.S. Department of Energy
Office of Scientific and Technical Information
P.O. Box 62
Oak Ridge, TN 37831

Telephone: (865) 576-8401
Facsimile: (865) 576-5728
E-Mail: reports@osti.gov
Online ordering: http://www.osti.gov/scitech

Available to the public from

U.S. Department of Commerce
National Technical Information Service
5301 Shawnee Road
Alexandria, VA 22312

Telephone: (800) 553-6847
Facsimile: (703) 605-6900
E-Mail: orders@ntis.gov
Online order: https://classic.ntis.gov/help/order-methods

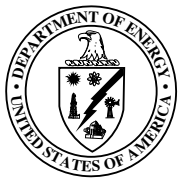

ABSTRACT

The process of determining that a computational physics code correctly implements the underlying governing equations is known as code verification. For shock physics codes, the simplest form of the governing equations are the hydrodynamic equations for conservation of mass, momentum, and energy, along with the appropriate equation of state (EOS) model.

This report documents code verification work for multiple Sandia shock physics codes (CTH, Alegra, SABLE, and Alegra-NG) using several benchmark problems for hydrodynamics with exact solutions - the well known Sedov and Noh problems. **As with all code verification studies, the results presented in the report cannot be quantitatively mapped onto actual performance in applications and should be interpreted as a qualitative guide only.** The key to making the qualitative connection to actual performance is to run the problems with typical user options that are representative of how analysts use the codes in practice.

The most comprehensive comparisons were performed using the cylindrical forms of the Sedov and Noh problems on two-dimensional domains. Comparisons were made to the exact solutions (implemented in the library ExactPack) using energy conservation, shock time of arrival, spatial solution profiles, and global error norms. Energy conservation for the Noh problem was assessed using a formulation of the problem containing two identical materials, such that the mass and energy of the inner material is conserved and can be tracked.

For the Sedov problem, three of the four codes (CTH, Alegra, and SABLE) exhibited total energy losses, ranging from 10-40% depending on the code, the mesh resolution, and which form of the problem (spherical or cylindrical). As a result, the solutions converged to the incorrect solutions with delay in shock time of arrival ranging from 5-15%. The next generation Alegra code (Alegra-NG) demonstrated energy conservation for Sedov and convergence to the exact solution with convergence rates approaching first order for both Sedov and Noh. Lack of radial symmetry from an instability significantly impacted the CTH results for two-dimensional versions of Sedov. CTH, SABLE and Alegra all exhibited velocity oscillations near the origin for Sedov.

For Noh, the energy losses for CTH, Alegra, and SABLE were smaller than for Sedov (2-6%) with smaller delays in shock time of arrival as well (2-8%). Energy conservation for Noh using Alegra-NG could not be assessed because energy sums over individual materials was not available. The non-physical "excessive wall heating" numerical artifact at the origin for Noh affected all of the codes tested, resulting in incorrect post-shock states and spurious overshoots in internal energy (undershoots in density) at the origin.

The author recommends future studies to identify the effect of energy conservation on mission relevant problems and to prioritize needed code improvements.

The work was funded from the W87-1 Shock Physics ModSim Mission Realization Partners (MRP) and from Advanced Simulation Computing (ASC) Shock Physics.

This page intentionally left blank.

CONTENTS

LIST OF FIGURES

LIST OF TABLES

This page intentionally left blank.

ACKNOWLEDGEMENTS

The author would like to thank the following individuals for their valuable feedback that resulted in a better study and report: Marissa Adams, Anthony Agelastos, Aaron Brundage, Jim Cox, Gabrielle Duncan-Reynolds, Dave Hensinger, Dan Ibanez, Nathan Peterson, Michael Powell, Bill Rider, Kevin Ruggirello, Maher Salloum, Erik Strack, and Justin Winokur.

This page intentionally left blank.

1. INTRODUCTION

1.1. Motivation and approach

Much work has been done over a period of many decades to improve the numerical accuracy of shock physics codes (hydrocodes) by both the National Nuclear Security Administration (NNSA) National Laboratories (Los Alamos, Lawrence Livermore, and Sandia) and the broader shock physics community. An important part of this process is selection of benchmark problems in order to assess accuracy relative to a known exact solution, a process known as code verification.

This report compares multiple Sandia hydrocodes using the widely studied Sedov and Noh benchmark problems, which have long been considered foundational problems used for verification of hydrocodes (included in the 2006 Tri-lab verification test suite [1] but used earlier as well [2]). The shock physics codes used in this work often have many other features beyond hydrodynamics; the use of the term "hydrocode" is meant to emphasize that the testing reported here only relies on the hydrodynamics capabilities for solving the Euler equations. The first of the two test cases was studied by the early pioneers Taylor, von Neumann, and Sedov; it was published by Sedov in 1959 [3]. The second problem was presented by Noh in his 1978 paper [4]. This work builds on prior code verification studies done at Los Alamos [2, 5, 6, 7], Lawrence Livermore [8], and Sandia [9].

The work began with investigations running just CTH [10, 11], and was eventually extended to a total of four Sandia hydrocodes including Alegra [12], SABLE [13, 14], and Alegra-NG (next generation Alegra code that will be deprecated in favor of the new SMASH code). All of the hydrocodes are developed at Sandia and currently used for Nuclear Deterrence (ND) applications; most have other users and stakeholders outside of the ND application area. Table 1-1 compares the codes used by several key features.

Table 1-1. Code feature comparison

Feature	CTH	Alegra	SABLE	Alegra-NG
discretization	finite volume	finite element	finite element	finite element
remap options	Eulerian	Lagrangian, Eulerian	Lagrangian, Eulerian	Eulerian
meshing strategy	structured grid	structured grid	structured grid	structured grid
time integrators	explicit	central difference	explicit	explicit
boundary conditions	symmetry	symmetry	symmetry	symmetry

The intent of the study is to apply the hydrocodes using *typical* user settings that are representative of how analysts use the codes in practice. Use of atypical settings is avoided in the study with the exception of specific studies around options such as remap (for example, see Sections 2.4 and 3.5).

The reason for this approach is to ensure that the results are *qualitatively* transferrable to applications. Comparisons of code performance such as runtime or memory usage are not considered in this report. However, efficiency could be considered elsewhere as a trade-off against accuracy. In applications where there is no exact reference solution, credibility studies should still be pursued to monitor energy conservation, quantify mesh convergence and assess solution stability.

The traditional approach to code verification considers the error between the computational solution and the exact solution in some global spatial norm at a given comparison time. The process is repeated for a decreasing sequence of mesh sizes and the errors are plotted as a function of mesh size on log-log scale. A linear fit of this data is used to estimate the rate of convergence of the errors. If the observed rate is sufficiently close to the expected rate, then the test is deemed successful. For problems like Sedov and Noh that are dominated by shock waves, the expected rate is typically first order when uniformly spaced meshes are used.

This work expands upon prior work [5, 6, 7, 8, 9] that uses the aforementioned traditional approach, emphasizing fundamental outputs in addition to global error norms, including

1. conservation of mass and total energy,
2. tracer histories at fixed point locations,
3. shock time of arrival, and
4. radial symmetry of solution fields.

Conservation of mass and energy is fundamental to the definition of the conservation laws that all hydrocodes are based on. However, this report will demonstrate that not all hydrocodes conserve total energy, even under mesh refinement. In ND applications, loss of mass or energy is typically associated with removal of material with nonphysical states - a procedure called material discard in CTH and SABLE or cell doctor in Alegra. In all of the examples tested here, no material discards are used. Energy conservation for CTH was discussed in a conference paper by Hertel et al. [11]

A recent report by Hensinger et al. [14] investigated a conservative remap algorithm that was implemented by the authors in the SABLE code in FY25. The method is called the "compatible energy conservation" method, which achieves better total energy conservation than the default remap in SABLE. The authors tested the algorithm across a large set of regression and verification test cases (Taylor anvil, high velocity impact with rigid surface, penetrator impact, inter-material fracture, and explosive cylinder) and considered quantities of interest found in this report such as total mass, total energy, internal energy, kinetic energy, and shock time of arrival. In addition the report considers phenomena such as shape change under advection, trailing edge energy losses for materials moving with uniform kinetic energy (rigid body motion), jet formation from material flow, inter-material fracture and void insertion, adaptive mesh refinement (AMR), and domain outflow boundary conditions.

The authors concluded that the algorithm "delivers very good results on canonical shock hydrodynamics tests,and it interoperates seamlessly with interface-tracking and complex constitutive models." However, in some test problems - such as the high velocity impact problem

and the explosive cylinder problem, the algorithm produces "pathological heating resulting [in] excessive temperatures." The authors concluded that these pathologies "make it unsuitable for general application in the SABLE application space."

A key output of hydrocodes is the time history of solution variables at specific locations called "tracers". These tracers can be fixed (Eulerian), or can move with the material flow (Lagrangian). For complex flows, the evolution of the pressure or velocity magnitude at a tracer location is often used as an indicator for shock time of arrival (TOA) at the tracer location. Tracers are also used to make comparisons with gauges in experiments.

Each benchmark problem has an associated comparison time when the computational solutions are compared to the exact solution. This time is used as the exact shock TOA when the tracers are placed at the exact shock location at this comparison time. Shock time of arrival is computed numerically as the time when the local value of the solution at a point (pressure, velocity magnitude, or internal energy) exceeds some constant threshold. When considered as part of a mesh convergence study, this enables another method to assess hydrocode accuracy.

Radial symmetry is a good indicator that the hydrocode can propagate a solution through a mesh without distortions from boundary conditions or grid alignment with a shock. One distortion that can break radial symmetry is a carbuncle instability, where a portion of the shock wave is moving faster than the rest of the solution, typically where the shock is aligned with the grid (see [15]). This can occur with grid aligned flows when there is not enough numerical dissipation in velocity components perpendicular to the flow and noise is allowed to grow in those components.

1.2. Sedov problem description

The Sedov-Taylor-von Neumann blast problem is a classic shock benchmark for conversion of internal to kinetic energy and shock propagation. It is challenging because the energy is released from a point source into a cold medium and the resulting shock has infinite Mach number. The problem can be solved analytically using self-similarity to reduce the problem to an ordinary differential equation (see Kamm and Timmes [5] for a complete derivation).

The Sedov problem actually has three different versions, depending on the form of symmetry and the expanding form of the shock. For example, the spherical version has radial symmetry in three dimensions, meaning that the shock expands spherically from the origin. The cylindrical and planar versions have radial symmetry in two and one dimensions, respectively. This enables various solution options, such as solving the spherical problem in multiple coordinate systems, including 3D cartesian, 2D cylindrical, and 1D spherical.

The key input parameters are the initial values of the total energy E_0 and density ρ. The key output is the shock position $r_{shock}(t)$ as a function of time and a parameter β:

$$r_{shock}(t) = \beta \left(\frac{E_0 t^2}{\rho} \right)^{1/5} .$$

For all cases the comparison time is defined to be $t = 1$. All three standardized Sedov problems are summarized in Table 1-2 for reference. The remaining values are for the gas constant γ=1.4,

the initial density of 1, the initial zero velocity, and the initial zero energy away from the origin. In this report, the exact solutions were computed using the ExactPack tool [16] that was developed at Los Alamos and is provided as an Open Source Python library.

Table 1-2. Parameters for all three standardized Sedov problems

geometry	E_0	r_{shock}
spherical	0.851072	1.0
cylindrical	0.311357	0.75
planar	0.0673185	0.5

The Sedov problem is run on a sufficiently large rectangular domain such that none of the mass and energy leaves the domain during the analysis. Thus it is expected that total mesh and energy should remain unchanged before reaching the comparison time. In this work, the domain is 20% larger in each coordinate direction than the shock position at the comparison time. The simulation time is also increased by 20% in order to capture the numerical value of the shock time of arrival.

A view of a small region of the mesh including the initial condition for the Cylindrical Sedov 2DR case is shown in Figure 1-1. The mesh size (0.0025) is equal to 1/8 of the radius of the cylinder (0.02) where the initial energy is placed. The cells are colored by the specific internal energy at time zero.

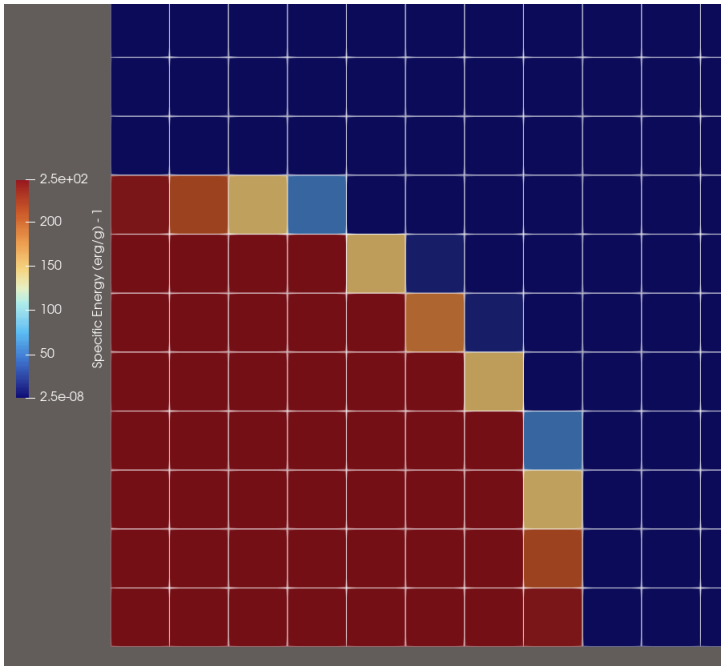

Figure 1-1. Cylindrical Sedov 2DR: initial condition for CTH on finest mesh

For the studies comparing all of the hydrocodes, the same common conditions were applied to enable the Sedov problem to be compared consistently across all four codes:

- cylindrical Sedov geometry,
- uniform structured grids,
- 2D rectangular mesh geometry, and
- Eulerian mode (Lagrangian plus remap).

1.3. Noh problem description

The Noh problem [4] is a classic shock benchmark for conversion of kinetic to internal energy and shock propagation from a rigid boundary with infinite Mach number. The kinetic energy is directed inward into a single point, causing a shock wave to radiate outward. The problem can be solved analytically in closed form (see [9] for the complete solution). The Noh problem is challenging because many hydrocodes have historically produced non-physical "excessive wall heating" at the origin, where density is very low and specific internal energy becomes very large relative to the exact *constant* post-shock states.

As with the Sedov problem (as documented in Table 1-2), the Noh problem also has three different versions, depending on the form of symmetry. Here only the cylindrical version is considered in the comparison studies because of the need to compare code results on 2D rectangular meshes. The parameter values are the gas constant $\gamma = 5/3$, the initial density of 1, and the initial radial velocity of $u_0 = -1$. The shock location is linearly proportional to time

$$r_{shock} = -\frac{1}{2}u_0(\gamma - 1)t$$

The comparison time is at $t = 0.6$ at which time the shock should be at a radial location of $r = 0.2$.

As with the Sedov problem, the Noh problem is run on a sufficiently large fixed domain such that the shock will be undisturbed by any far-field boundary conditions. However, the total mass and energy is expected to vary over time because of the far-field inflow boundary where material flows into the domain.

In this work, conservation of total mass and energy are verified by dividing the rectangular domain into two different materials with identical equation of states. The inner material encloses the shock at comparison time, and the outer material includes the far-field boundary. By construction, the inner material should radially compress at the speed u_0 and conserve its mass and total energy.

The inner material is placed in a circle of radius $r = 1$, and the outer material is placed in the remaining volume. At the comparison time of $t = 0.6$, the inner material should compress to a radius of $r = 0.4$, a region that still contains the outward propagating shock at $r = 0.2$. Thus, the total mass and energy of the inner material should remain constant and provide similar quantities to assess as in Sedov.

A view of the mesh including the initial velocity condition for the Cylindrical Noh 2DR case is shown in Figure 1-2. The mesh size (0.02) is the coarsest size used. The cells are colored by the

volume fraction of the inner material that is used to track mass and energy conservation over time.

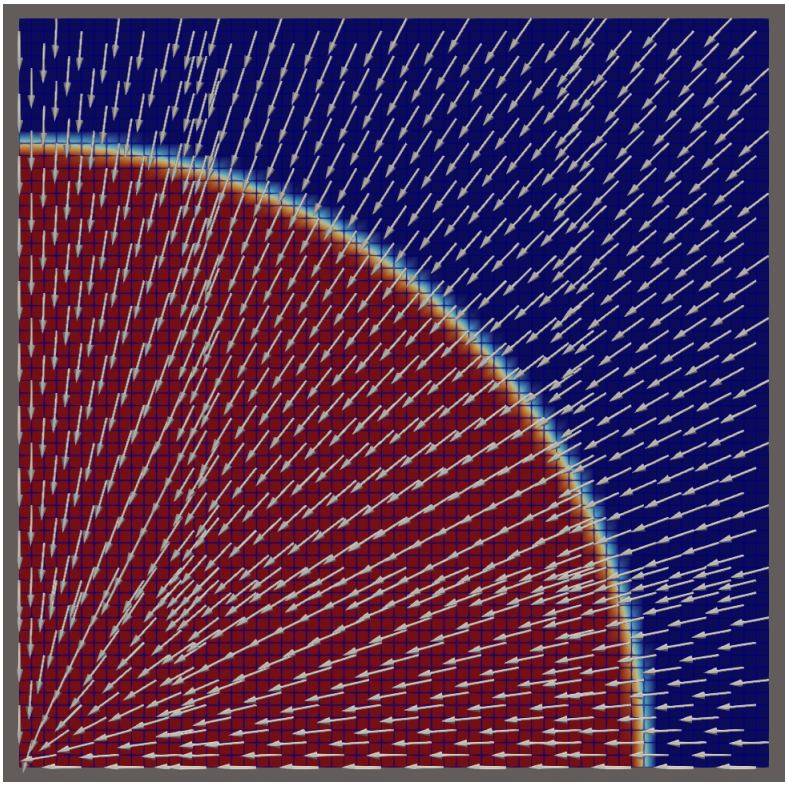

Figure 1-2. Cylindrical Noh 2DR: initial condition for CTH on coarsest mesh

For the study comparing all of the hydrocodes on Noh, the same common conditions listed at the end of Section 1.2 were applied as for Sedov.

1.4. Hydrocode comparison strategy

The various approaches used to compare hydrocodes are described in this section.

The same problem can be run in different dimensions. For example, the spherical Sedov problem can be run in multiple coordinate systems, including 1D spherical (1DS), 2D cylindrical (2DC) and 3D rectangular (3DR). These studies are only performed for hydrocodes that have these capabilities. For 1DS the only case is CTH; for 2DC cases, CTH, Alegra and SABLE can be compared. The comparisons made using *all four* hydrocodes are done using cylindrical forms of the benchmark problems in 2D rectangular (2DR) geometry.

Comparisons are made using time evolution of scalar quantities such as total mass and energy, as well as Eulerian tracers using pressure and velocity magnitude. The exact values of these quantities can be computed using the exact solution for comparison. In this work, all exact solutions are computed using the library ExactPack [16].

Convergence under mesh refinement is assessed for various scalars extracted from the solution:

1. total energy (initial and comparison times),
2. total mass at comparison time, and
3. shock TOA.

Solution fields at the comparison time are plotted along with the exact solution. These are presented from all mesh sizes for a single hydrocode in order to assess trends under mesh refinement. In these plots, the independent variable is always the radial coordinate variable and the numerical solutions are plotted using scatter plots to assess radial symmetry.

In most plots, the input and output variables are scaled to enable ease of assessing relative changes. For example, Figure 1-3 shows comparisons of total energy for two different problems. The scalings applied to total energy (using the initial value) and to time (using the comparison time) make the different problems more comparable, since the values of initial energy and comparison time vary between the two problems. The colors in the plots are also made to be consistent across the report so that CTH is always blue, Alegra is orange, SABLE is green, and Alegra-NG is red.

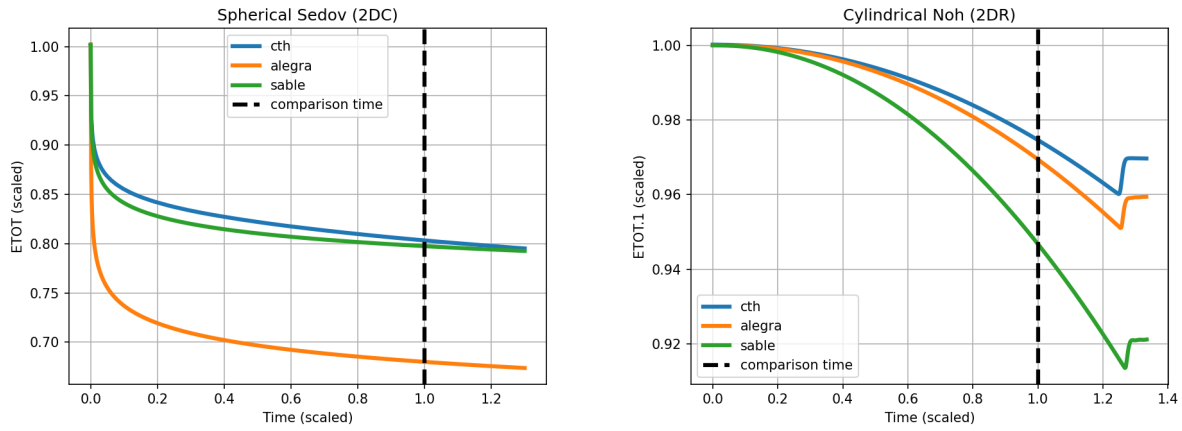

Figure 1-3. Examples of scaled variables for comparison purposes

Table 1-3. Parameters used for each shock physics code

Option	Value Used	Code
convection	0	CTH
iteration	5	All
lilvf	0.5	CTH
pwdiom	1	CTH, Alegra, SABLE
mmp0	N/A	CTH
interface	smyra	CTH
boundary type	symmetry	All
time integrator	central difference	Alegra

This page intentionally left blank.

2. MAIN RESULTS FOR SEDOV

The main results for the Sedov problem are provided in this section, using the cylindrical version of the Sedov problem run in 2D rectangular (2DR) geometries. A mesh convergence study was completed for each code in order to assess convergence of quantities such as total energy at comparison time and shock TOA.

The key results obtained using the Sedov test case are the following:

- Production codes (CTH, SABLE, Alegra) do not conserve total energy
- Shock TOA is delayed for production codes (some tracers for CTH arrive early)
- CTH has large instabilities in pressure, density, and velocity near the shock
- Remap options exist for all production codes that improve energy conservation
- Energy losses arise from the remap step in Eulerian mode
- The choice of initial condition has little impact on the final shock position
- All production codes have instabilities in velocity near the origin

2.1. Energy conservation

The first result is that production codes do not conserve total energy when run in Eulerian mode using typical user settings. This is illustrated by Figure 2-1, which shows log-time history of total energy (scaled by the reference value) for all codes tested. Each curve represents a fixed value of mesh resolution. For the production codes CTH, SABLE, and Alegra, the total energy increases under mesh refinement but does not converge to the true value after losing energy during the transient shock propagation. Alegra-NG maintains a nearly constant total energy over time, converging to the true value under mesh refinement.

In this study, the main method to insert the initial energy has been to use a circular or spherical region of fixed radius with uniform temperature chosen to match the given initial energy for the Sedov problem (cylindrical or spherical). This introduces some numerical error in the initial total energy because of the diatom insertion process used in all the hydrocodes.

Errors in the initial total energy are confirmed to be small and decrease under mesh resolution as shown in Figure 2-2, where scaled initial energy is plotted as a function of mesh size. The production codes have errors in initial total energy at most 1%. The higher errors from Alegra-NG are a result of a different material insertion algorithm, which mixes temperature instead of energy when inserting material into diatoms.

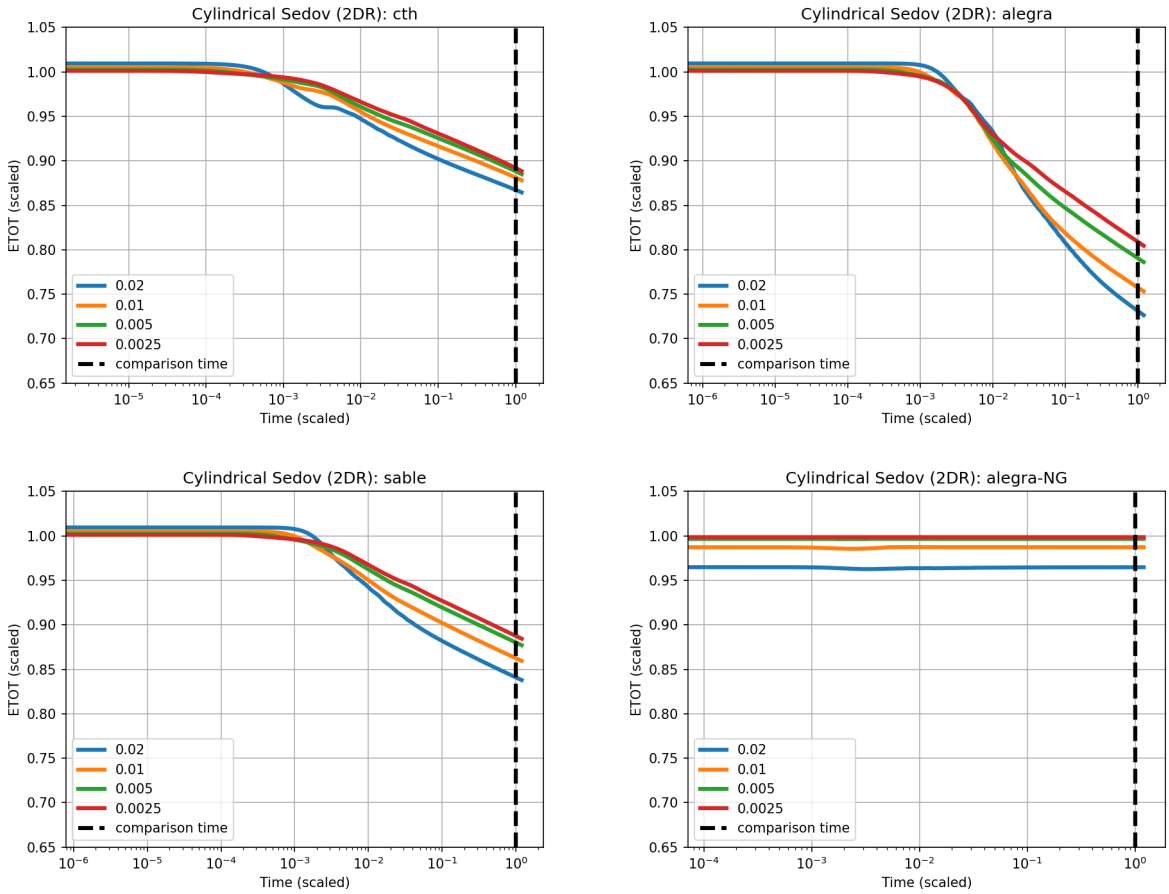

Figure 2-1. Cylindrical Sedov 2DR: convergence of total energy

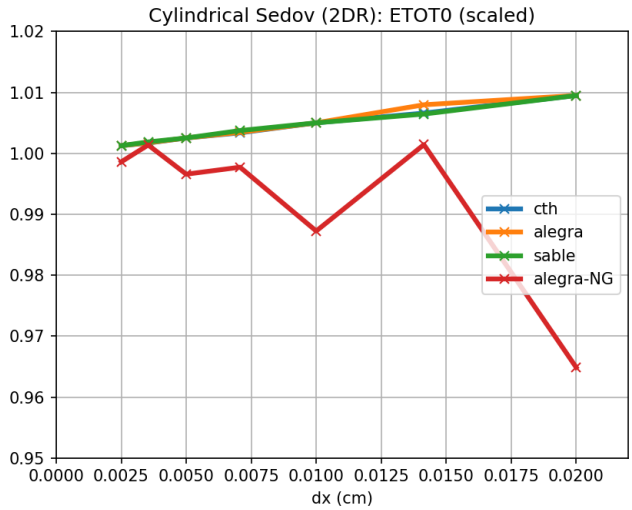

Figure 2-2. Cylindrical Sedov 2DR: convergence of scaled initial energy

Results in Section 2.4 will show that these energy losses for production codes can be alleviated using alternative options for remap that are not yet widely used.

2.2. Tracers and shock time of arrival

The Cylindrical Sedov 2DR models are instrumented with Eulerian tracers at the shock location ($r = 0.75$) at comparison time ($t = 1$). Multiple angular positions are selected (45, 0, and 90°) to provide an indication of the symmetry of the solution and to detect anomalies, since the shock TOA is expected to be identical at these locations.

The impact of the loss of total energy on shock TOA at the 45° tracer is quantified in Figure 2-3, where it is shown that loss of total energy at final time (left plot) correlates well with increase in shock TOA (right plot). Results for shock TOA at the other two tracers (0 and 90°) is shown in

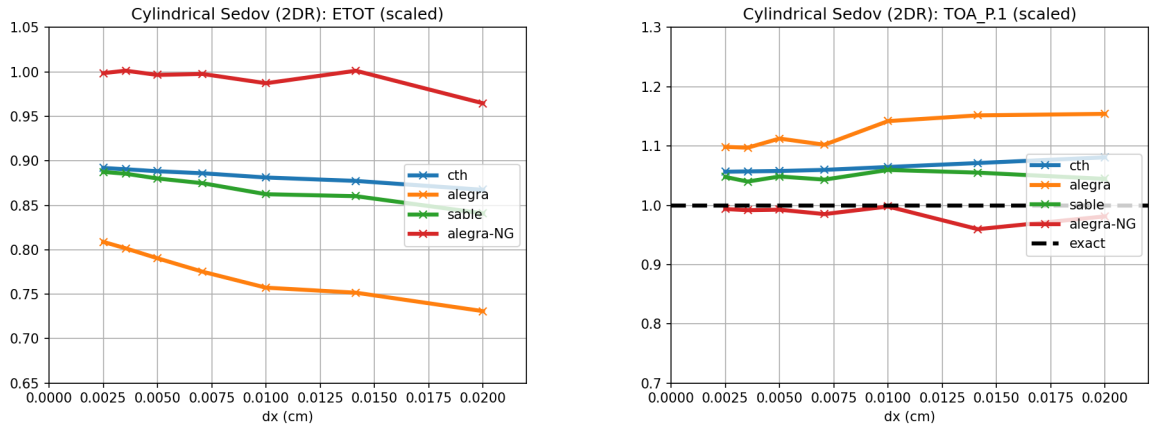

Figure 2-3. Cylindrical Sedov 2DR: convergence of ETOT and shock TOA at 45°

Figure 2-4. Here the situation seems to improve for CTH, but this is actually a result of a more serious pressure instability in the CTH solution.

2.3. Solution field instabilities

This study identified large instabilities in CTH results for pressure, density, and velocity near the shock for all of the 2D Sedov problems tested. No resolution of this issue has been identified to date, though the CTH developers are continuing to work to resolve if this is a bug or a feature of the code. This issue is only present in CTH and not in any of the other codes.

Figure 2-5 shows pressure plots at comparison time for CTH for two forms of the Sedov problem tested. The left plot is for the spherical Sedov problem run in 2DC mode; the right plot is for the cylindrical Sedov problem run in 2DR mode. Both problems use symmetry boundary conditions, though these are not the source of the problem, since the instabilities persist on larger meshes without symmetry boundary conditions.

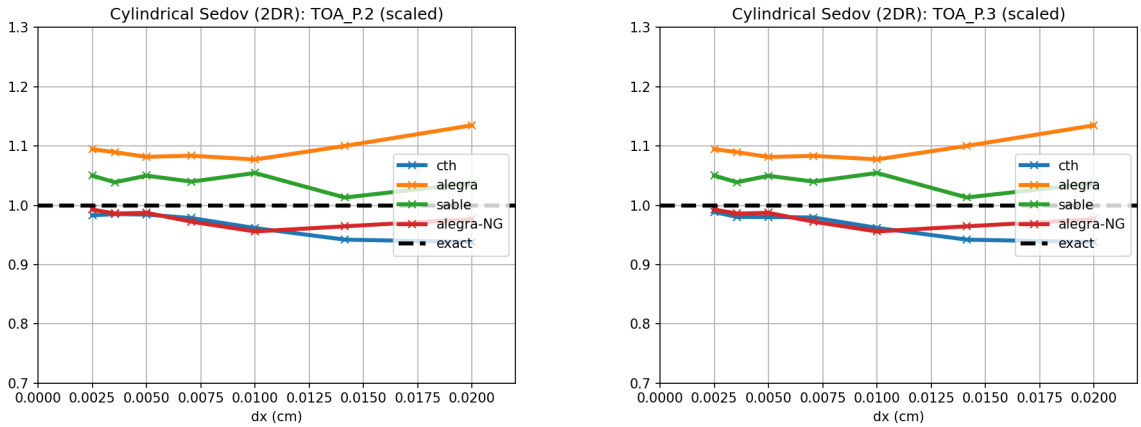

Figure 2-4. Cylindrical Sedov 2DR: convergence of shock TOA at 0 and 90°

All of the production codes exhibited instabilities in the velocity near the origin. Figure 2-6 compares the results using the spherical Sedov 2DC case.

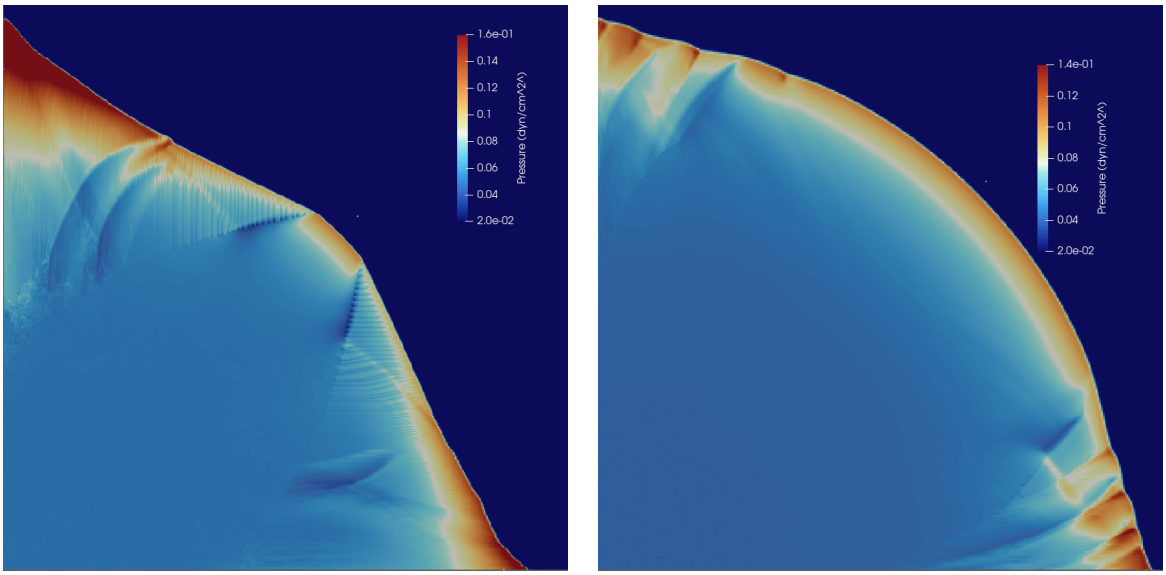

Spherical Sedov 2DC Cylindrical Sedov 2DR

Figure 2-5. CTH pressure solutions at final time

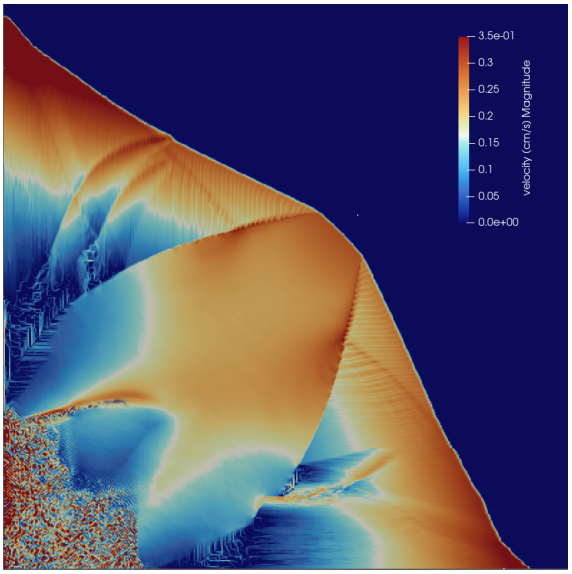

CTH

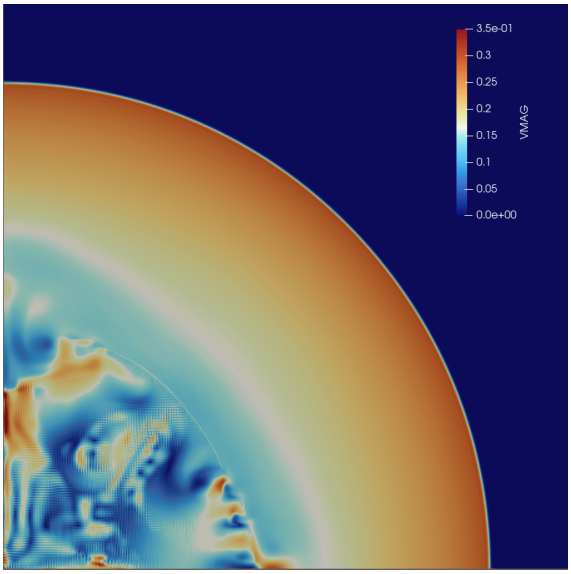

Alegra

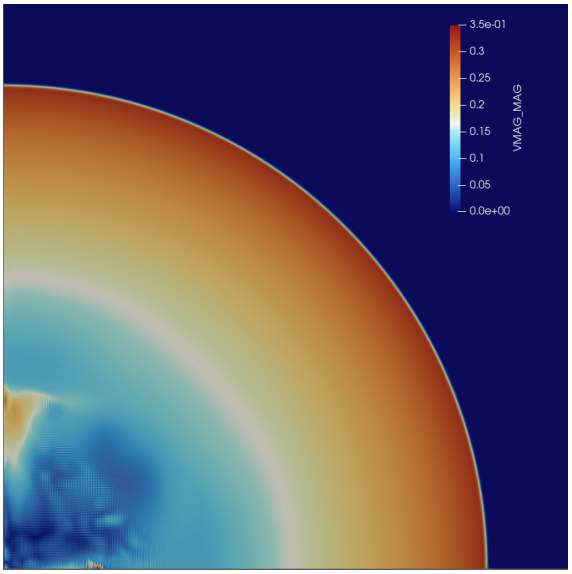

SABLE

Figure 2-6. Spherical Sedov 2DC: velocity magnitude solutions at final time

2.4. Comparison of remap options

New code development in SABLE occurred in FY25 that provides an improved energy conservation option to users (called "compatible energy conservation"). Likewise, the other production codes provide users additional options for remap. In CTH, this is done by setting "convection = 2" in the input file. For Alegra, multiple options exist; here the option "debar energy advection" is tested.

Figure 2-7 plots convergence of total energy for the original production code results along with the remap option tested. All three options have resolved the energy losses and improved shock

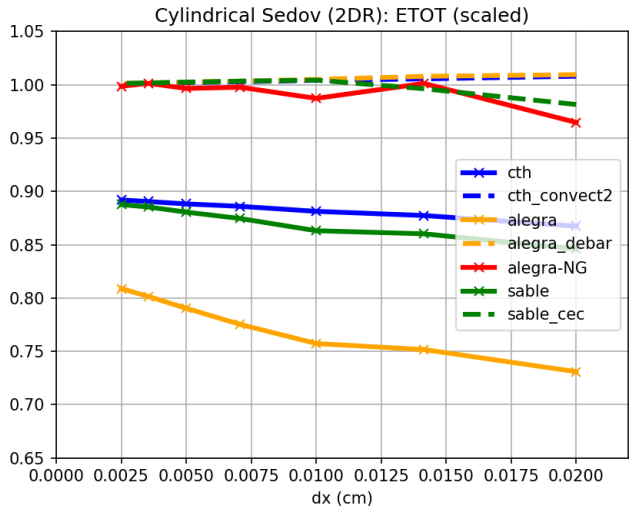

Figure 2-7. Cylindrical Sedov 2DR: convergence of ETOT for different remap options

TOA. However, the CTH implementation still has the pressure oscillations, as seen by the convergence of a coordinate-aligned tracer at 90°.

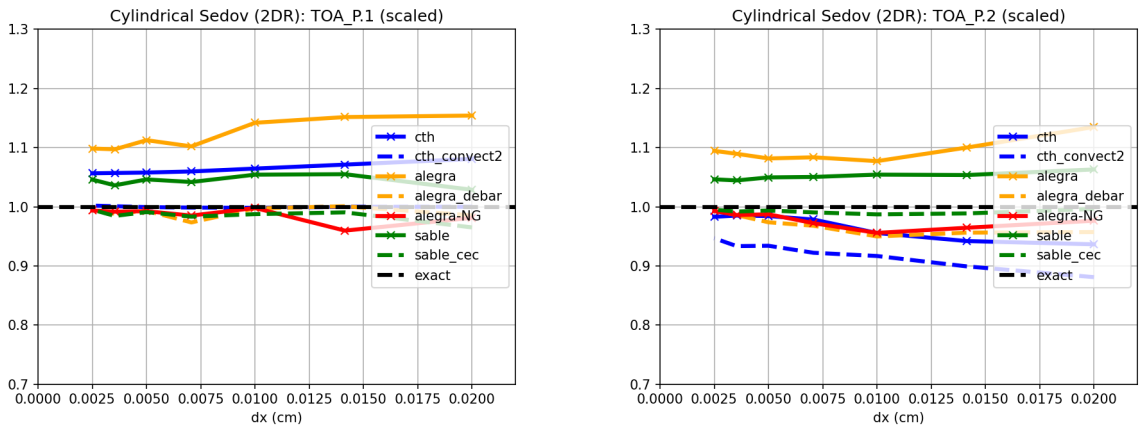

Figure 2-8. Cylindrical Sedov 2DR: convergence of shock TOA at 45° (left) and 90° (right) for different remap options

2.5. Comparison of Eulerian and Lagrangian modes

In order to isolate the source of the energy losses in production codes, a study was done using Alegra comparing a Lagrangian solution mode with the more common Eulerian solution mode, which is a Lagrangian step followed by a remap step. This study could not be performed in CTH, which only provides Eulerian mode, but could be performed in SABLE.

Figure 2-9 shows the time histories of total energy. Here it is shown that total energy is conserved in Lagrangian mode (as expected), in contrast to the Eulerian mode. This suggests that for Alegra (and potentially all of the production codes) the energy is most likely lost in the remap step.

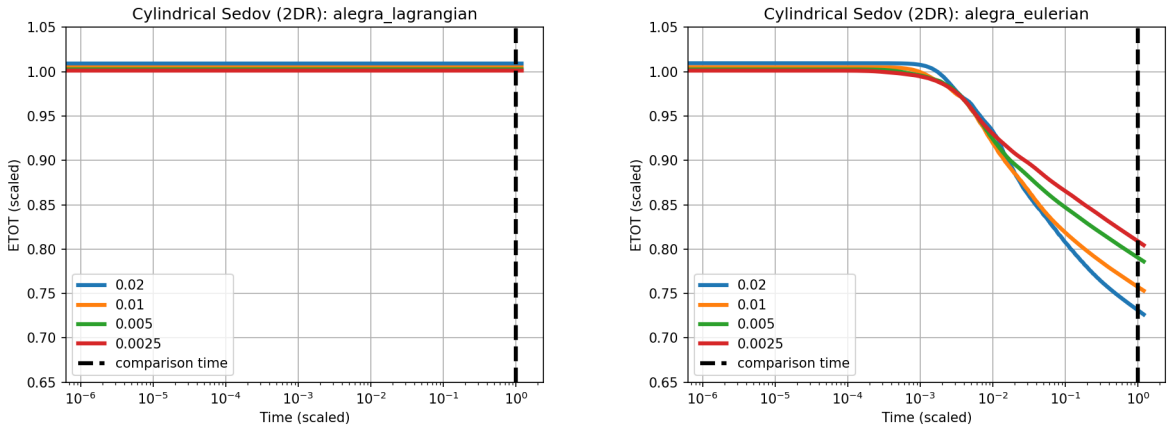

Figure 2-9. Cylindrical Sedov 2DR: comparison of (left) Lagrangian vs (right) Eulerian using Alegra.

2.6. Effect of the initial condition

Additional studies were performed to isolate issues from the choice of the initial condition (IC) for Sedov, which has been a source of controversy in the literature. As stated earlier, this study uses a finite circular or spherical region to insert the initial energy at uniform temperature.

Replacing the finite circle of initial energy with a finite square provides a method to remove all error in the initial energy. However, the evolution of total energy remained very similar across codes (results not shown here).

Replacing the finite circle with a point source within a single mesh cell did improve the results for Alegra-NG. However, the energy losses in the production codes were much worse. Figure 2-10 compares the convergence of total energy at comparison time using the nominal finite circle IC with a point source IC applied within a single grid cell.

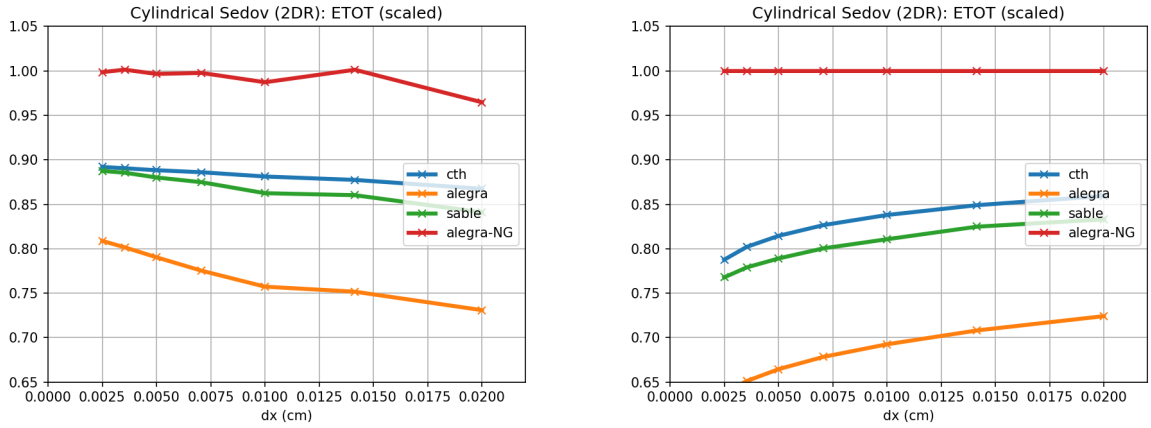

Figure 2-10. Cylindrical Sedov 2DR: convergence of ETOT for different initial conditions. (left) Finite circle (right) Point source within single grid cell

3. SPHERICAL SEDOV PROBLEM: 1DS RESULTS USING CTH

The simplest and most efficient way to run the spherical Sedov problem in CTH is using 1D spherical (1DS) mode. Because only CTH has a 1DS mode, results in this section are shown only for CTH.

The computational domain is defined as $[0, L]$, where $L = 1.2$ is large enough to include the solution with shock at $r = 1$ at the comparison time of $t = 1$. The final time for the simulations is $t = 1.2$. The mesh sizes (denoted dx) range from $2e{-}2$ down to $1.25e{-}3$ using a mesh size ratio of $\sqrt{2}$ to produce a total of nine meshes.

The convection option in CTH determines the type of remap used within each time step. A remap is needed after the material is advected using a Lagrangian step. The values can of the convection option can be 0 (default) or 2. The default option "convects internal energy and discards the kinetic energy discrepancy"; the non-default option "convects total energy (internal plus kinetic) then substracts the new kinetic energy (computed from the remapped momentum) from the total energy to recover the internal energy" [10].

The initial condition for the analytical solution is based on a point source at the origin, which is well defined for the analytical solution, since it is defined using a similarity coordinate (scaled shock position). Implementation of the point source in simulations requires placing the initial energy in a single grid cell, resulting in increasing specific internal energy values under mesh refinement. With the exception of the comparison in Section 3.5, the results shown in this report all apply the initial energy within a finite size region that is independent of mesh size. This *approximate* form of the initial condition results in a finite maximum value of specific internal energy independent of mesh size. For the 1DS case, the source region is chosen to be $[0, R]$, where $R = 0.02$ (as done in [9]).

3.1. Conservation

Figure 3-1 shows the time evolution of total mass (MTOT), total energy (ETOT), internal energy (EINT) and kinetic energy (EK) under mesh convergence. Here the variable names used are taken from their names in the CTH history output. Mass is normalized by the initial mass and energy variables are normalized by the input total energy of the blast. Mass is conserved exactly (all lines in the plot overlap) but the overall energy loss ranges from around 30% on the coarsest mesh to around 15% on the finest mesh shown. The energy losses occur most quickly at the first time step and then at a slower rate at later times. The exact time histories of EINT and EK are not currently available, but could be used for comparison purposes. The trend for EINT is to increase with mesh refinement for all time values; the trend for EK is unusual, with increasing values under mesh refinement at earlier times and then decreasing values at later time.

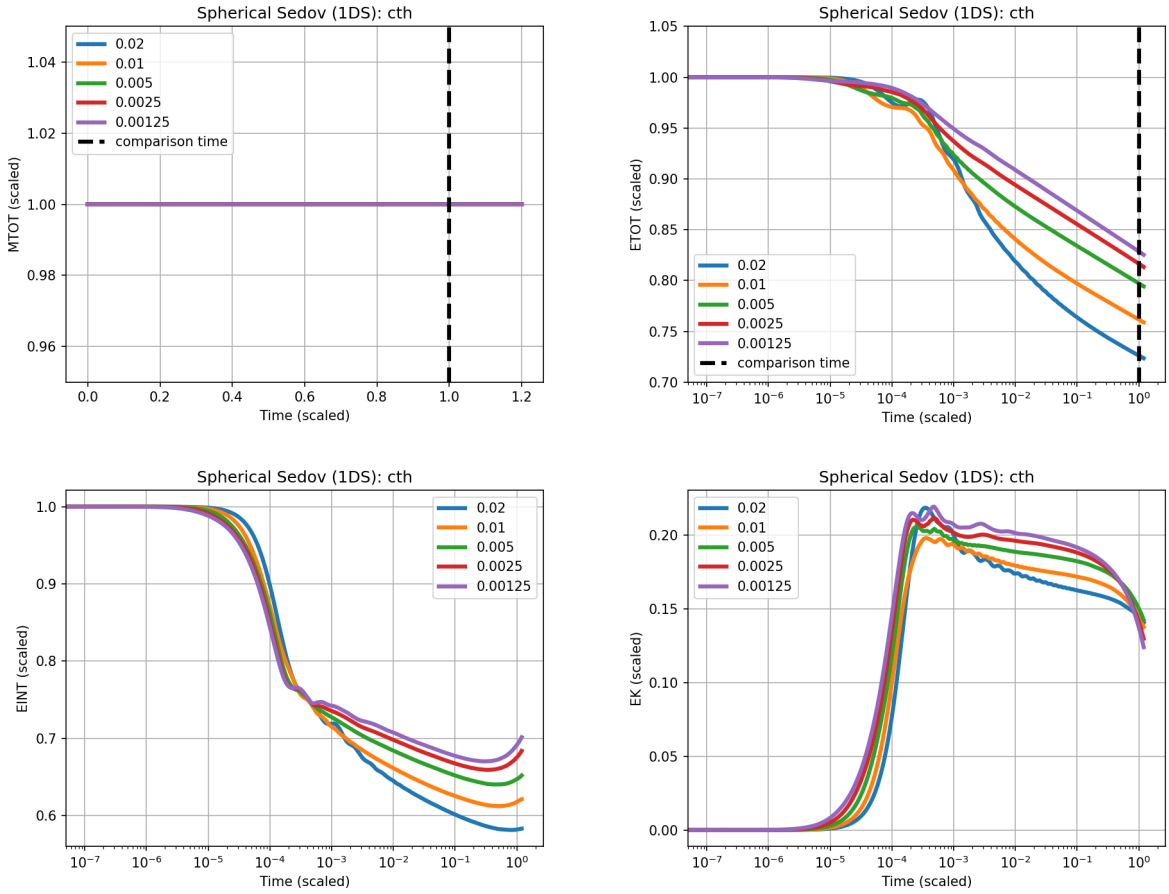

Figure 3-1. Spherical Sedov 1DS: convergence of mass and energy

3.2. Tracers and shock TOA

The CTH models are instrumented with Eulerian tracers at a location of $r = 1$, which is the shock position for the exact solution at the comparison time. This produces time histories of variables such as pressure (P) or velocity magnitude (VMAG) that can be post-processed to estimate outputs such as shock time of arrival (TOA). The shock wave for the exact solution arrives at the tracer location at exactly $t = 1$.

Figure 3-2 shows the mesh convergence for the pressure and velocity magnitude tracers along with a solid black line for the tracer history based on the exact solution. The shock TOA is delayed in the CTH results by 10-15%. The peak value also appears to be less than the value of the exact solution. This result will be representative of later results for most of the hydrocodes applied to Sedov when energy is not conserved and the solutions converge to the wrong solution.

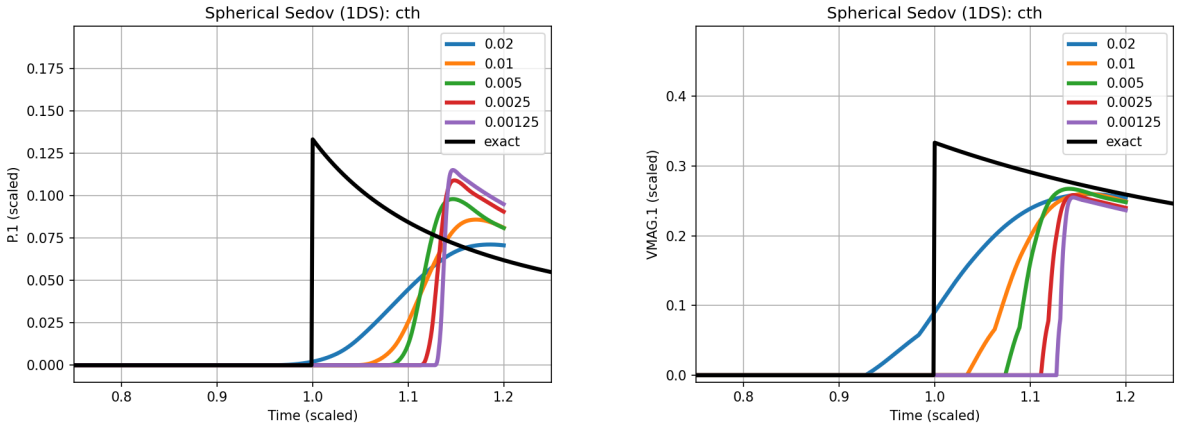

Figure 3-2. Spherical Sedov 1DS: convergence of tracers

3.3. Mesh convergence of energy and shock TOA

Each of the time histories in the previous sections can be post-processed to extract a scalar quantity. These include total energy at the comparison time of $t = 1$ and shock TOA at the tracer location (using either P or VMAG). Figure 3-3 shows the mesh convergence of mass and energy at comparison time. The total energy appears to be converging to a value about 85% of the exact value. Internal energy also appears to converge, while kinetic energy does not exhibit a convergent trend across the range of mesh sizes considered.

Figure 3-4 shows the convergence for shock TOA using both pressure and velocity magnitude using thresholds of 0.05 and 0.15, respectively. See Section 1.1 for the definition of how the TOA values are extracted. The convergence for pressure-based TOA is very noisy, with a sharp increase on the finest meshes. The velocity-based TOA is less noisy, but has the same sharp increase on the finest meshes.

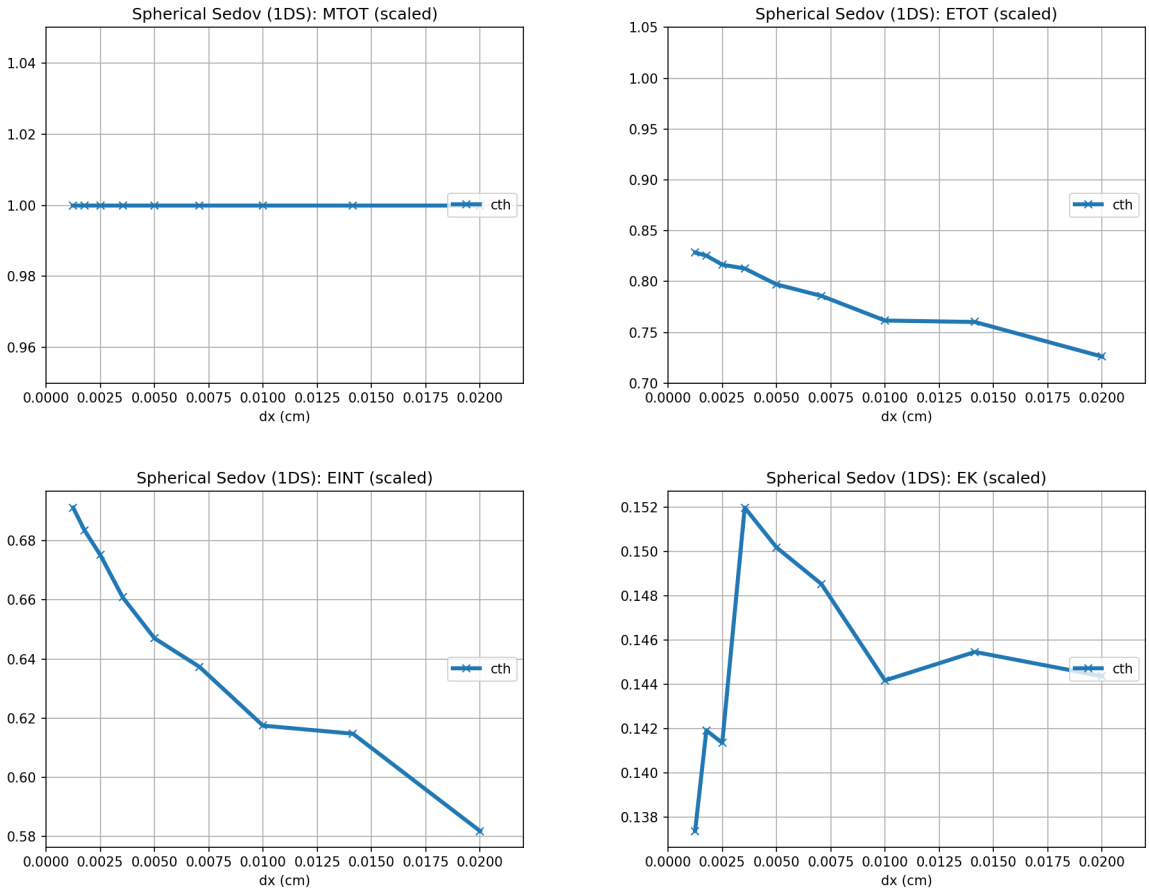

Figure 3-3. Spherical Sedov 1DS: convergence of mass and energy at final time

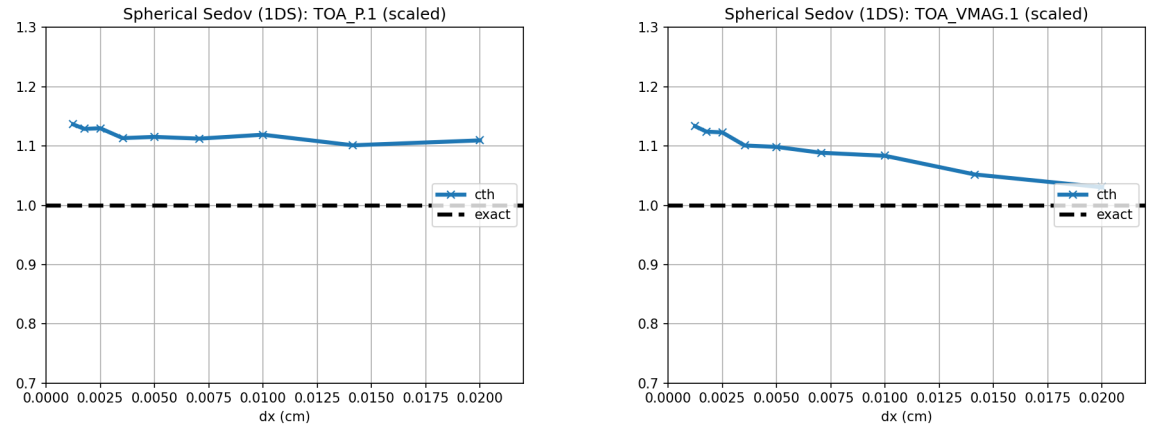

Figure 3-4. Spherical Sedov 1DS: convergence of shock TOA

The convergence to a lower total energy in Figure 3-3 mirrors the convergence to a higher shock TOA in Figure 3-4 . This will become a common theme over all hydrocodes that do not conserve total energy.

3.4. Solution fields

The final comparisons in this chapter use the solution fields as a function of the radial coordinate at the comparison time. In higher dimensions (2DC and 2DR), these would be scatter plots. For 1DS they can be displayed as line plots. The exact solutions were computed using the ExactPack Python library [16] and are plotted in black.

Figure 3-5 shows convergence of the main four solution fields - density, velocity, pressure, and specific internal energy. In all plots, the shock location is behind the exact solution. The peak velocity and density are lower than the exact solution, while the peak pressure is comparable. Large oscillations in velocity are visible near the origin, which become more localized near the origin at finer mesh scales.

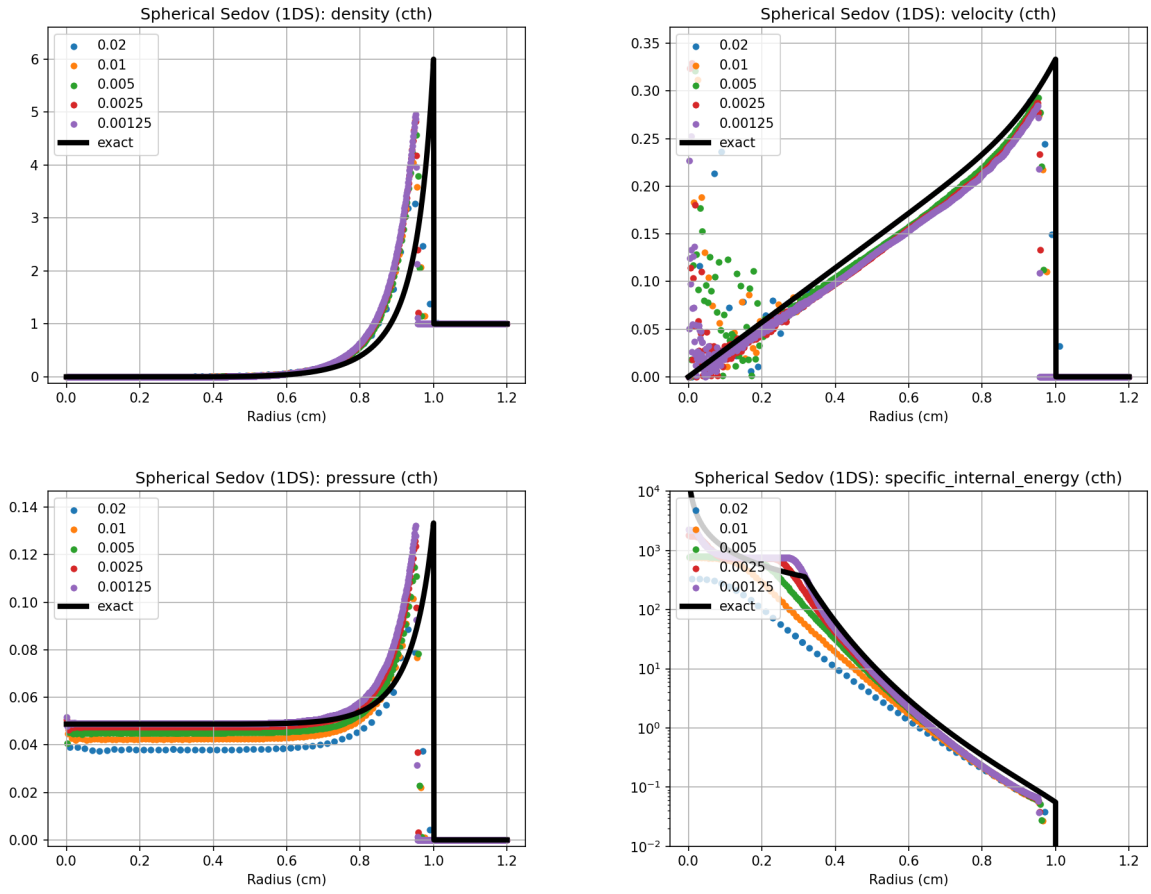

Figure 3-5. Spherical Sedov 1DS: solution convergence

3.5. Additional studies: convection option and point source

Additional studies were performed comparing the remap (convection) options and using a point source initial condition.

Figure 3-6 compares the velocity solutions and energy using the non-default convection=2 option over a range of mesh sizes. The resulting shock position is much better aligned with the exact solution; the oscillations near the origin are largely unaffected by the convection option. Total energy is not conserved, but the energy losses are much less, now only 1-3%.

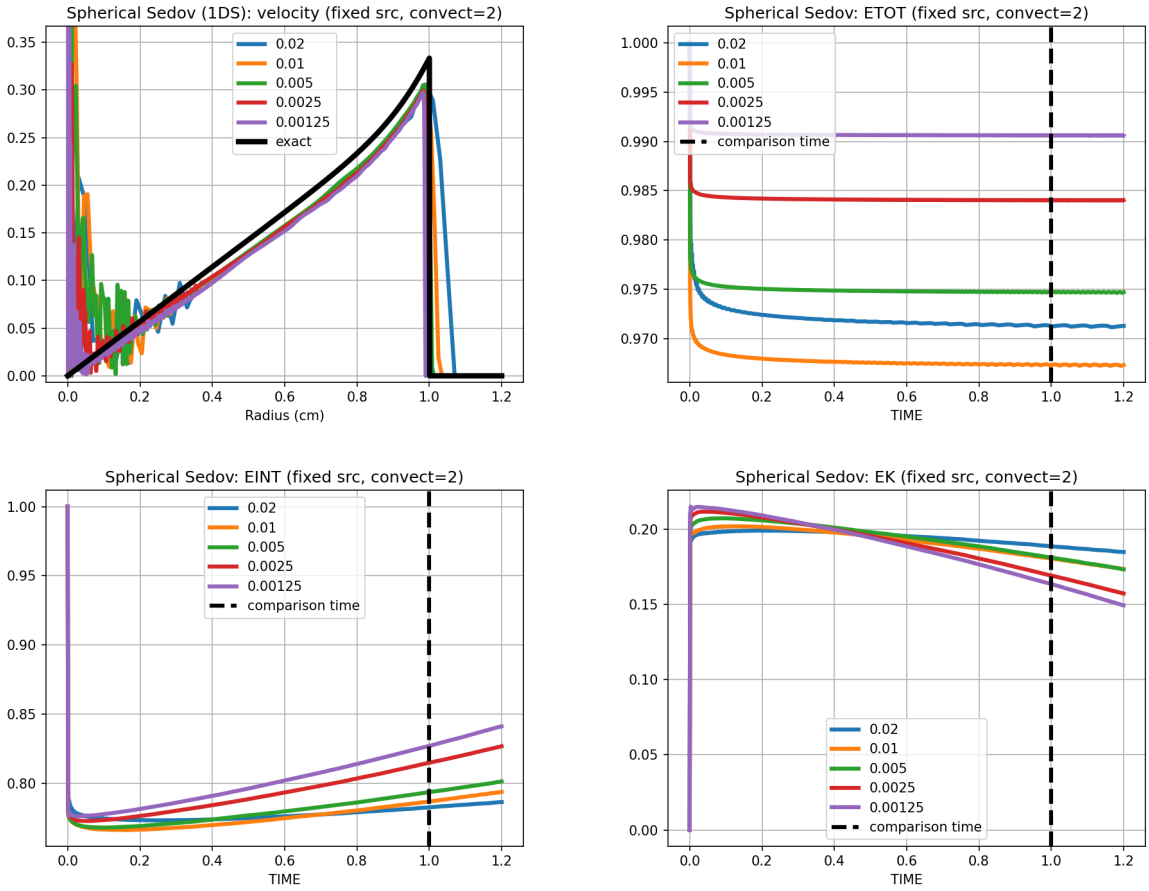

Figure 3-6. Spherical Sedov 1DS: use of convection=2 for velocity and energy

Figure 3-7 compares the density solutions and energy using a point source approximation (all energy placed in a single grid cell). In contrast to the finite source region, the total and kinetic energy are both *decreasing* with mesh refinement. As a result the shock wave eventually *stops moving* as seen in the plots of density at the comparison time.

3.6. Conclusions

For the spherical Sedov problem run in 1D spherical (1DS) mode, the following conclusions can be made about the results shown for CTH:

- total energy is not conserved, with losses ranging from 15-30%

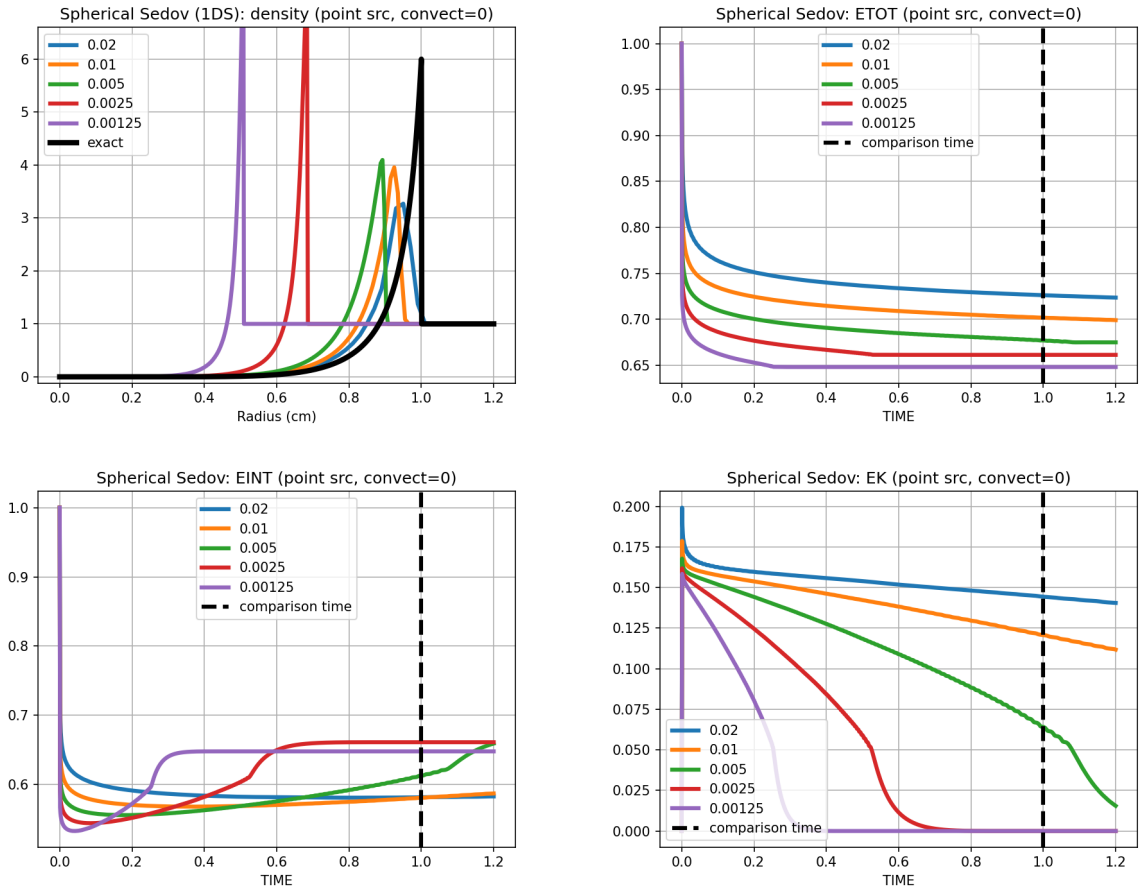

Figure 3-7. Spherical Sedov 1DS: use of point source for density and energy

- shock time of arrival is delayed by 10-15%
- energy conservation and shock TOA are significantly improved by the convection=2 option
- large oscillations in velocity occur near the origin
- the point source option for the initial condition causes decreasing total energy with mesh refinement and eventually results in loss of all kinetic energy

This page intentionally left blank.

4. SPHERICAL SEDOV PROBLEM: 2DC RESULTS USING CTH, ALEGRA, AND SABLE

In this chapter the spherical Sedov problem is run using 2D cylindrical (2DC) coordinates in all of the production codes (CTH, Alegra and SABLE). In addition to conservation and shock TOA, this enables evaluation of solution symmetry and detection of any anomalies from the use of a 2DC coordinate system. At the time of publication, Alegra-NG did not have a 2DC capability. Unless specified otherwise, the default convection=0 option for CTH is used in all results in this and the remaining chapters.

The computational domain is defined as the rectangle $[0, L]^2$, where $L = 1.2$ is large enough to include the solution at the comparison time of $t = 1$. Symmetry boundary conditions are applied to all four boundaries.

The mesh sizes (denoted dx) range from $2e{-}2$ down to $2.5e{-}3$ using a mesh size ratio of $\sqrt{2}$ to produce a total of seven meshes. The finest two mesh sizes from the 1DS study were not used in any of the 2D studies because of computational cost.

As with the 1DS case, the results shown in this chapter all use a finite size region to apply the initial energy. The source region is chosen to be a circle of radius $R = 0.02$. This approximate form of the initial condition results in a finite maximum value of specific internal energy independent of mesh size.

4.1. Conservation

Because a circular region of initial energy is inserted into a mesh of rectangular grid cells, some error is expected in the initial energy. Figure 4-1 shows the convergence of the scaled *initial* total energy (denoted as ETOT0). The initial total energy is never more than 1.5% and decreases linearly to the expected value in a consistent way for all three codes.

Figure 4-2 compares the time evolution of total energy (ETOT) for all three codes using a range of mesh sizes. Energy losses at the comparison time range from 30-40% for Alegra and 20-25% for CTH and SABLE. The energy losses occur most quickly at the first time step and then at a slower rate at later times.

A comparison of internal and kinetic energy using the finest mesh resolution (0.0025) is shown in Figure 4-3. Internal energy mirrors the trends in total energy; kinetic energy shows a large spike near initial time followed by a slow decay over time (linear for CTH and non-linear for Alegra and SABLE).

Mass conservation was exact for all codes and is not plotted here.

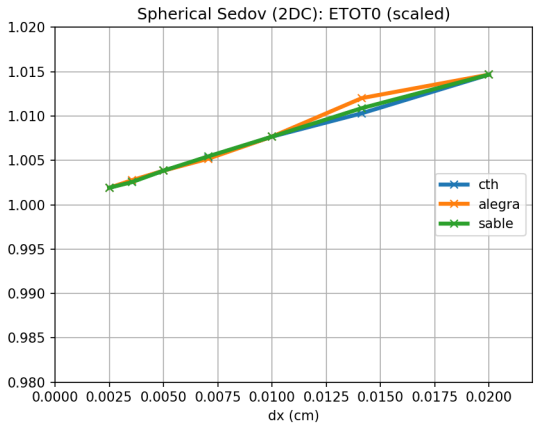

Figure 4-1. Spherical Sedov 2DC: convergence of scaled initial energy

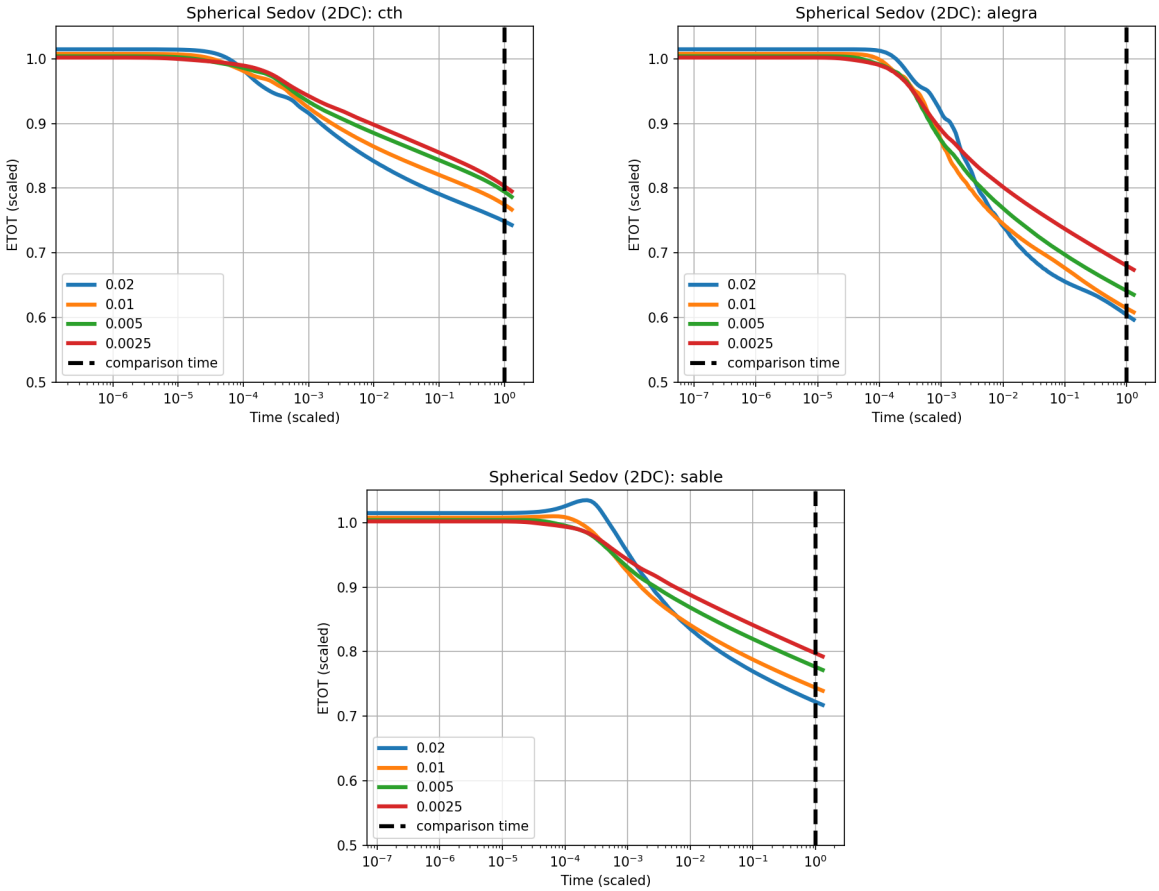

Figure 4-2. Spherical Sedov 2DC: convergence of total energy

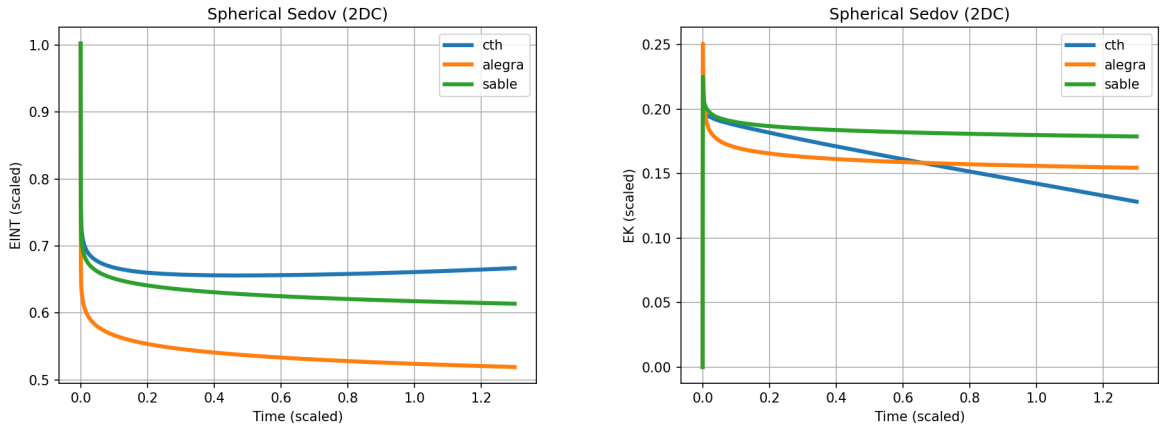

Figure 4-3. Spherical Sedov 2DC: comparison of internal and kinetic energy

4.2. Tracers and shock TOA

As with the 1DS case, the models are instrumented with Eulerian tracers at the shock location at comparison time. The radial location is $r = 1$ and multiple angular positions are selected (45, 0, and 90 ° for tracers numbered 1 through 3). These provide an indication of the symmetry of the solution and can be useful to detect anomalies, since the time histories for the exact solution should be identical at each location.

Figure 4-4 illustrates convergence of pressure tracers at 45° for multiple codes and meshes (results for velocity magnitude are similar), along with a solid black line indicating the time history of the exact solution. Each code exhibits convergence of the time histories, but not necessarily to the exact solution. For the 45° tracers, the shock arrives about 15% late for CTH, 10% late for SABLE and 20% late for Alegra.

Figure 4-5 provides a similar comparison for pressure tracers at 0 and 90°. CTH exhibits a 10% *earlier* shock TOA at 0° and a 15% earlier shock TOA at 90°. CTH also exhibits even higher values for both pressure and velocity than the exact solution. The large discrepancies in shock TOA for CTH as a function of angle will be shown later in this chapter to be from a significant asymmetry in the CTH solution. Alegra and SABLE again shows similar 20% and 10% delay in the shock TOA, respectively, with SABLE exhibiting better symmetry between the two tracer locations.

4.3. Mesh convergence of energy and shock TOA

Each of the time histories in the previous sections can be post-processed to extract a scalar quantity. These include total mass and energy at $t = 1$ and shock TOA at each of the tracer locations (for either P or VMAG). Figure 4-6 shows the mesh convergence of mass and energy at comparison time. The total energy (ETOT) converges to about 80% of the exact value for CTH

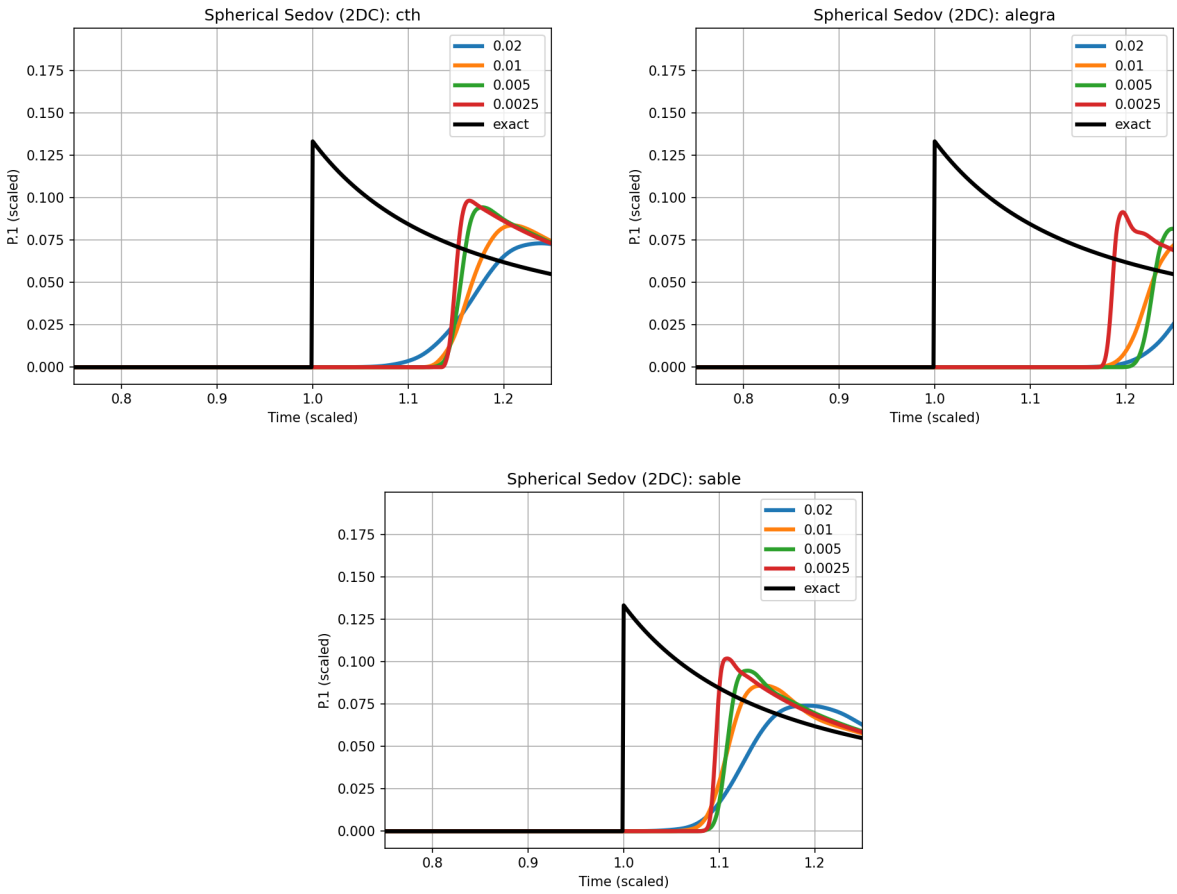

Figure 4-4. Spherical Sedov 2DC: convergence of tracer histories at 45°

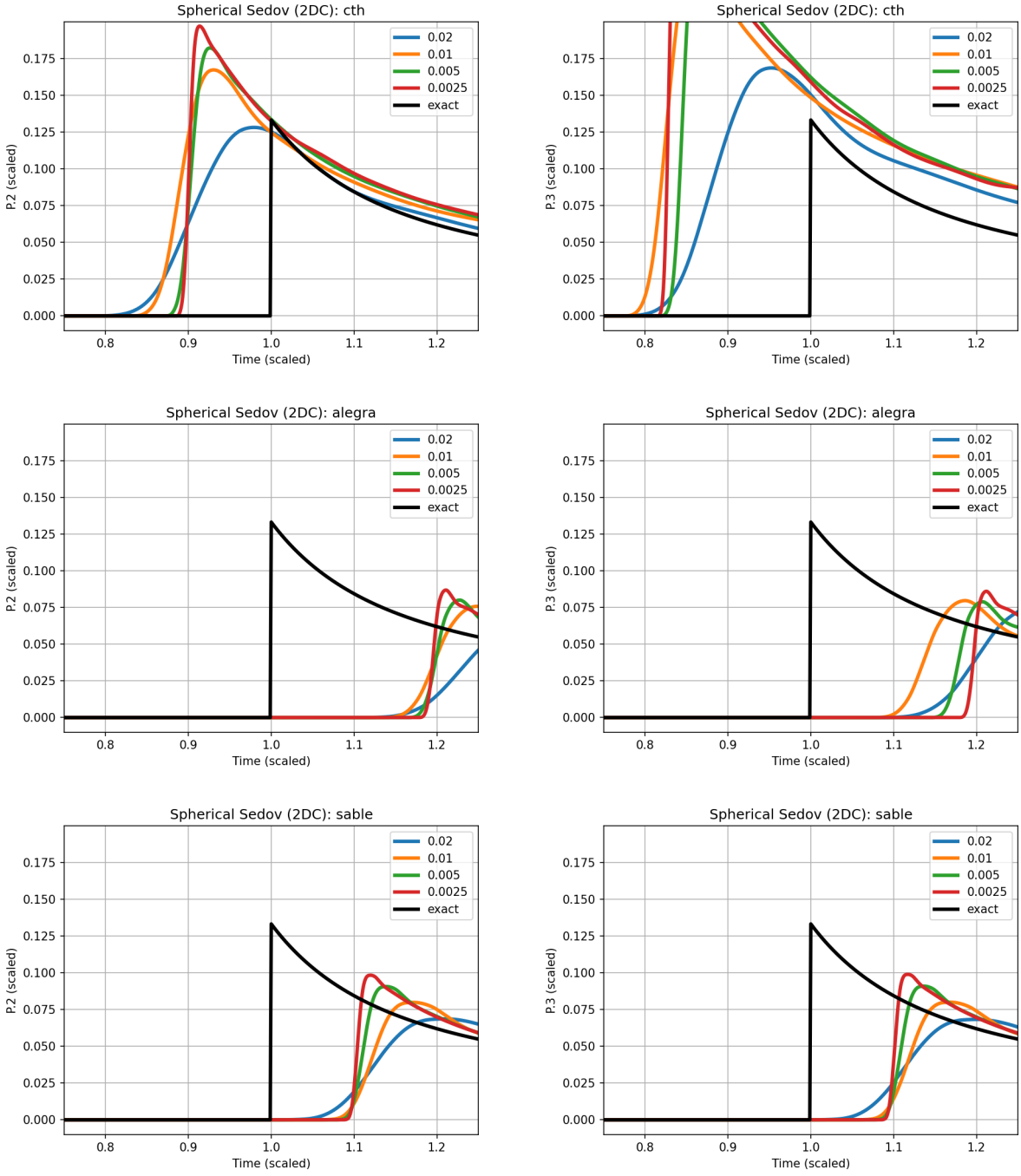

Figure 4-5. Spherical Sedov 2DC: convergence of tracer histories at 0° (left) and 90° (right)

and SABLE, and to about 70% for Alegra. Trends in internal and kinetic energy are less clear than with total energy.

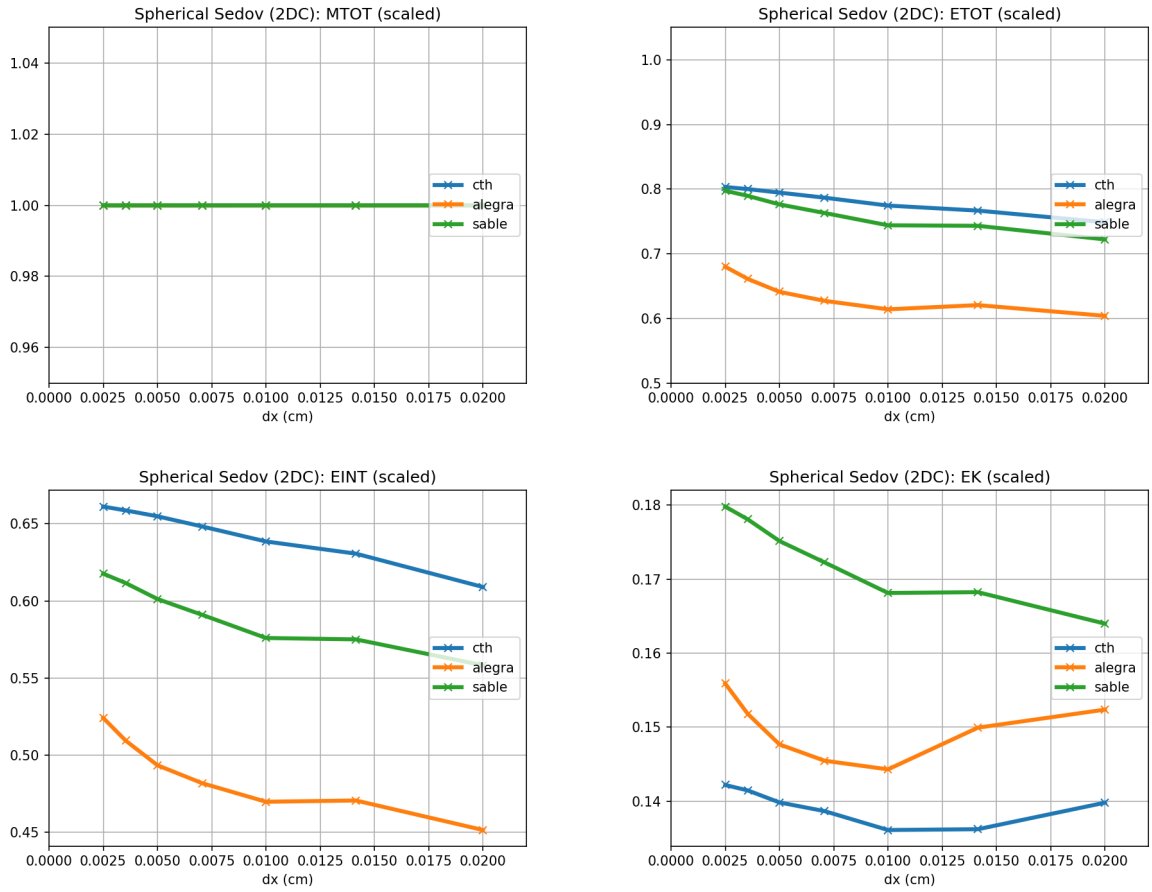

Figure 4-6. Spherical Sedov 2DC: convergence of mass and energy at final time

Figure 4-7 plots the extracted shock TOA data for pressure (results for velocity magnitude are similar). Alegra converges to a 20% delayed TOA, while SABLE converges to a 10% delayed TOA. CTH convergence depends on the angle, with 15% later TOA at 45°, 10% earlier TOA at 0°, and 15% earlier TOA at 90°.

4.4. Solution fields

The final comparisons are scatter plots using the solution fields as a function of the radial coordinate at the comparison time of $t = 1$. The exact solutions were computed using the ExactPack [16] Python library and are plotted in black.

Figure 4-8 shows convergence of density for each hydrocode. CTH has significantly more scatter in the solution than Alegra, while all the codes exhibit large errors in the shock location. SABLE has the most symmetry in the solution.

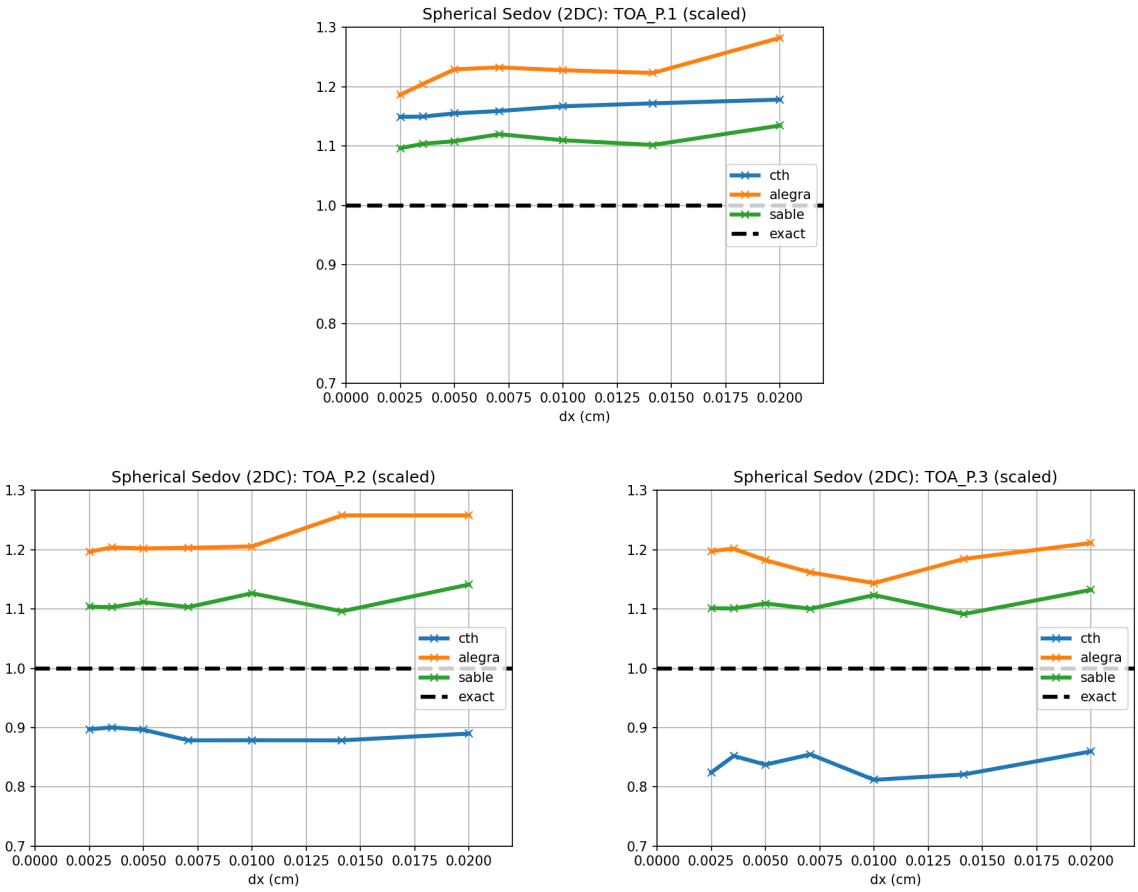

Figure 4-7. Spherical Sedov 2DC: convergence of shock TOA for pressure at 45° (top), 0° (lower left), and 90° (lower right)

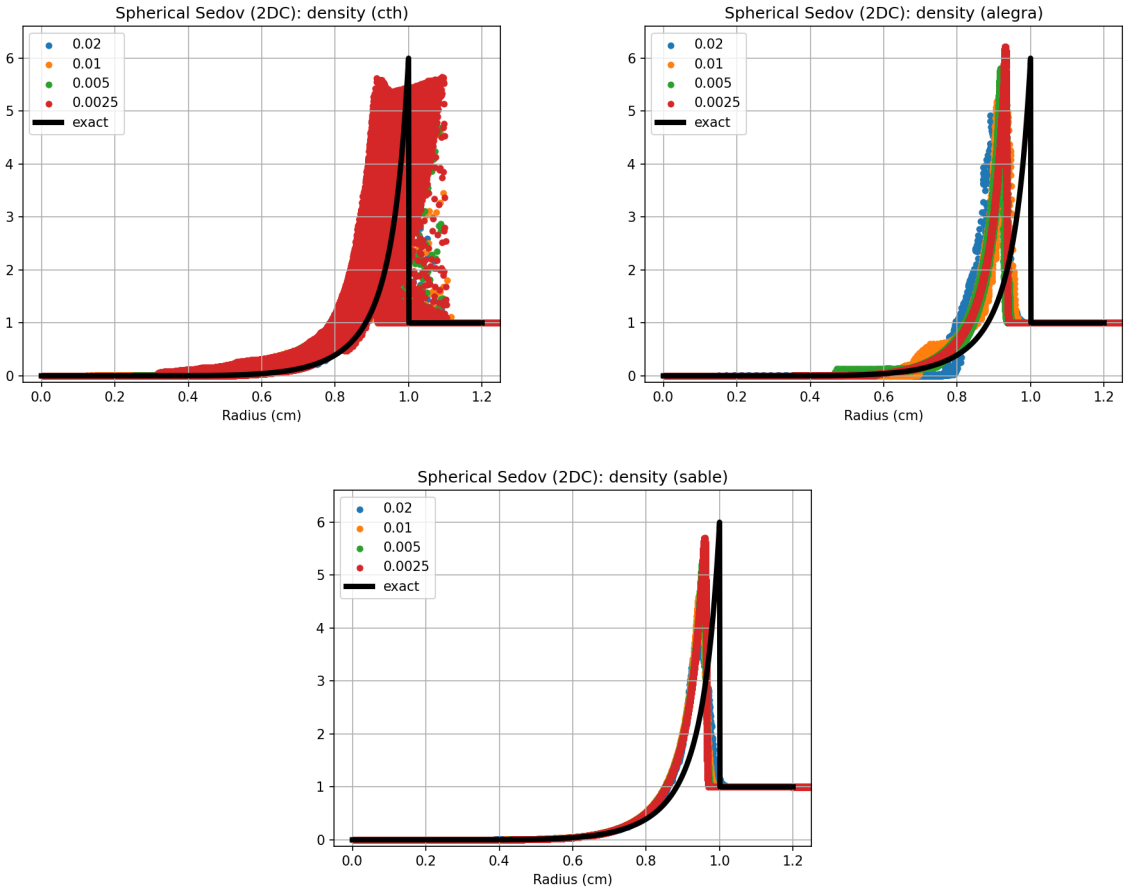

Figure 4-8. Spherical Sedov 2DC: convergence of density at final time

Figure 4-9 shows convergence of velocity magnitude for each hydrocode. Again CTH shows significant asymmetry in the solution near the shock. All the codes have large velocity oscillations in the post-shock region.

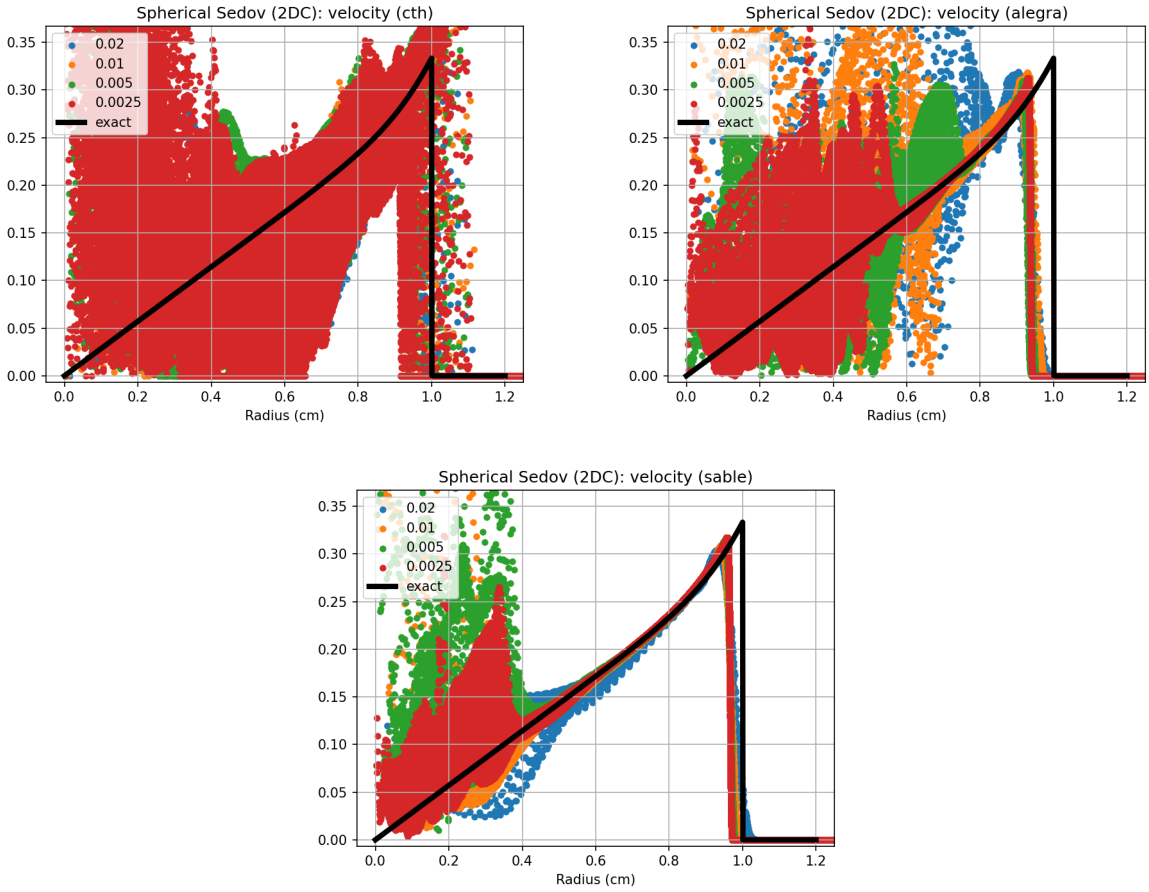

Figure 4-9. Spherical Sedov 2DC: convergence of velocity at final time

Figure 4-10 shows convergence of pressure for each hydrocode. CTH shows pressure oscillations behind the shock but appears to be converging to a more accurate post-shock state than Alegra and SABLE, which under-estimate the post-shock pressure by 20%. All the codes have noticeable post-shock pressure oscillations; SABLE has the lowest amplitude oscillations.

Figure 4-11 shows convergence of specific internal energy for each hydrocode. Here the effect of the initial condition approximation using a finite circular region can be seen by the fact that the energy hits a plateau near the origin for all codes. Alegra shows overshoots behind the shock that improve with mesh refinement. Again SABLE has the most symmetry in the solution behind the shock.

The final plots in Figure 4-12 compare velocity magnitude and pressure solutions at the comparison time and the finest mesh resolution. The color scales are the same in each plot (velocity ranges over [0,0.6] and pressure over [0.04,0.24]). The most serious issue is the significant instability in the CTH result, which is driving the large changes in shock TOA for

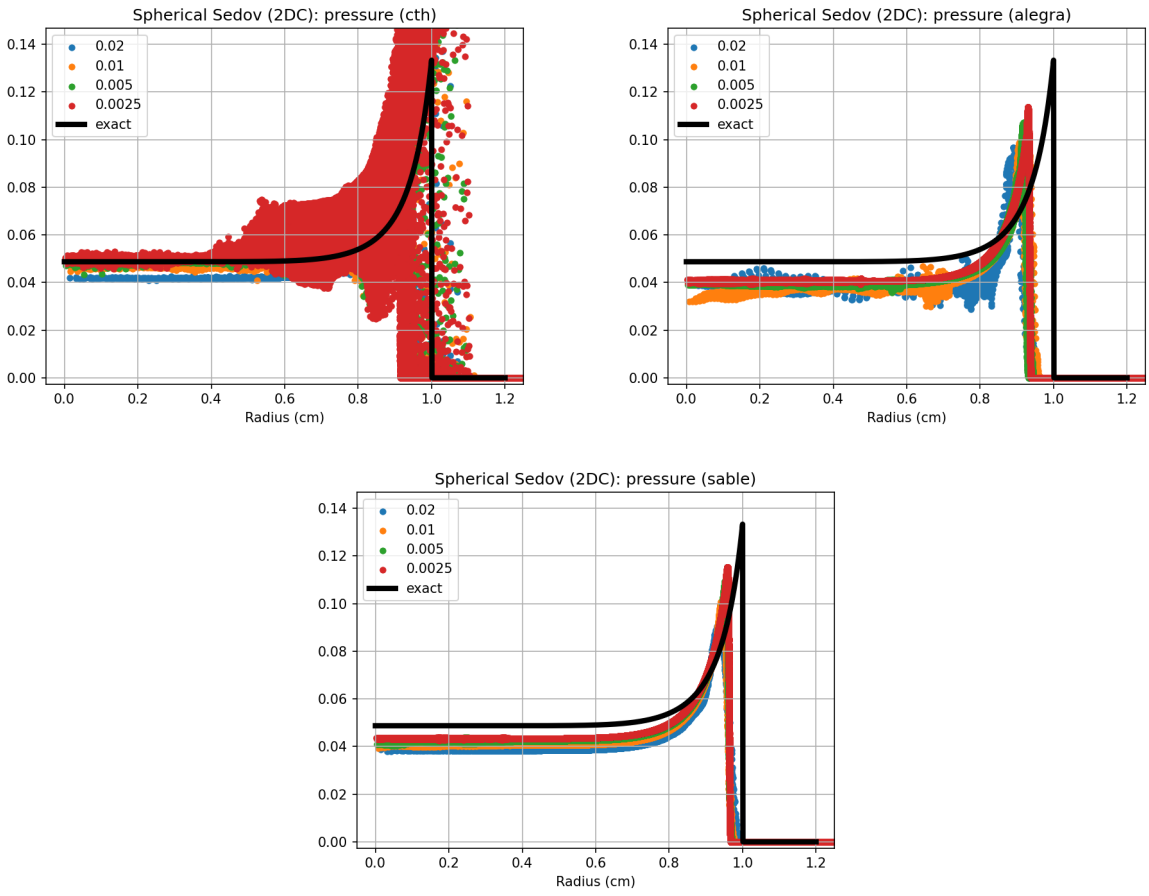

Figure 4-10. Spherical Sedov 2DC: convergence of pressure at final time

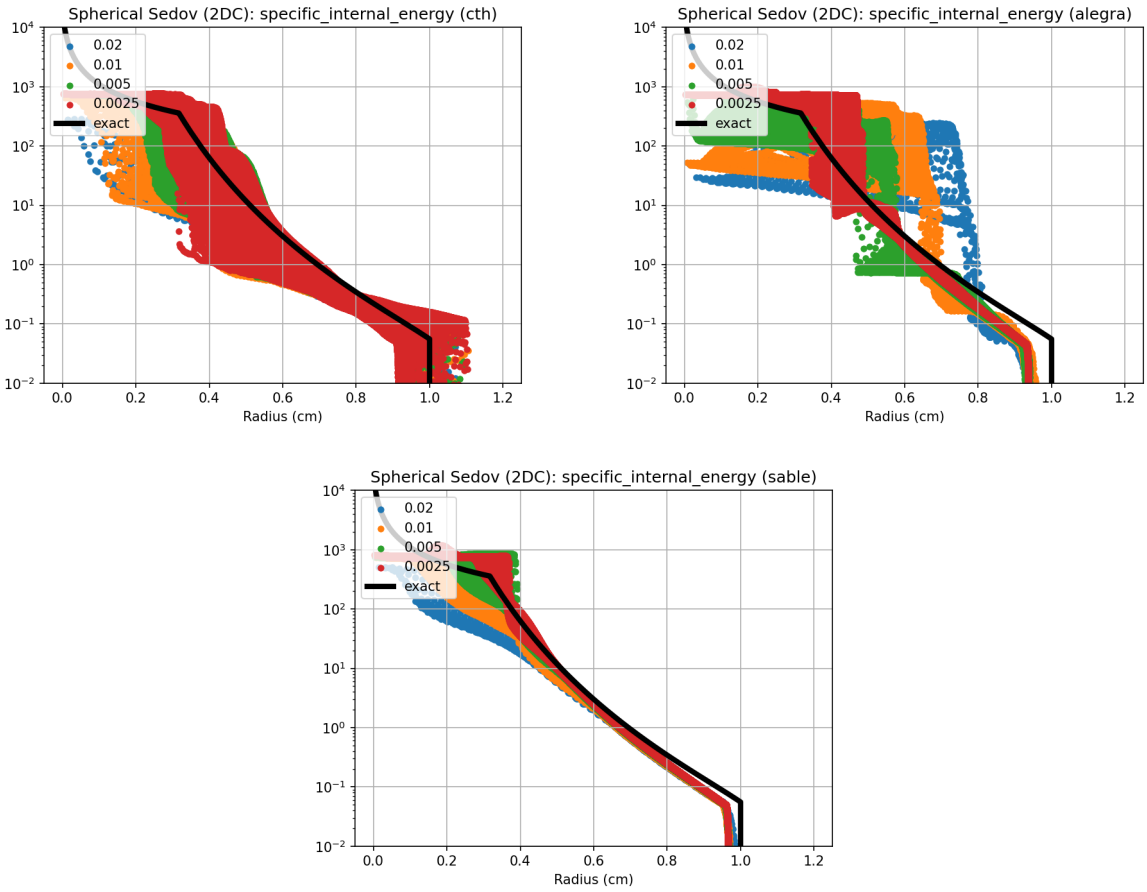

Figure 4-11. Spherical Sedov 2DC: convergence of specific internal energy at final time

tracers at different angles. The pressure solutions for Alegra and SABLE exhibit the nearly 10% delay in the shock but are highly symmetrical. All codes exhibit different kinds of velocity oscillations near the origin.

4.5. Conclusions

For the spherical Sedov problem run in 2D cylindrical (2DC) mode, the following conclusions can be made:

- errors from initial total energy are less than 1.5% and decrease with mesh refinement
- total energy is not conserved, with losses around 30-40% for Alegra and 20-25% for CTH and SABLE
- shock TOA is delayed by 10% for SABLE and 15% for Alegra
- shock TOA for CTH is delayed by 15% at 45° and arrives 10% earlier at 0 and 90°
- significant asymmetry is present for CTH in all fields near the shock
- velocity oscillations are present near the origin for all codes
- the post-shock pressure for SABLE and Alegra is 20% lower than the exact value.

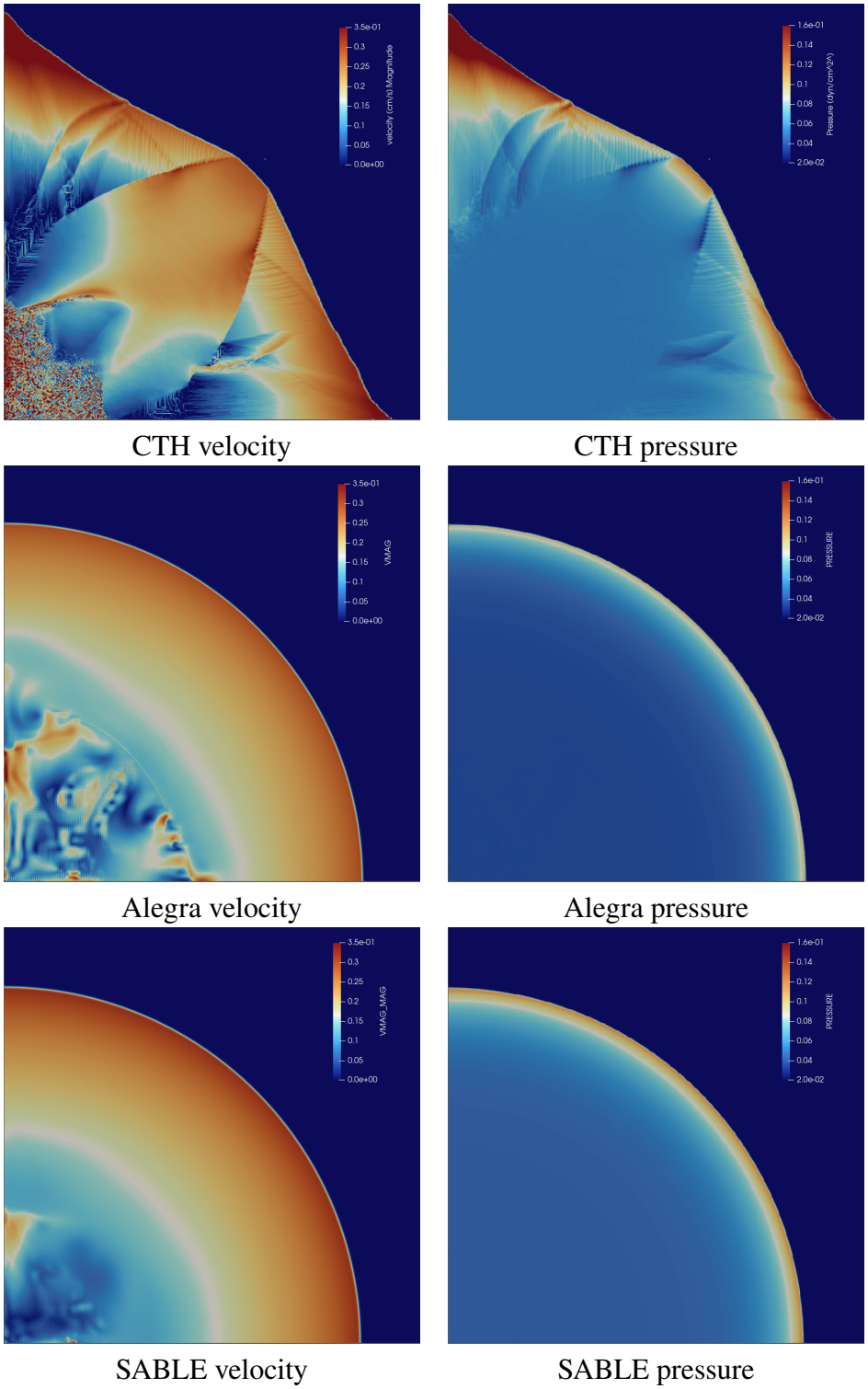

Figure 4-12. Spherical Sedov 2DC: velocity magnitude and pressure solutions at final time

This page intentionally left blank.

5. CYLINDRICAL SEDOV PROBLEM: 2DR RESULTS USING MULTIPLE CODES

In order to be able to compare all of the codes of interest, the cylindrical Sedov problem is used. The simulations are all run using 2D rectangular coordinates, using quarter symmetry, and in Eulerian mode (Lagrangian plus remap back to the original mesh). As with the spherical 2DC case, the initial energy is averaged over a circle of radius $r = 0.02$. The domain and boundary conditions are the same as for the spherical 2DC case.

5.1. Conservation

Because a circular region of initial energy is inserted into a mesh of rectangular grid cells, some error is expected in the initial energy. Figure 5-1 shows the convergence of the scaled *initial* total

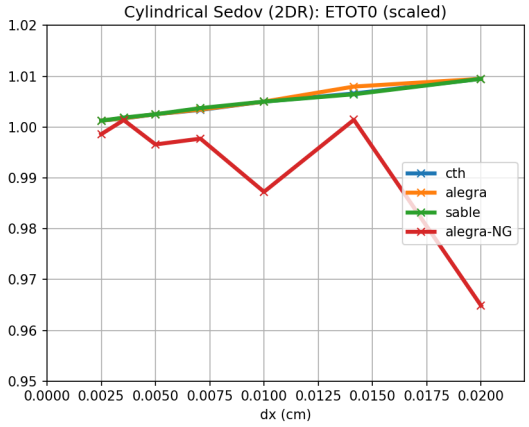

Figure 5-1. Cylindrical Sedov 2DR: convergence of scaled initial energy

energy (ETOT0). Consistent convergence of the initial energy is seen across three of the four codes, with errors no more than 1% on the coarsest mesh. The exception is the Alegra-NG code, which differs in the insertion of initial energy, using a temperature-based mixing rather than energy-based mixing. The errors in ETOT0 are larger, but do still converge to the exact value.

Figure 5-2 compares the time evolution of total energy (ETOT) for all codes using a range of mesh sizes. As with the 1DS and 2DC cases, all but one code loses energy, ranging from 5-10% for CTH, 20-30% for Alegra, and 20-25% for SABLE. The energy losses occur at the first time step and then at a slower rate at later times. The Alegra-NG code is able to conserve energy much more accurately with errors ranging from 0.01-3%.

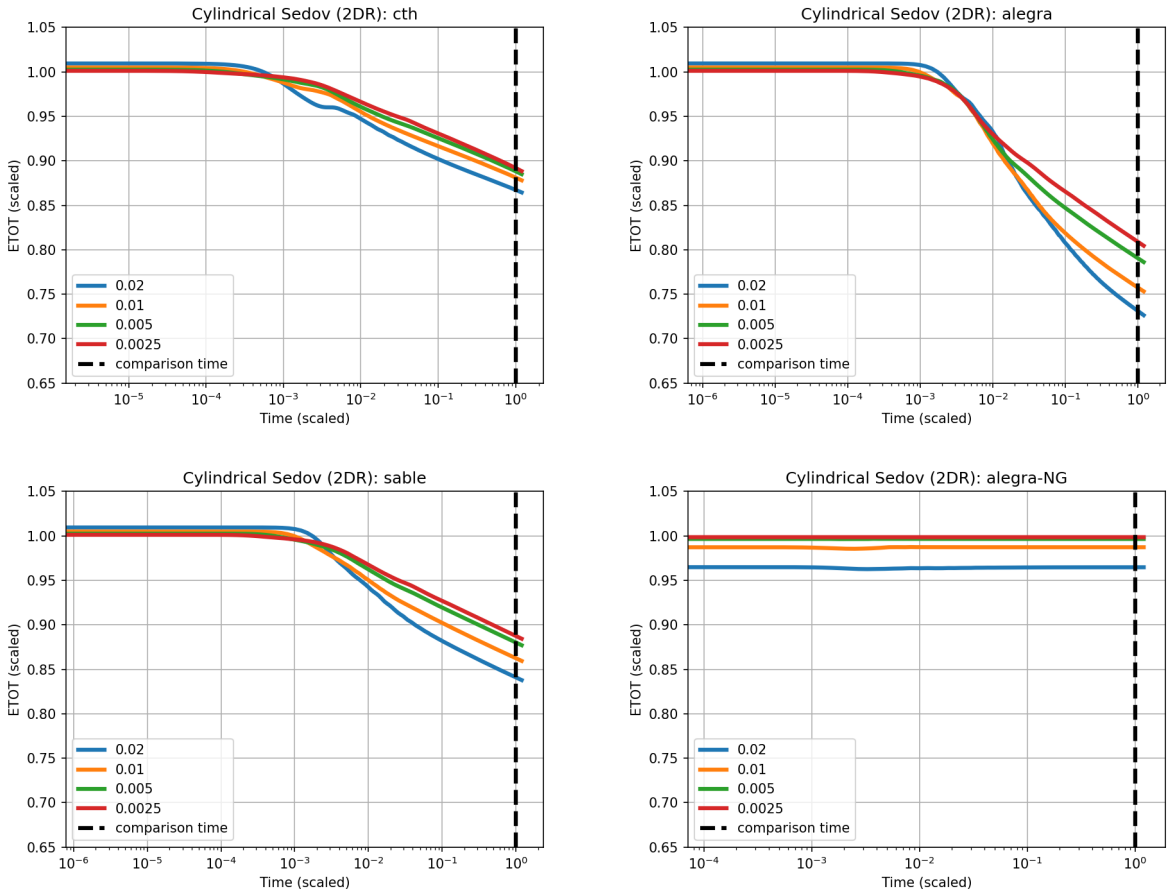

Figure 5-2. Cylindrical Sedov 2DR: convergence of total energy

A comparison of internal and kinetic energy using the finest mesh resolution (0.0025) is shown in Figure 5-3. Here the missing energy can be seen as a discrepancy in both internal and kinetic energy when comparing the energy-conserving results from Alegra-NG with the other three codes.

Mass conservation was exact for all codes and is not plotted here.

5.2. Tracers and shock TOA

As with the 2DC spherical case, the models are instrumented with Eulerian tracers at the shock location at comparison time. The radial location is $r = 0.75$ and multiple angular positions are selected (45, 0, and 90°) to provide an indication of the symmetry of the solution and to detect anomalies.

Figure 5-4 illustrates convergence of pressure tracers at 45° for multiple codes and meshes (results for velocity magnitude are similar), along with a solid black line indicating the time history of the exact solution. Each code exhibits convergence of the time histories, but not necessarily to the

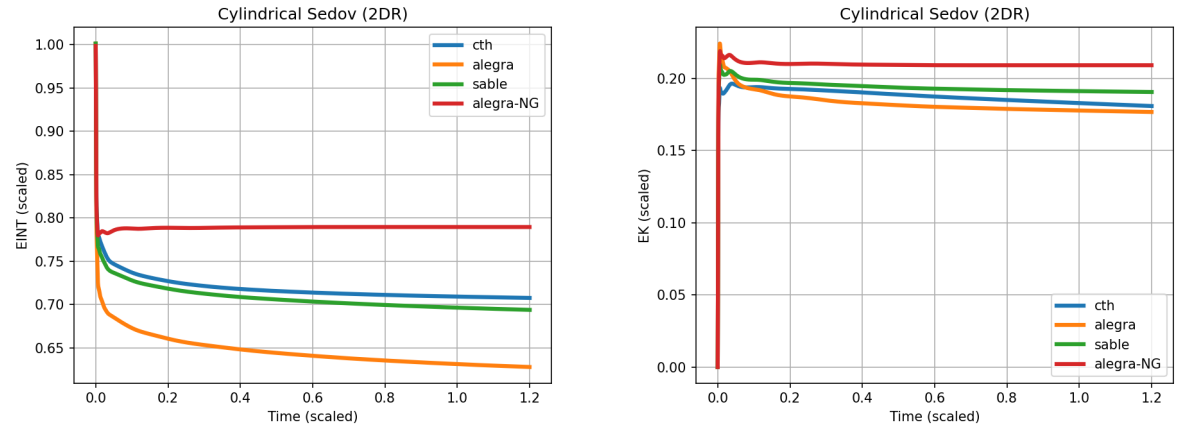

Figure 5-3. Cylindrical Sedov 2DR: convergence of internal and kinetic energy

exact solution. For the 45° tracers, the shock arrives about 5% late for CTH and 10% late for SABLE and Alegra. The energy conserving Alegra-NG code produces tracer histories that are much closer to the analytical solution.

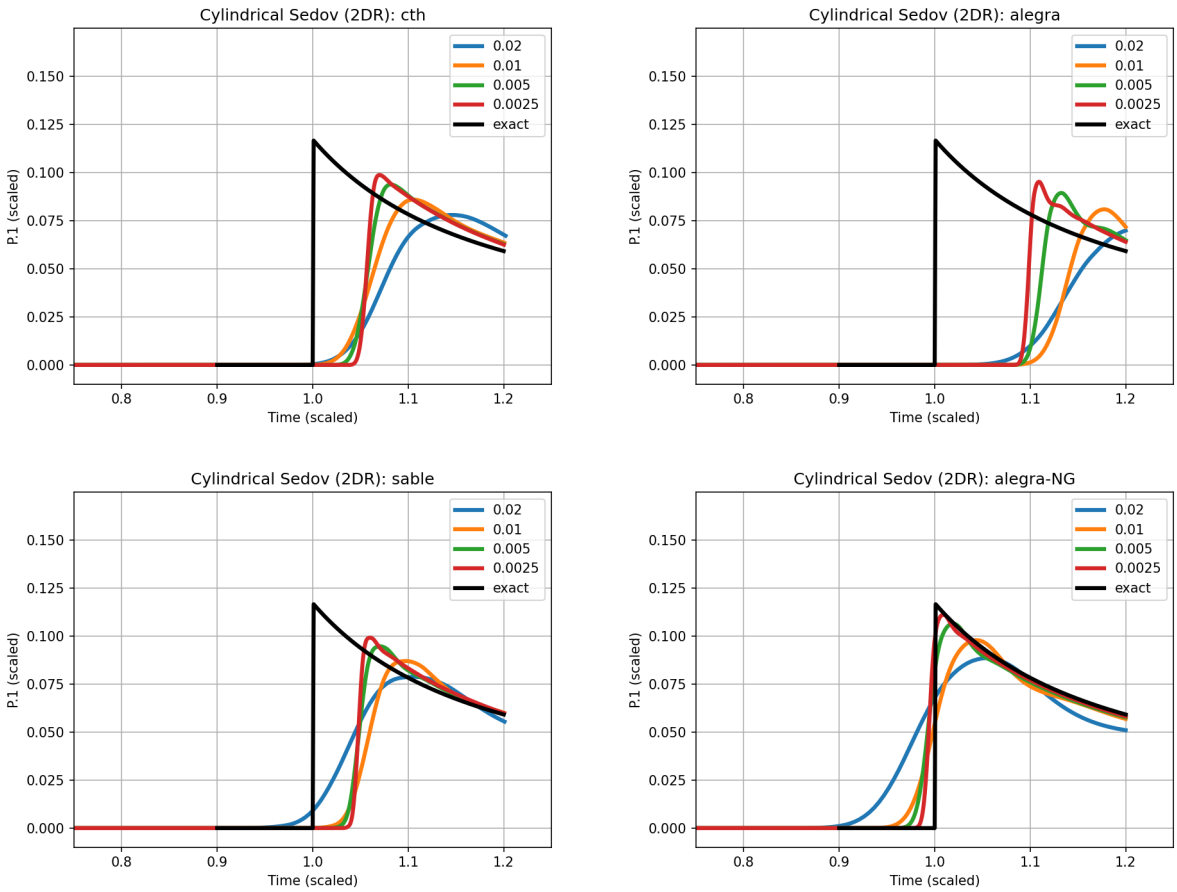

Figure 5-4. Cylindrical Sedov 2DR: convergence of tracer histories at 45°

Figure 5-5 provides a similar comparison for pressure tracers at 0° (results for 90° are very similar). For the 0 and 90° tracers, Alegra and SABLE show similar delay in the shock TOA, while CTH exhibits a shock TOA that is slightly earlier than the exact TOA. This result will be shown later in this chapter to be from a significant asymmetry in the CTH solution arising from a large instability, similar to what was observed for the Spherical Sedov problem using 2DC.

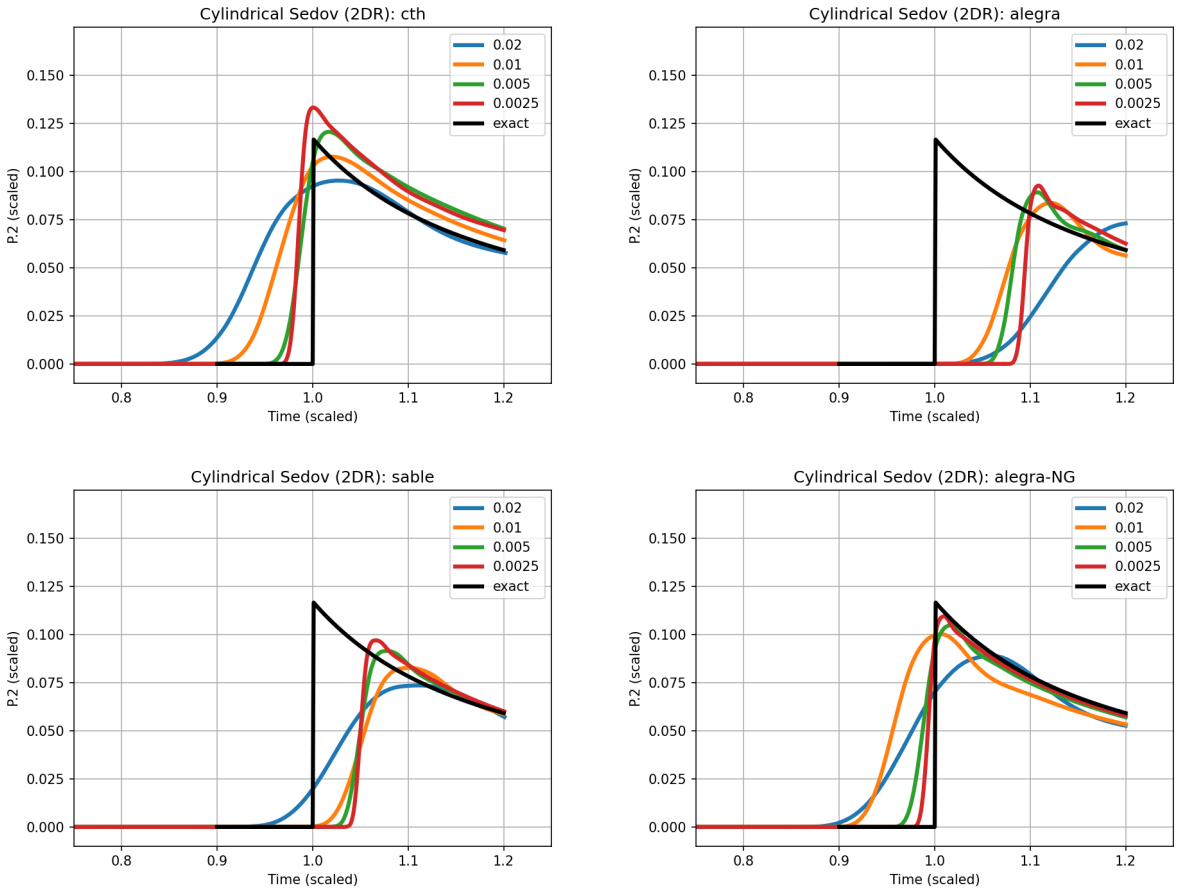

Figure 5-5. Cylindrical Sedov 2DR: convergence of tracer histories at 0°

5.3. Mesh convergence of energy and shock TOA

Figure 5-6 shows the mesh convergence of mass and energy at the comparison time. For CTH, Alegra, and SABLE the total energy converges to about 90%, 82%, and 78% of the exact value, respectively. Alegra-NG is converging to within less than 0.1% of the exact value.

Figure 5-7 shows the convergence of the TOA for two tracer locations for both pressure (P) and velocity magnitude (VMAG). In all cases Alegra and SABLE consistently converge to TOA values about 10% higher than the exact value. CTH converges to a TOA value about 5% larger for the 45° tracer and about 1% lower for the 0 and 90° tracers (for the wrong reason). Alegra-NG converges to nearly the correct TOA in all cases.

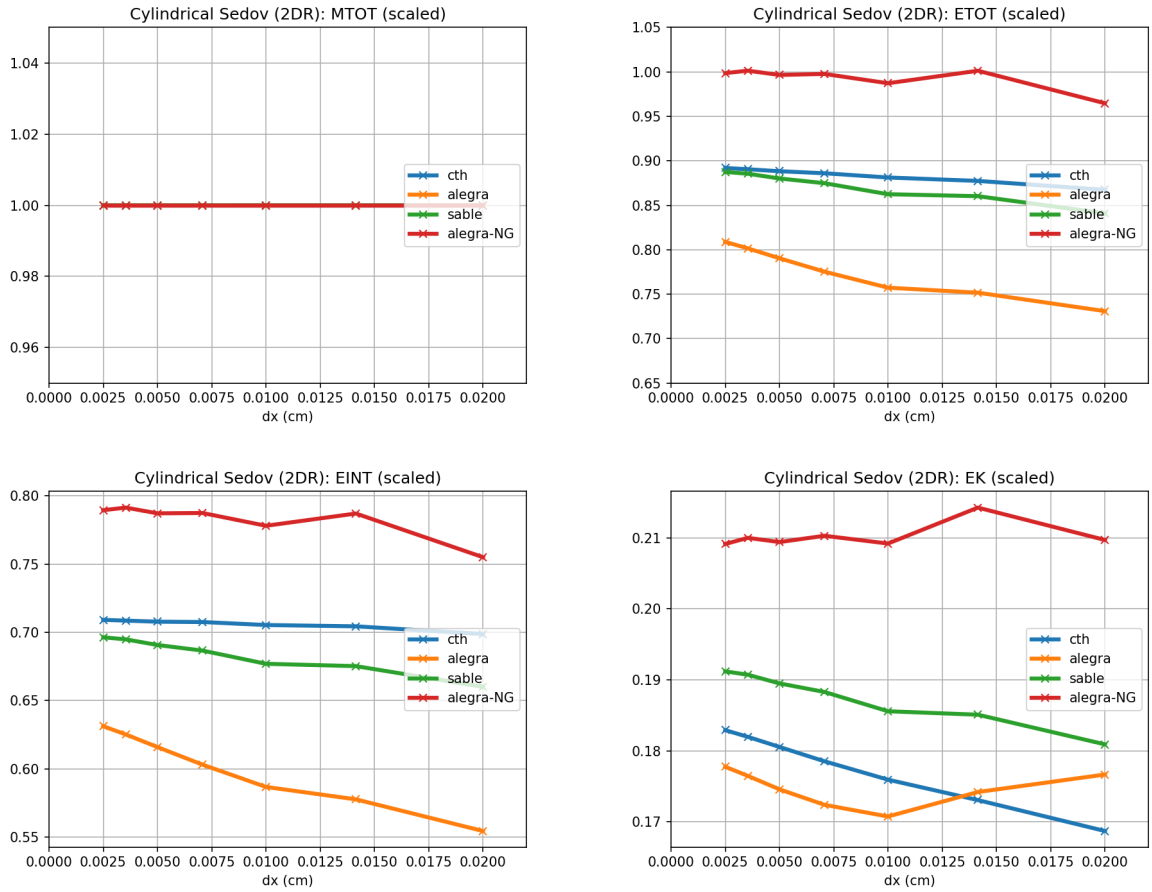

Figure 5-6. Cylindrical Sedov 2DR: convergence of mass and energy at final time

5.4. Solution fields

The final comparisons are scatter plots using the solution fields as a function of the radial coordinate at the comparison time of $t = 1$. The exact solutions were computed using the ExactPack Python library [16] and are plotted in black.

Figure 5-8 shows convergence of density for each hydrocode. CTH has the most scatter in the solution, while Alegra-NG converges closest to the exact solution. As in the 2DC case, SABLE has good symmetry in the solution, along with Alegra-NG.

Figure 5-9 shows convergence of velocity magnitude for each hydrocode. Again CTH shows significant asymmetry in the solution near the shock. Both CTH and SABLE also have large velocity oscillations near the origin. Alegra also exhibits asymmetry in the velocity field near the origin. Again Alegra-NG is converging well to the exact solution with good symmetry.

Figure 5-10 shows convergence of pressure for each hydrocode. CTH shows pressure oscillations behind the shock but appears to be converging to a closer post-shock state than Alegra or SABLE. The pressure in Alegra-NG is largely free of oscillations and is converging to the correct solution.

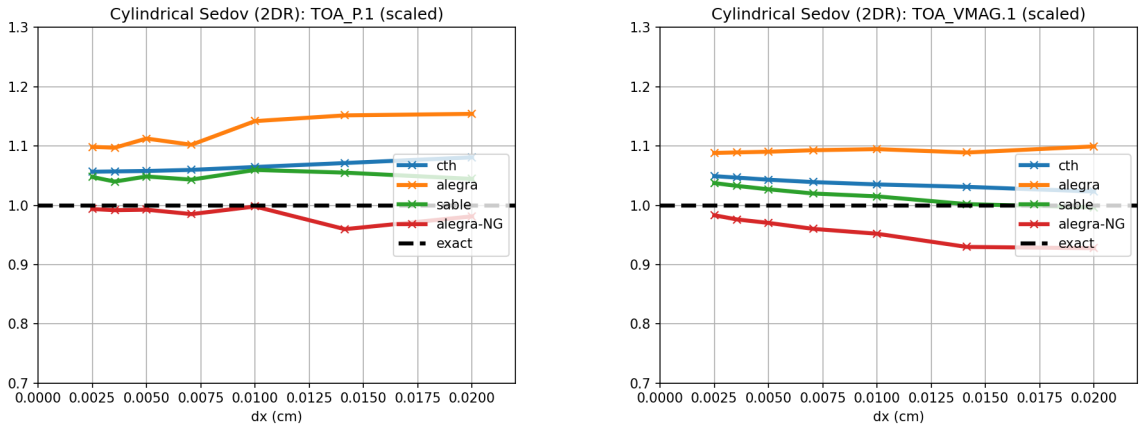

Tracers at 45°

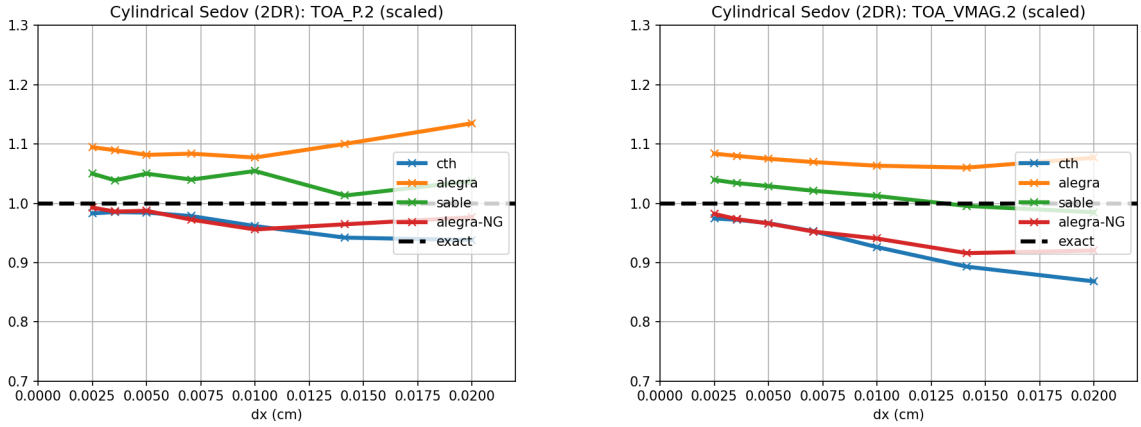

Tracers at 0°

Figure 5-7. Cylindrical Sedov 2DR: convergence of shock TOA at 45 and 0°

Figure 5-11 shows convergence of specific internal energy for each hydrocode. Here the effect of the initial condition approximation using a finite region can be seen by the fact that the energy hits a plateau near the origin for all codes. Alegra has the largest errors on coarse grids in the post-shock region. Alegra-NG again shows the best convergence near the shock.

Figure 5-12 compares pressure solutions at the comparison time. The most serious issue is the significant instability in the CTH result, which is driving the large changes in shock TOA for tracers at different angles. The solutions for Alegra and SABLE exhibit the nearly 10% delay in the shock and lower peak pressure compared to the Alegra-NG solution.

Figure 5-13 compares velocity magnitude solutions at the comparison time. As with the pressure plots, there is a significant instability in the CTH result near the shock. The solutions for CTH, Alegra and SABLE exhibit velocity instabilities near the origin that are not present in the Alegra-NG solution.

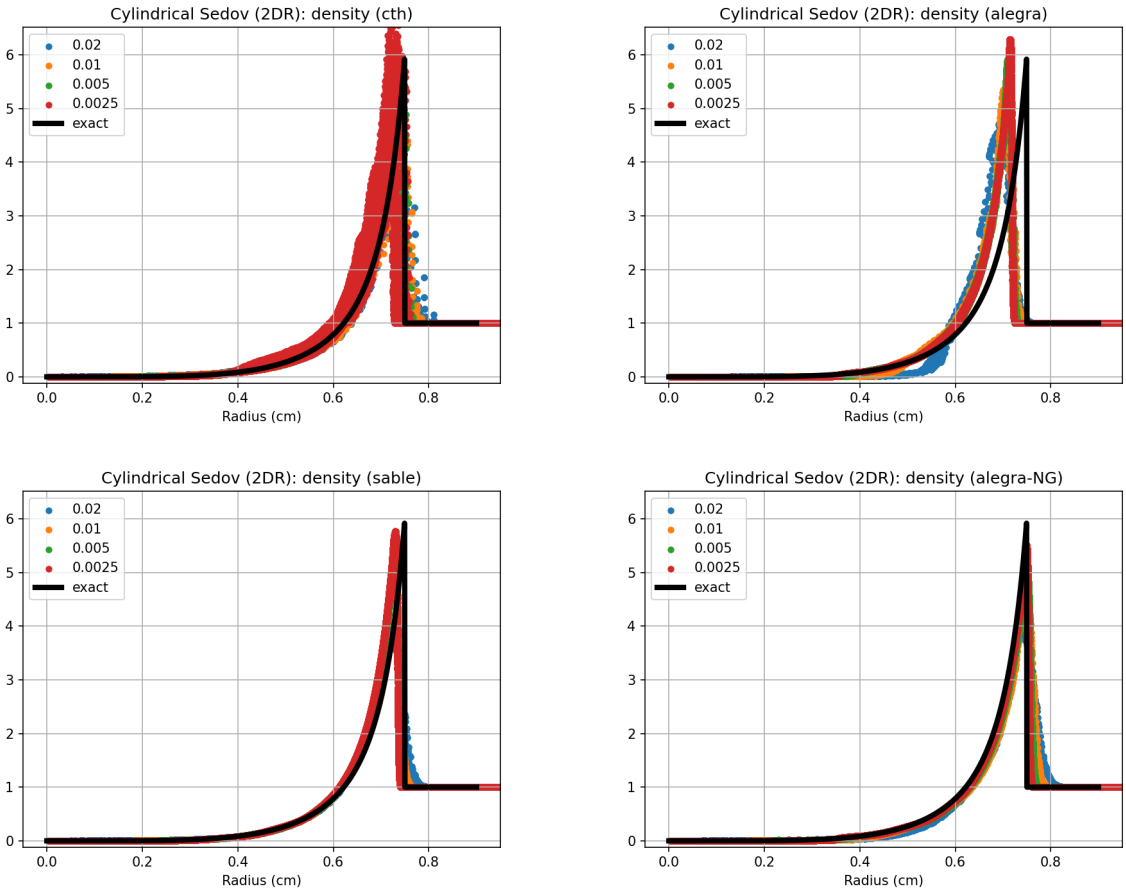

Figure 5-8. Cylindrical Sedov 2DR: convergence of density at final time

5.5. Convergence using error norms

For two studies comparing all four codes such as Cylindrical Sedov and Cylindrical Noh, a comparison is made using global error norms. These norms are computed for each variable, and are computed using the average cell error between the compute solution and the exact solution at the same radial location. Because of the finite size region for the initial condition, the resulting plateau for the internal energy results will cause error norms for this variable to fail to converge. To prevent this, the region of averaging for internal energy is limited to cells with radial location greater than $r = 0.4$, which is more than half the distance to the shock location at $r = 0.75$.

Figure 5-14 provides log-log plots of the global errors as a function of the mesh size along with a dashed line to indicate a first order error rate. The best convergence is shown to be from Alegra-NG. CTH begins to converge on the coarser meshes, but the errors eventually flatline. Alegra and SABLE show similar poor convergence at all mesh resolutions. All four codes eventually produce flat error profiles for internal energy, even with the limitations on the integration region for the error norms.

Figure 5-15 provides semi-log plots of the resulting error rates, computed as pairwise slopes of

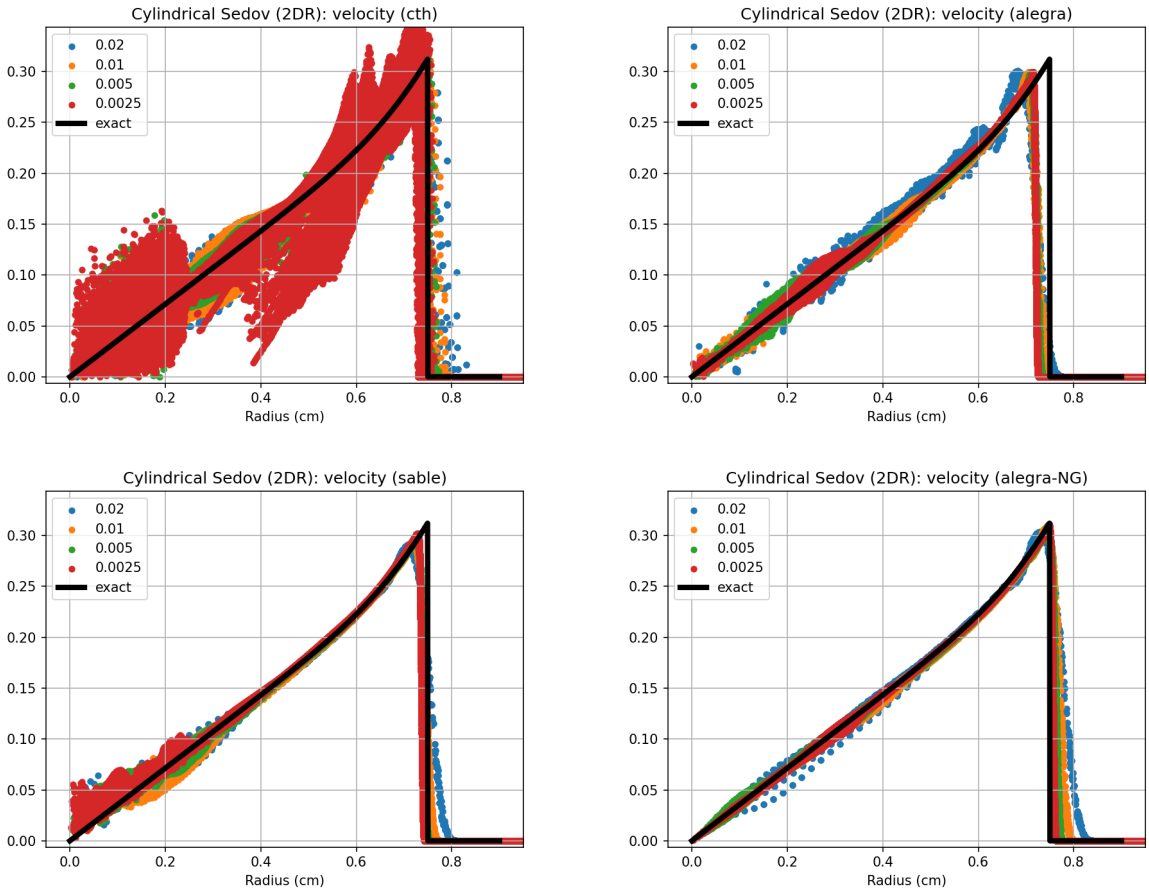

Figure 5-9. Cylindrical Sedov 2DR: convergence of velocity at final time

the data in the log-log error plots in Figure 5-14. The dashed line indicates the formal convergence rate of one. While there is significant noise - especially for internal energy, again the only convergence is shown to be from Alegra-NG with rates approaching one from below. CTH exhibits some positive convergence rates on coarser meshes, but the rates for CTH, Alegra, and SABLE are all nearly zero on the finest three meshes, indicating a lack of convergence to the exact solution.

These plots support the hypothesis that the finite source region for the initial condition is not the reason for lack of convergence of CTH, Alegra and SABLE. This is because the convergence of Alegra-NG is still observed over the range of mesh sizes tested (with the exception of internal energy in the post-shock region). Further studies at finer mesh resolution would be expected to eventually reveal degradation of the convergence rates of Alegra-NG because of the finite source region approximation.

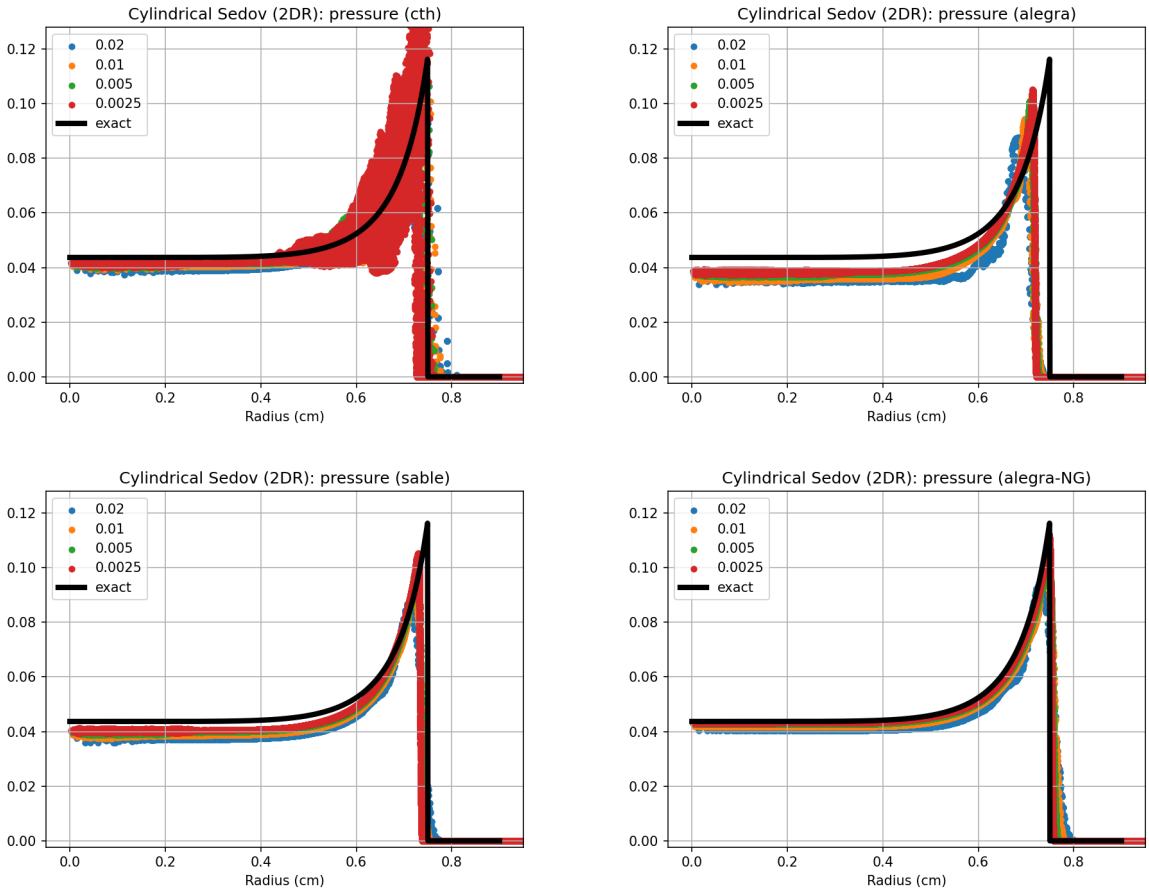

Figure 5-10. Cylindrical Sedov 2DR: convergence of pressure at final time

5.6. Conclusions

The inclusion of Alegra-NG provides an example of a code that conserves total energy. This also produces much more accurate shock TOA, with values converging to nearly the expected values. The symmetry of the solutions is also quite good, with no major defects visible.

Energy losses at the comparison time are about 20% for SABLE and Alegra, and 10% for CTH. Shock TOA is delayed for Alegra and SABLE by about 10%. For CTH, shock TOA is delayed 5% for 45° tracers and accelerated slightly for 0 and 90° tracers because of the significant asymmetry in the pressure and velocity in the shock region, arising from a numerical instability.

As with the Spherical Sedov 2DC case in Section 4.4, CTH, Alegra and SABLE have large velocity oscillations near the origin. Alegra-NG shows the best convergence to the exact solution, except for internal energy near the origin, which all codes incorrectly resolve because of the initial condition approximation as a finite region.

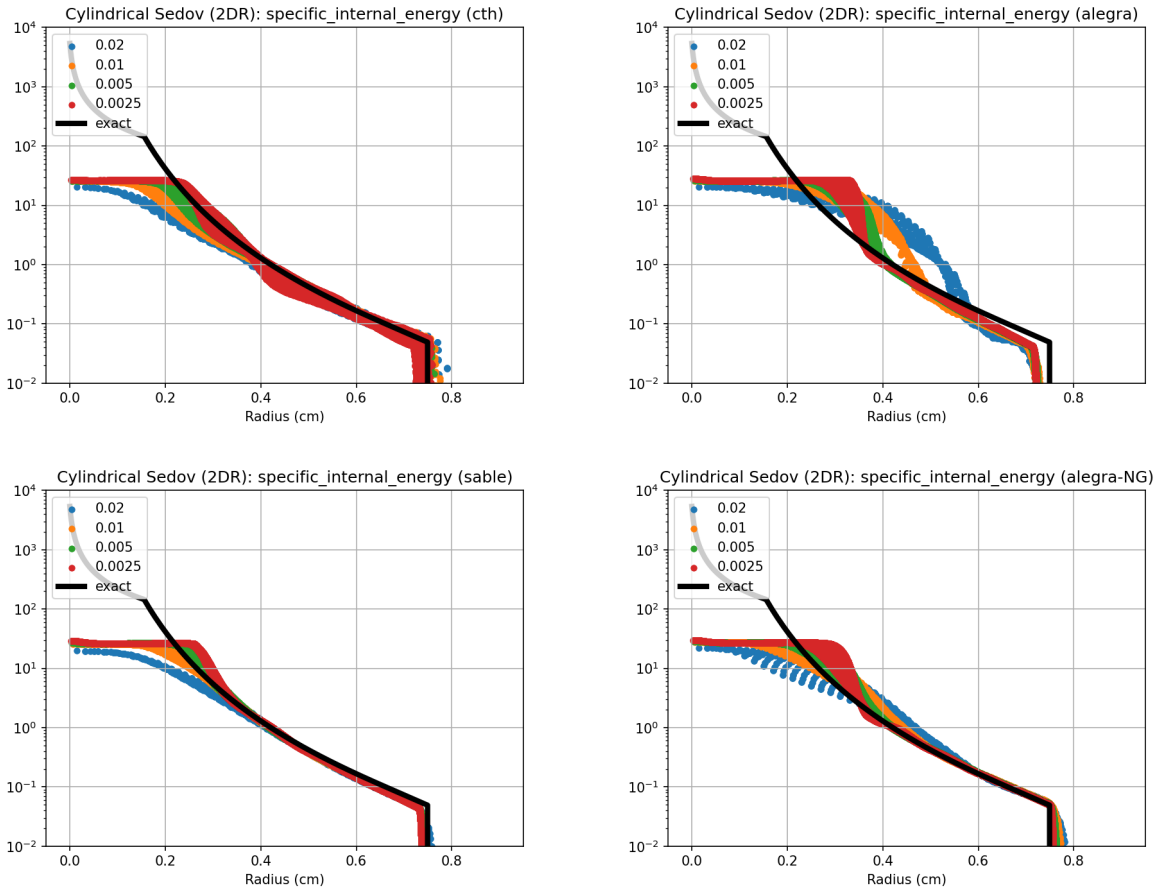

Figure 5-11. Cylindrical Sedov 2DR: convergence of specific internal energy at final time

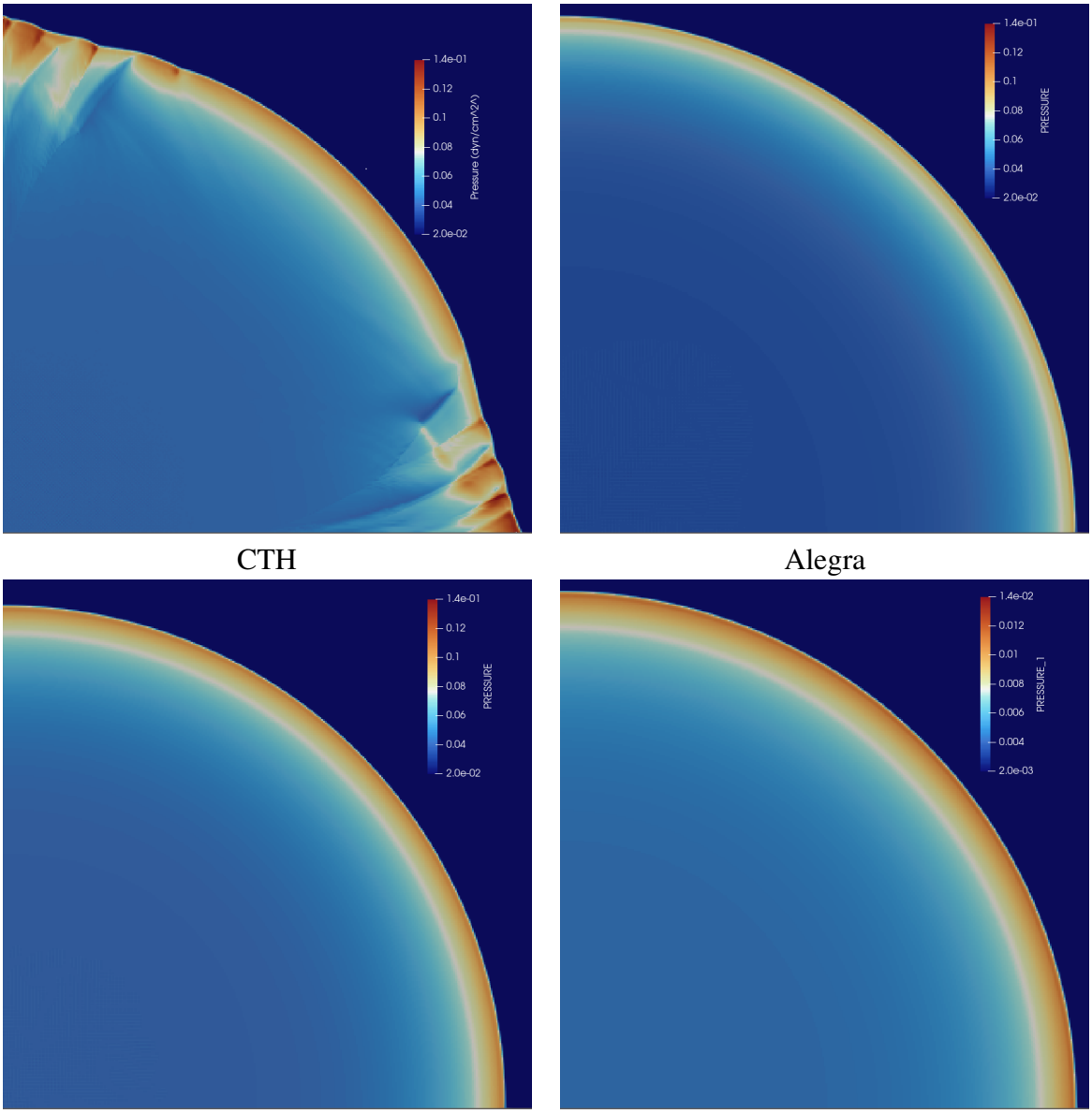

CTH Alegra

SABLE Alegra-NG

Figure 5-12. Cylindrical Sedov 2DR: pressure solutions at final time

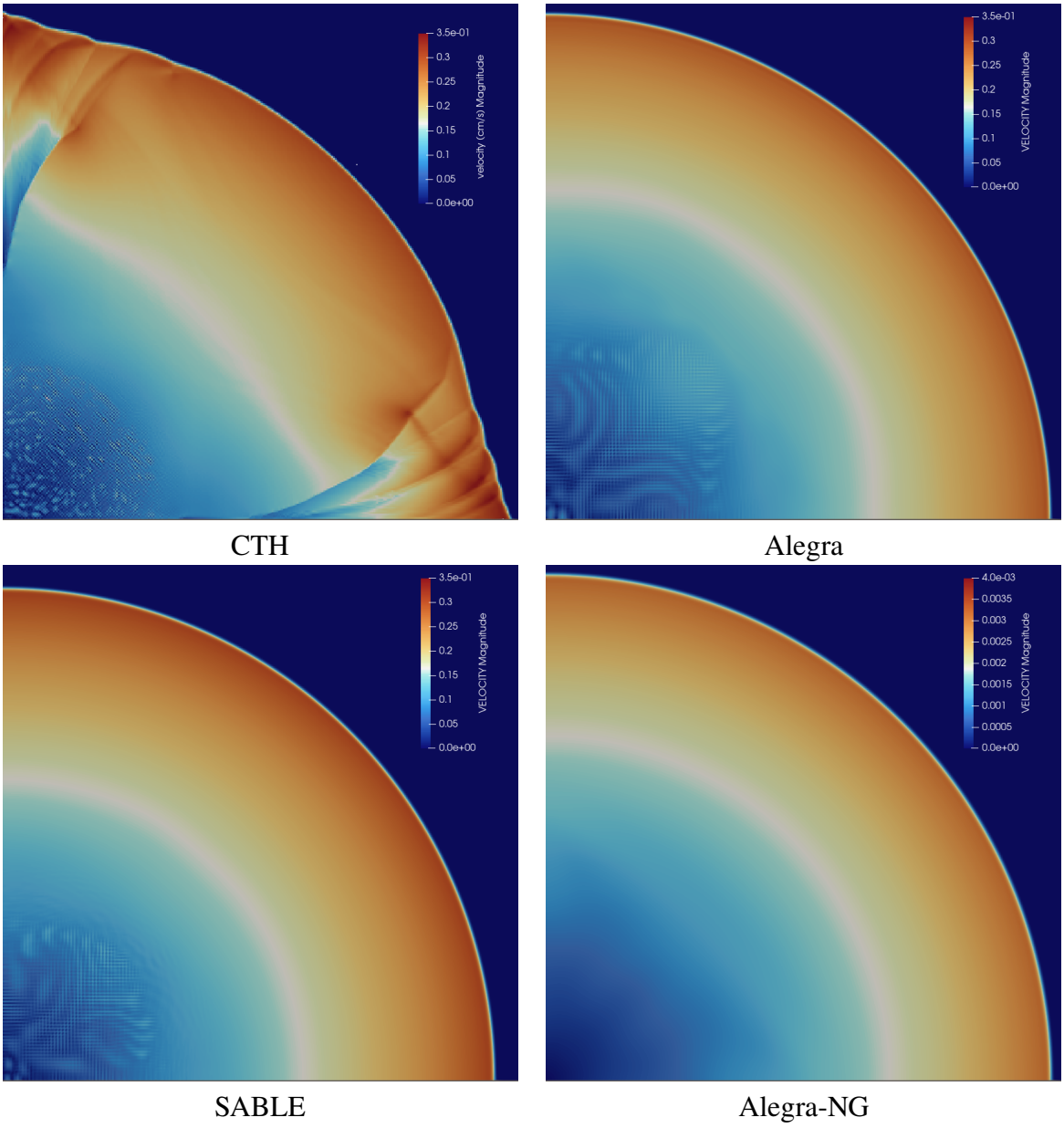

Figure 5-13. Cylindrical Sedov 2DR: velocity magnitude solutions at final time

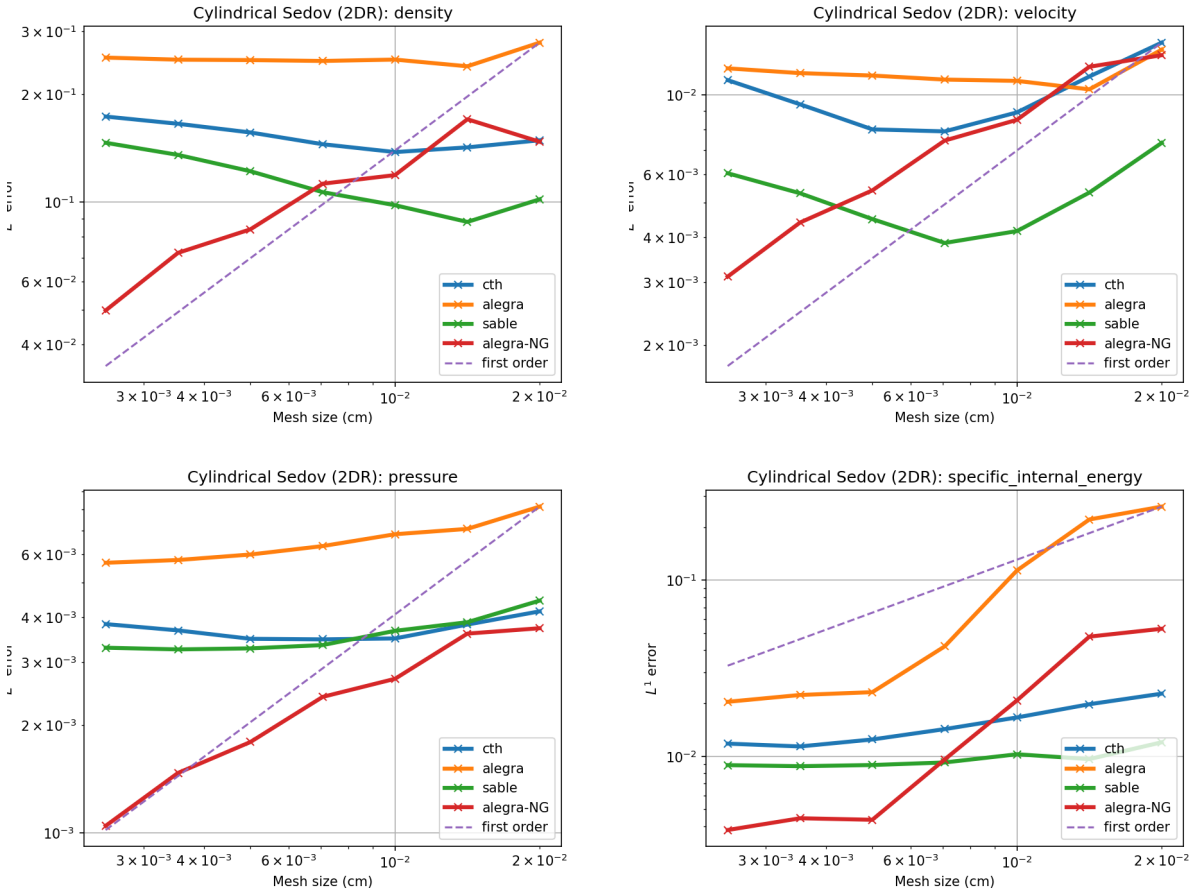

Figure 5-14. Cylindrical Sedov 2DR: error norms

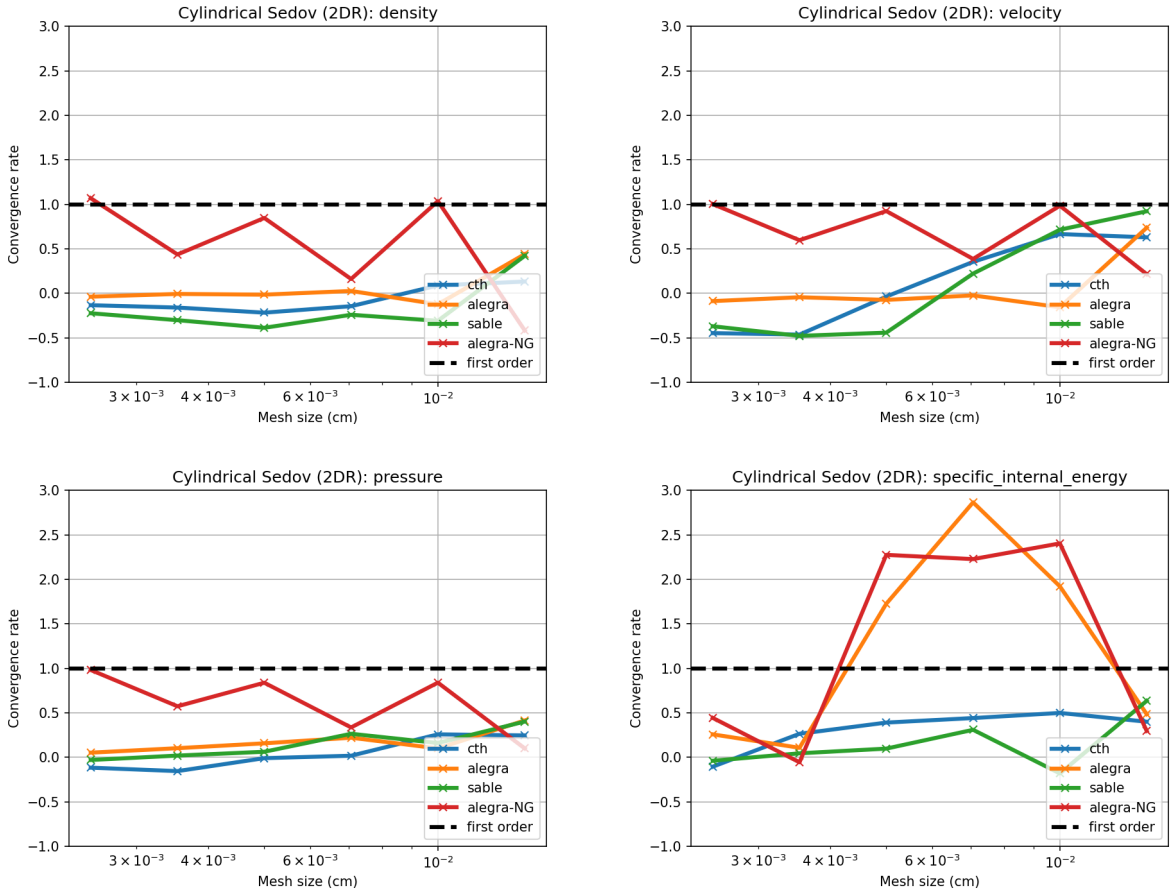

Figure 5-15. Cylindrical Sedov 2DR: convergence rates

6. CYLINDRICAL NOH PROBLEM: 2DR RESULTS USING MULTIPLE CODES

The final benchmark problem considered in this report is the Noh problem. As in the previous chapter, in order to be able to compare all of the codes of interest, the cylindrical version of the Noh problem is used. The simulations are all run using 2D rectangular coordinates, using quarter symmetry, and in Eulerian mode (Lagrangian plus remap back to the original mesh).

The computational domain is defined as the rectangle $[0, L]^2$, where $L = 1.2$ is large enough to include the solution at the comparison time of $t = 0.6$. Symmetry boundary conditions are applied to all four boundaries and the final time of the simulations is $t = 0.8$.

6.1. Conservation

Total energy and mass for were computed for a circular region initially of radius $r = 1$, using a separate material. The remaining material in the larger box was defined to be identical to the material in the inner circle. All energy and mass calculations in this chapter are computed with respect to the material that is originally located within the inner circular region, ignoring the material outside this region. Energy and mass conservation within the circular region could not be assessed for Alegra-NG code because material-specific energy and mass tallies are not available from the code's output.

Figure 6-1 compares the time evolution of total energy for all codes and mesh sizes except Alegra-NG. As with Sedov problem, each code loses energy. However the energy losses at the comparison time are much less than for Sedov, ranging from 2-3% for CTH and Alegra, and 4-6% for SABLE. The extent of energy losses is expected to be very problem-dependent. The energy losses occur gradually, at an increasing rate for later times. The increases in energy at the latest times are when the far field boundary condition is interfering with the shock; these could be removed by increasing the size of the domain boundary.

6.2. Tracers and shock TOA

The models are instrumented with a single Eulerian tracer at a radial location of $r = 1$ and angular position of 45°. Figure 6-2 shows the convergence history of pressure at this location for three of the hydrocodes along with a solid black line indicating the time history of the exact solution. The shock arrives about 3% late for CTH and Alegra, and 8% late for SABLE, but in all cases the shock appears to be converging. However, there are post-shock oscillations (Gibbs phenomena) in

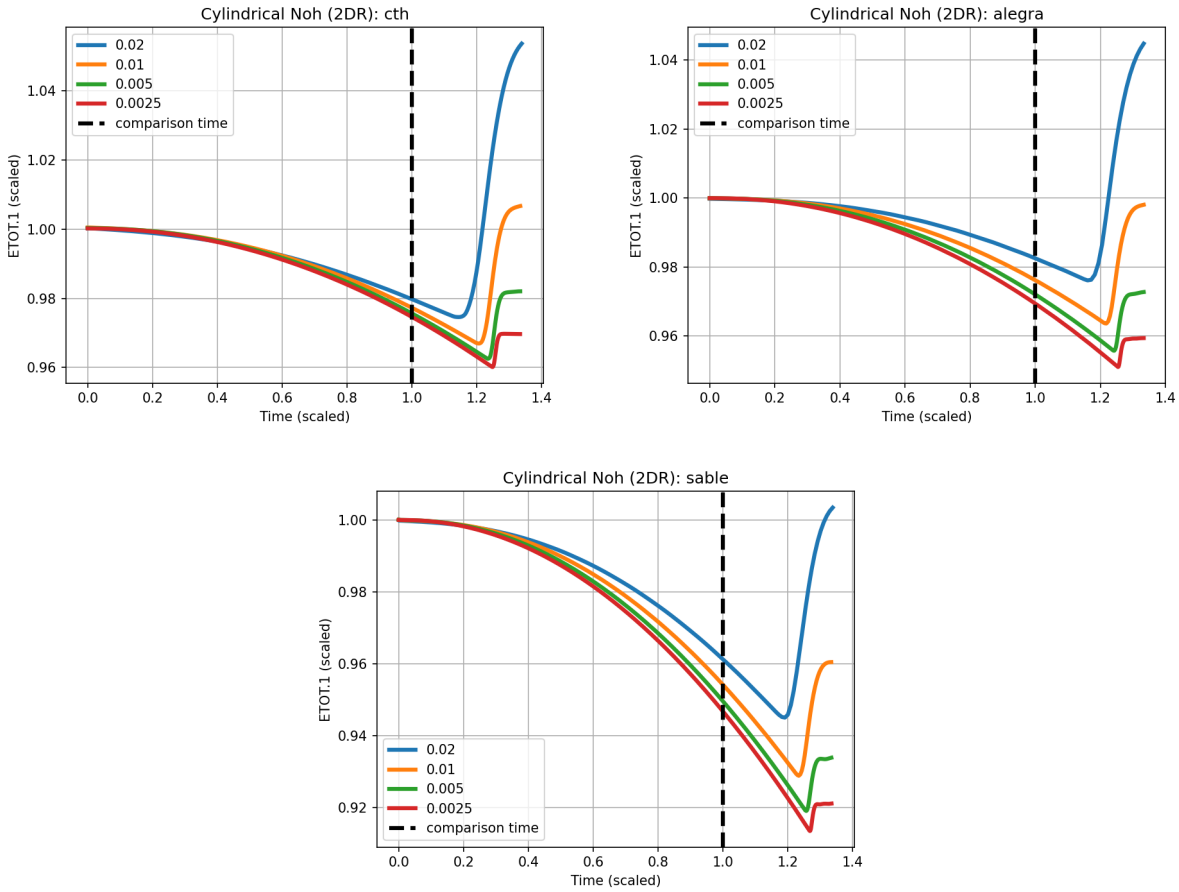

Figure 6-1. Cylindrical Noh 2DR: convergence of total energy

all cases that are not being resolved under mesh refinement, but are instead increasing in frequency. Alegra and SABLE also show increase in peak oscillation with mesh refinement.

6.3. Mesh convergence of energy and shock TOA

Figure 6-3 shows the mesh convergence of mass and energy within the inner material at comparison time. For CTH and Alegra the total energy converges to about 97% of the exact value; for SABLE to about 94%. Unlike Sedov, in this case CTH has larger values of mass than expected in the inner material using this two material formulation of Noh, which do converge under mesh refinement.

Figure 6-4 compares convergence of TOA for pressure and specific internal energy. In all cases, the values are converging to a result later than the exact solution. The largest error is 10% for SABLE, with errors about 3-4% for CTH and Alegra.

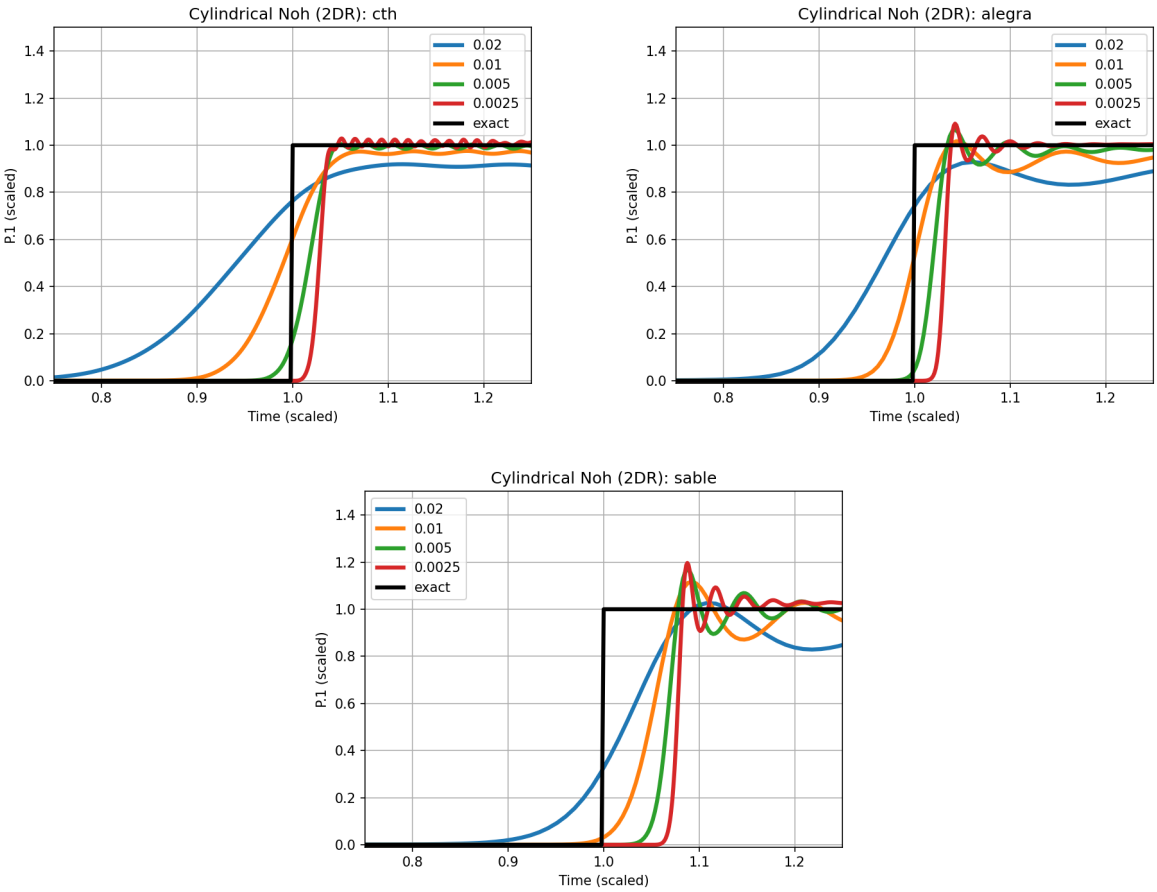

Figure 6-2. Cylindrical Noh 2DR: convergence of pressure tracer histories at 45°

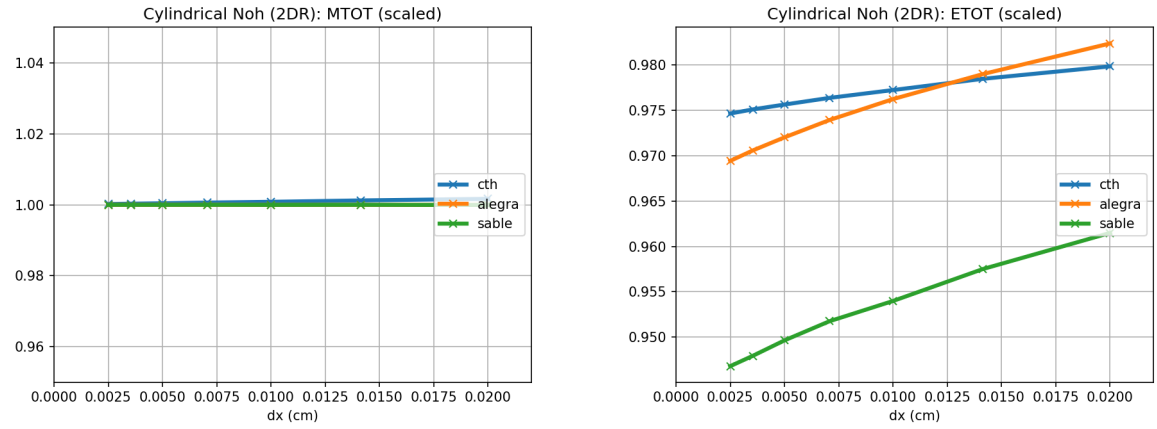

Figure 6-3. Cylindrical Noh 2DR: convergence of mass and energy at final time

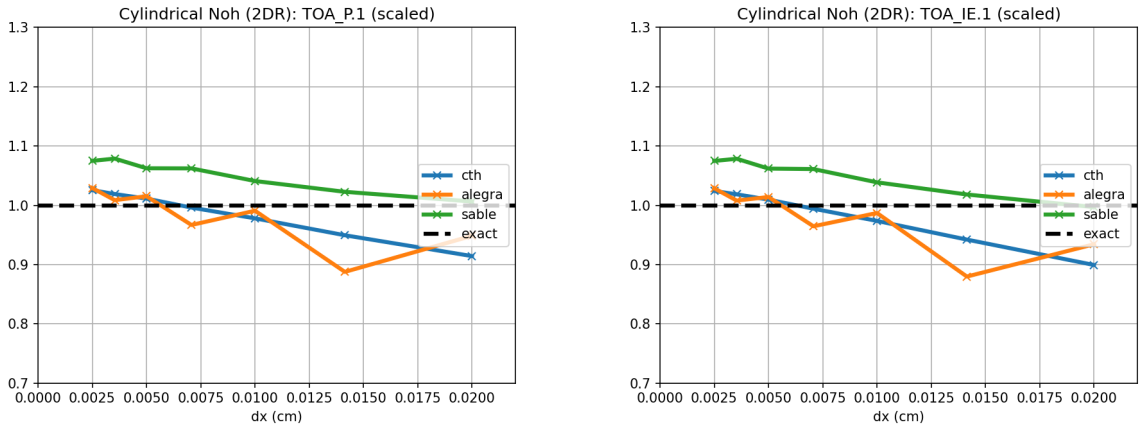

Figure 6-4. Cylindrical Noh 2DR: convergence of shock TOA at 45°

6.4. Solution fields

The final comparisons are scatter plots using the solution fields as a function of the radial coordinate at the comparison time of $t = 0.6$. The exact solutions were computed using the ExactPack [16] Python library and are plotted in black.

Figure 6-5 shows convergence of density for each hydrocode. All codes exhibit the numerical artifact known as "excessive wall heating" for density, where the values near the origin drop off precipitously rather than maintain a constant post-shock state. SABLE has the largest overshoot in post-shock density with a spike just behind the shock. Alegra-NG and CTH converge closest to the exact solution.

Figure 6-6 shows convergence of velocity magnitude for each hydrocode. SABLE exhibits the largest error in the shock location, with the other codes converging closer to the correct shock location. Some velocity oscillation is seen near the origin in all codes, with the largest magnitude observed for CTH.

Figure 6-7 shows convergence of pressure for each hydrocode. All codes exhibit pressure oscillations in the post-shock region. Pressure spikes are visible just behind the shock for Alegra and SABLE.

Figure 6-8 shows convergence of specific internal energy for each hydrocode. The "excessive wall heating" artifact impacts the energy, resulting in non-physical increases near the origin for all codes. SABLE has the lowest post-shock energy state, followed by CTH and Alegra. The best post-shock state for energy is seen in the results from Alegra-NG.

The final plots are surface plots of pressure at comparison time in Figure 6-9. Here the values are scaled near the range of the post-shock pressure to emphasize any oscillations that occur in the solution fields. The problems that were seen in Sedov for CTH are not present in the Noh results. All of the codes exhibit some amount of pressure oscillation; the largest oscillations occur in the SABLE results and are aligned with the mesh.

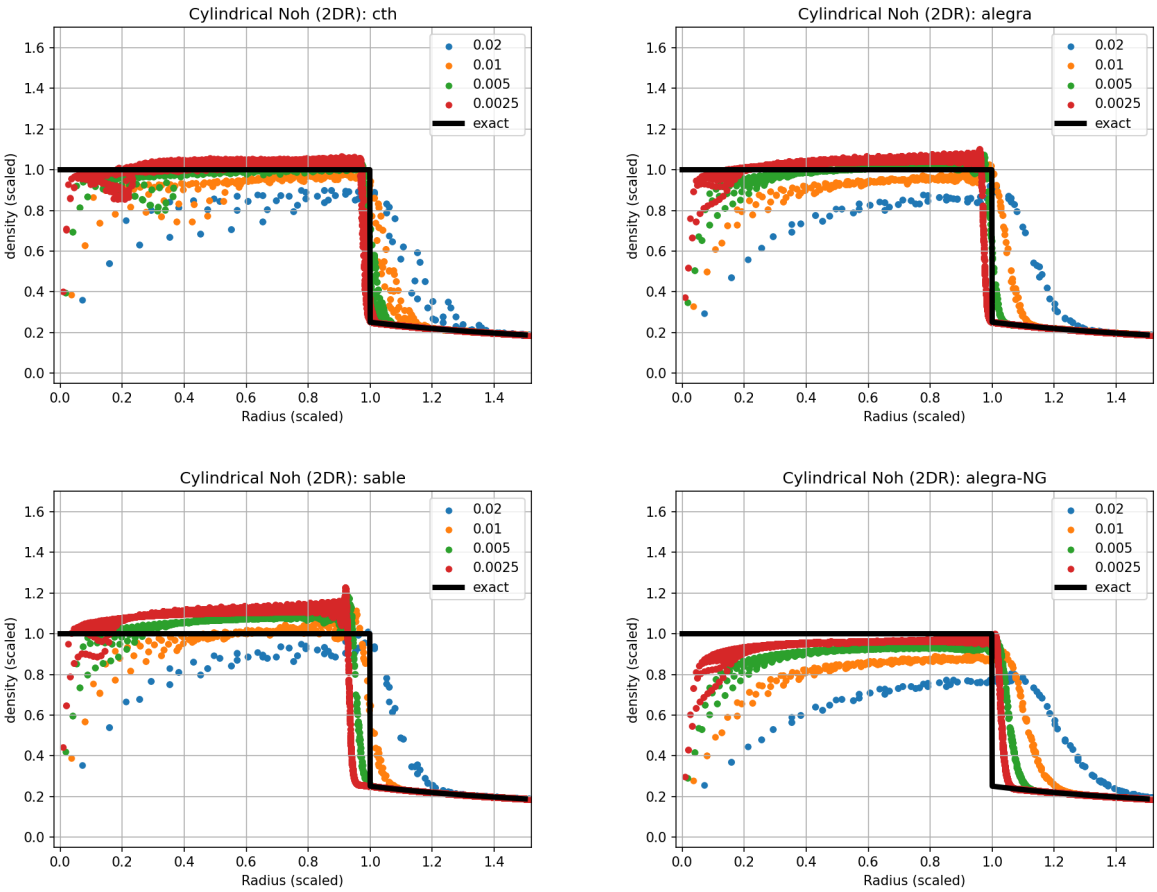

Figure 6-5. Cylindrical Noh 2DR: convergence of density at final time

6.5. Convergence using error norms

Since this study compares all four codes, a comparison is made using global error norms. These norms are computed for each variable, and are computed using the average cell error between the compute solution and the exact solution at the same radial location. Because of the errors in front of the shock because of the incorrect far field boundary condition, the region of averaging for all variables is limited to cells with radial location less than $r = 0.24$ (120% of the shock location at $r = 0.2$). Figure 6-10 provides log-log plots of the global errors as a function of the mesh size along with a dashed line to indicate a first order error rate. The best convergence is shown to be from Alegra-NG, followed by CTH and Alegra, and finally by SABLE. The wall heating effect is not driving the lack of convergence, since the error slopes are not flattening for Alegra-NG at the resolutions used.

Figure 6-11 provides semi-log plots of the resulting error rates, computed as pairwise slopes of the data in the log-log error plots in Figure 6-10. The dashed line indicates the formal convergence rate of one. The best convergence is shown to be from Alegra-NG with rates approaching one. All codes exhibit some positive convergence rates on coarser meshes, but the rates for CTH, Alegra, and SABLE eventually go negative on the finest three meshes, where errors

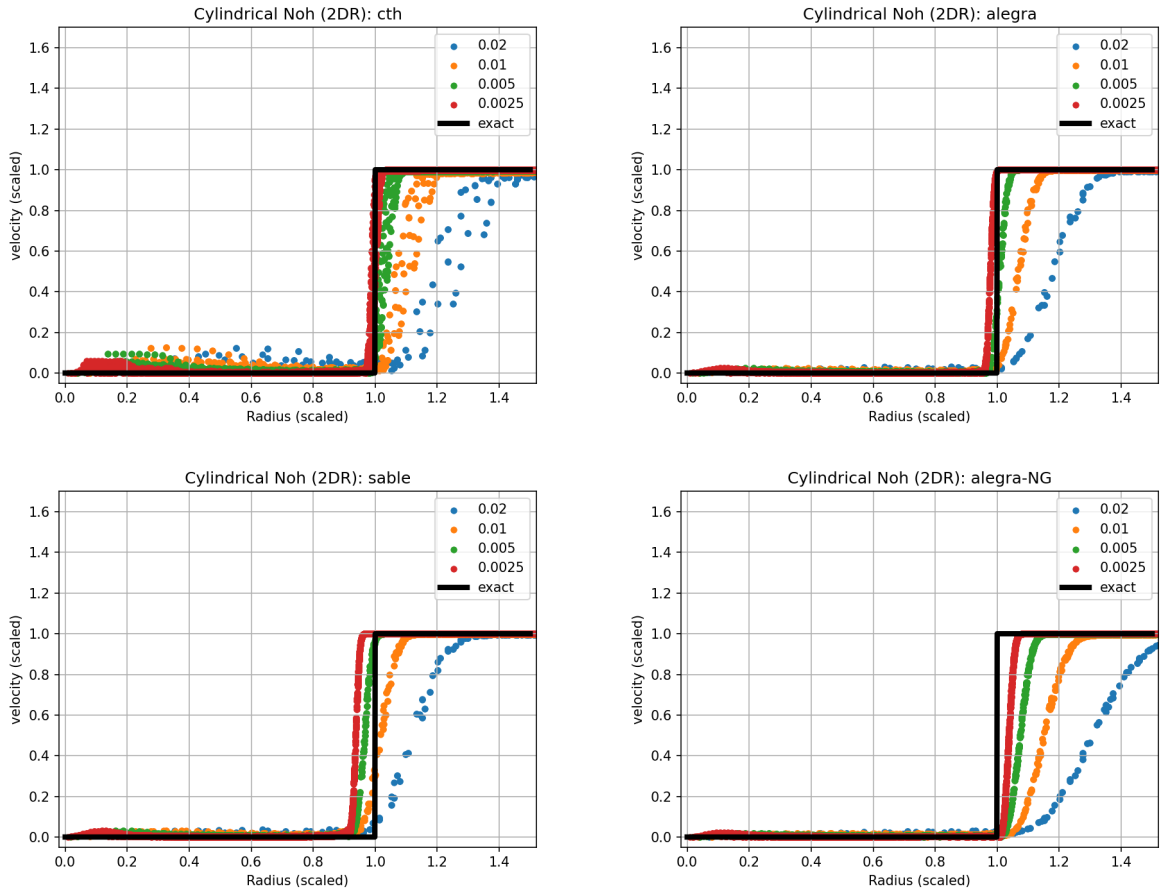

Figure 6-6. Cylindrical Noh 2DR: convergence of velocity at final time

are *increasing* with mesh refinement. The one exception is velocity for CTH, which maintains a convergence rate greater than one.

6.6. Conclusions

The strategy to assess conservation for Noh could not be implemented for Alegra-NG. An alternate approach that was not tested would be to compute material-specific energies from the output files using a tool such as ParaView. For the remaining codes, energy losses were much less than for Sedov, with about 2.5% for CTH, 3% for Alegra, and 4% for SABLE. Convergence of shock TOA for the same code indicated delays of 10% for SABLE and 5% for CTH and Alegra.

The issues with significant asymmetry and instability for CTH running Sedov are not present for Noh. All codes exhibit some issues with symmetry for Noh, with the largest pressure asymmetry seen in the SABLE results.

Unfortunately, all four codes exhibit the numerical artifact of "excessive wall heating" near the origin, where density is very low and specific internal energy is very high.

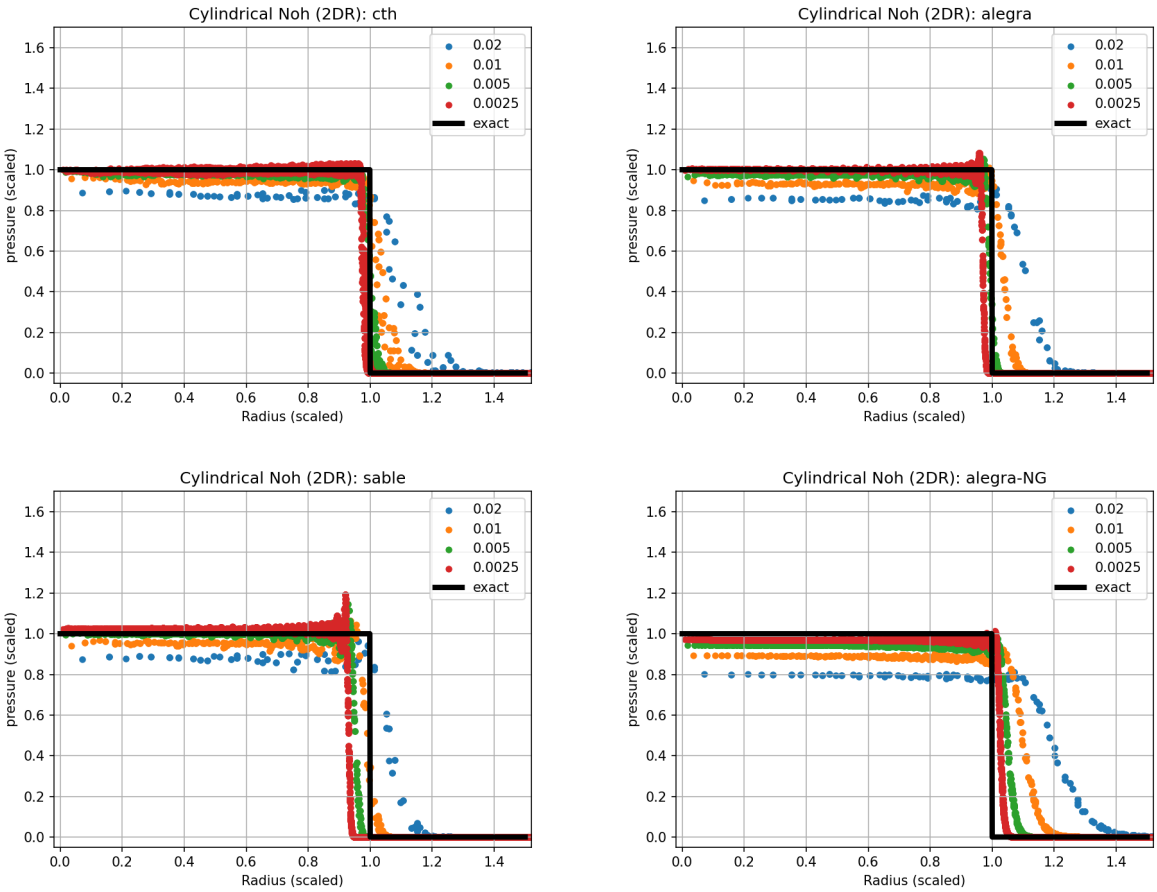

Figure 6-7. Cylindrical Noh 2DR: convergence of pressure at final time

SABLE has about 10% higher post-shock density and 10% lower post-shock internal energy. CTH and Alegra have about half these values for post-shock states.

Finally, numerical oscillations are still seen in the post-shock state for all codes, but the magnitudes are generally decreasing with mesh size. The exceptions are SABLE and Alegra, which exhibit distinct post-shock spikes in density, pressure, and specific internal energy.

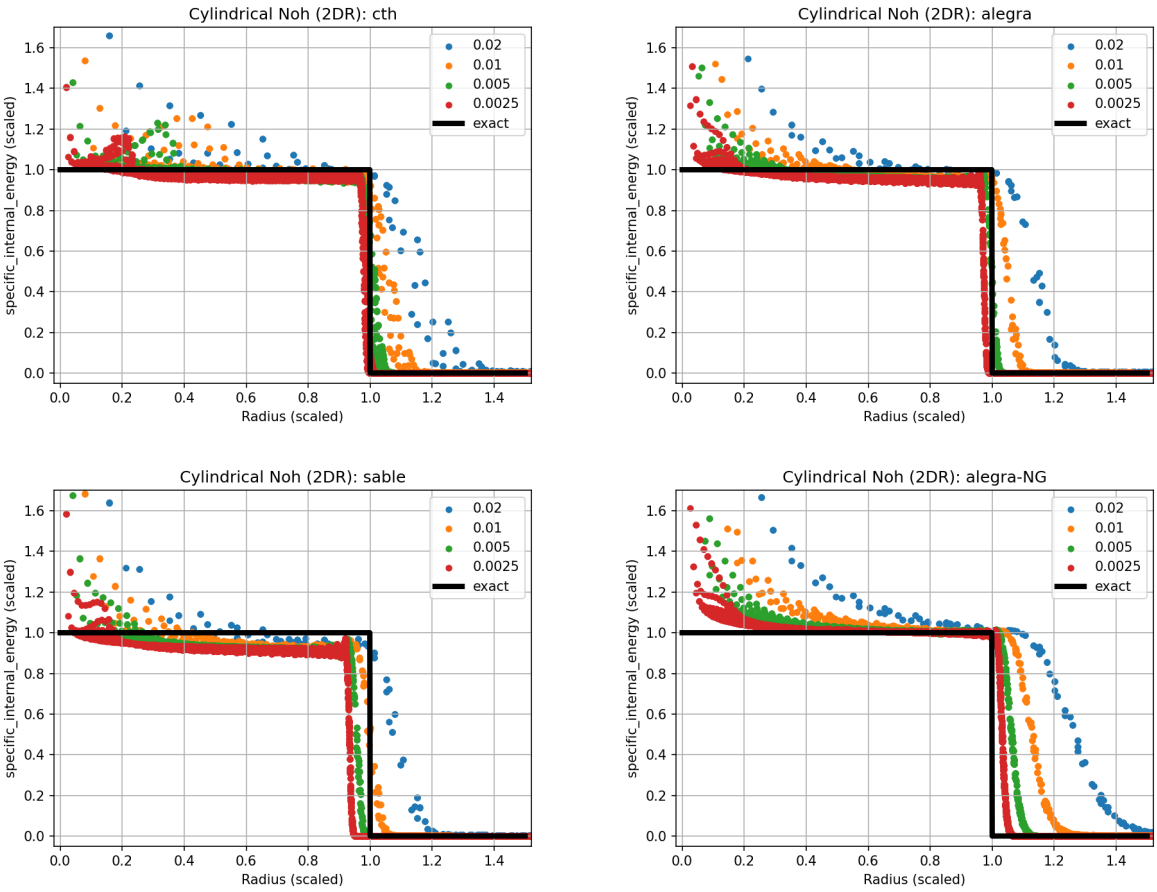

Figure 6-8. Cylindrical Noh 2DR: convergence of specific internal energy at final time

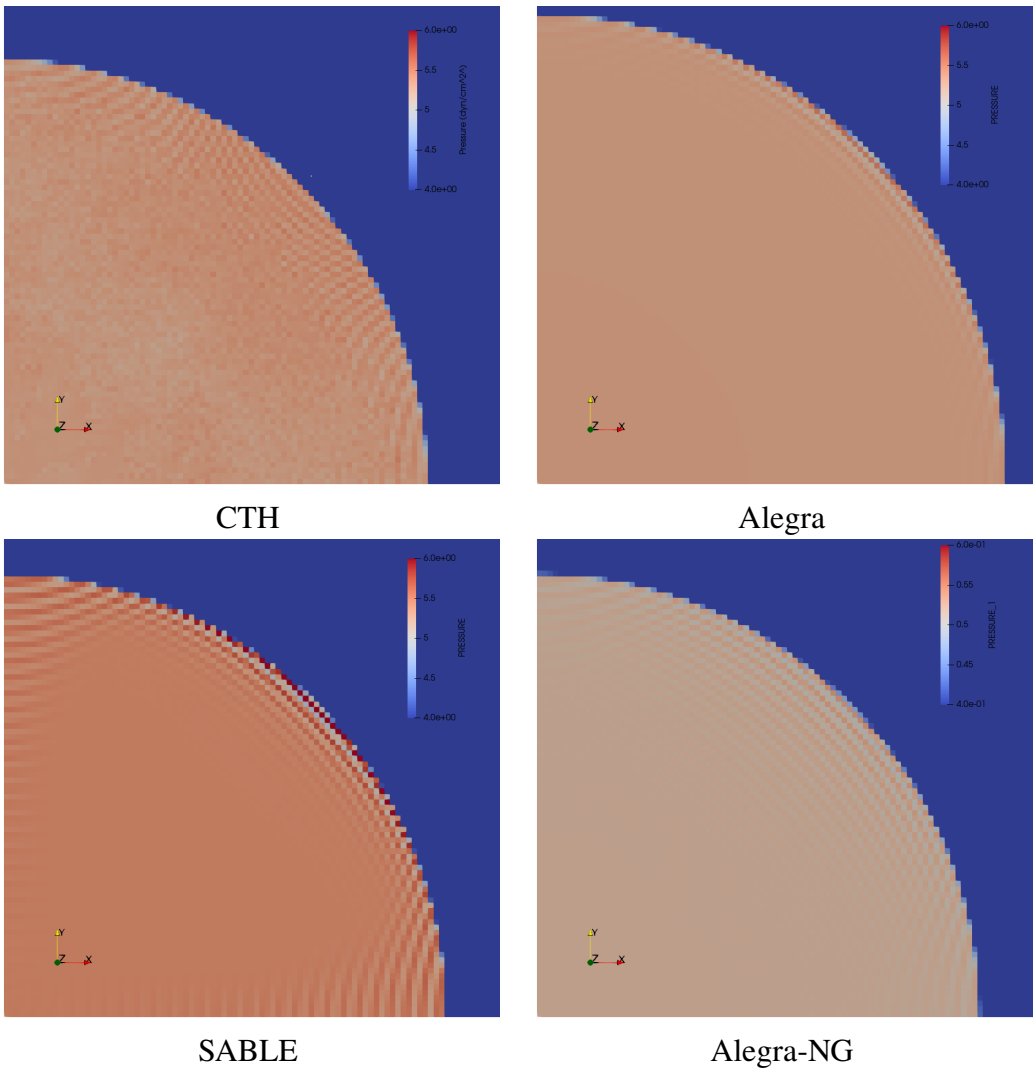

Figure 6-9. Cylindrical Noh 2DR: pressure solutions at final time

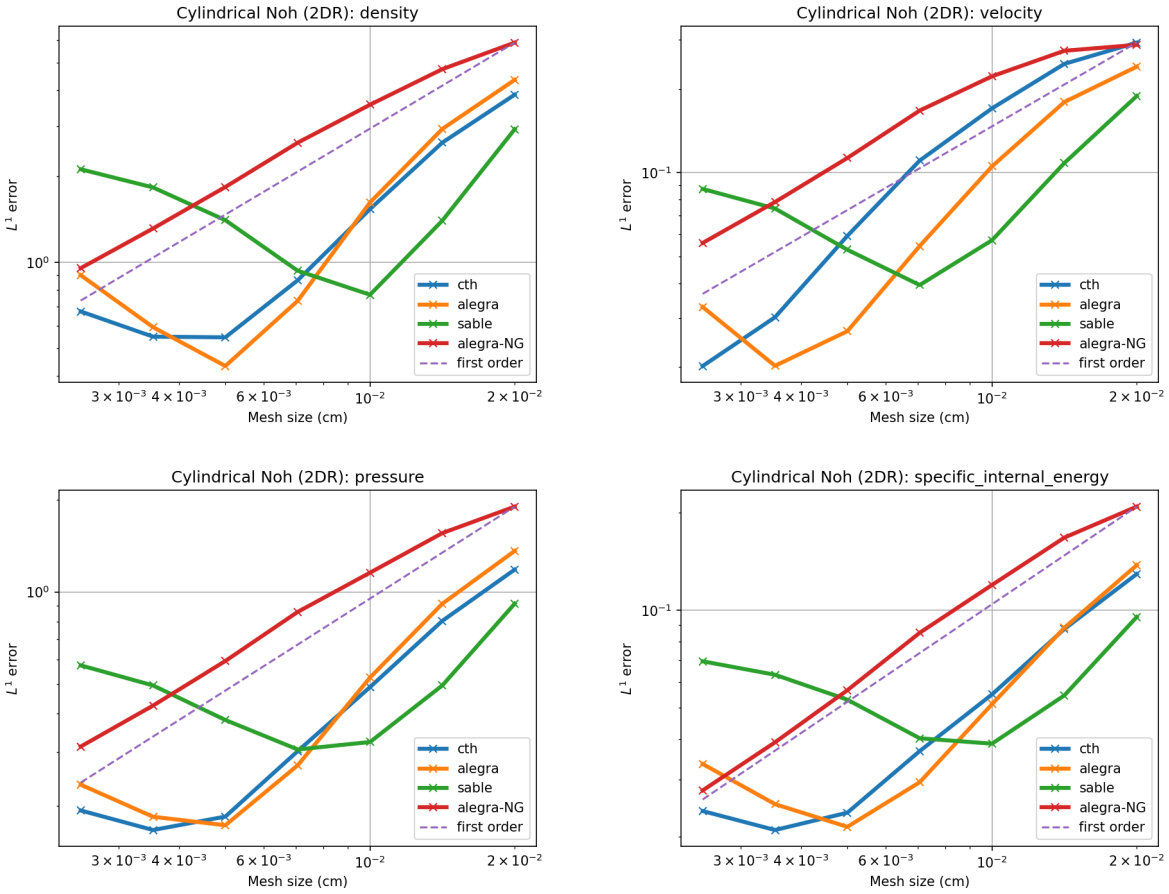

Figure 6-10. Cylindrical Noh 2DR: error norms

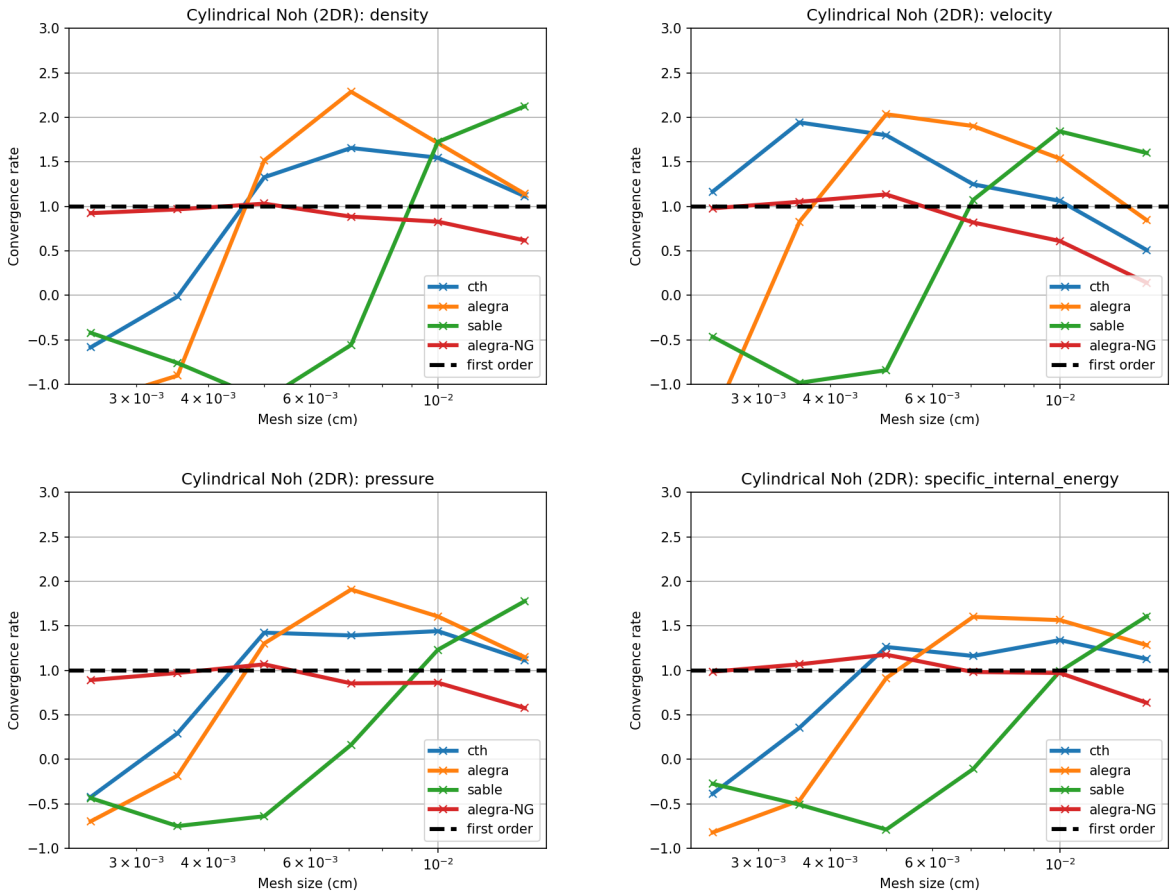

Figure 6-11. Cylindrical Noh 2DR: convergence rates

This page intentionally left blank.

7. CONCLUSION

A number of issues are summarized here that warrant improvement in each of the codes.

The most serious issue is the lack of conservation of total energy in three of the four codes when run using Eulerian methods and typical user options that are representative of how analysts use the codes in practice. Figure 7-1 shows scatter plots of total energy at comparison time versus shock TOA for both Sedov and Noh (2DR cylindrical cases using the finest mesh resolution). There is roughly a linear correlation between the two. Mesh refinement is shown to improve conservation in some cases, but energy still converges to a lower value.

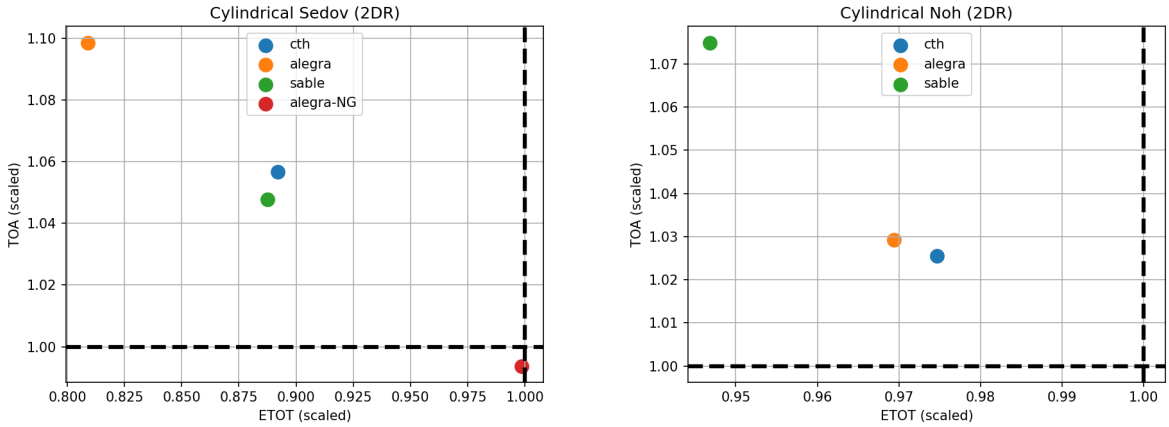

Figure 7-1. Cylindrical Sedov and Noh: scatter plot of total energy versus shock TOA

Another major issue is the "excessive wall heating" effect for Noh that is clearly visible for all four codes in density and internal energy (see Figures 6-5 and 6-8). The high temperatures and low densities near the origin could result in loss of mass and energy in problems with material discards activated. The post shock state for Noh is incorrect for several codes and may be affected by the wall heating.

Finally, the instability in the CTH results for Sedov (see Figure 2-5), with coordinate-aligned large spurious shocks behind the main shock and significant asymmetry for both 2DC and 2DR is concerning.

Additional issues in order of severity include:

- velocity oscillations near the origin for CTH, Alegra, and SABLE (mainly Sedov but also Noh);

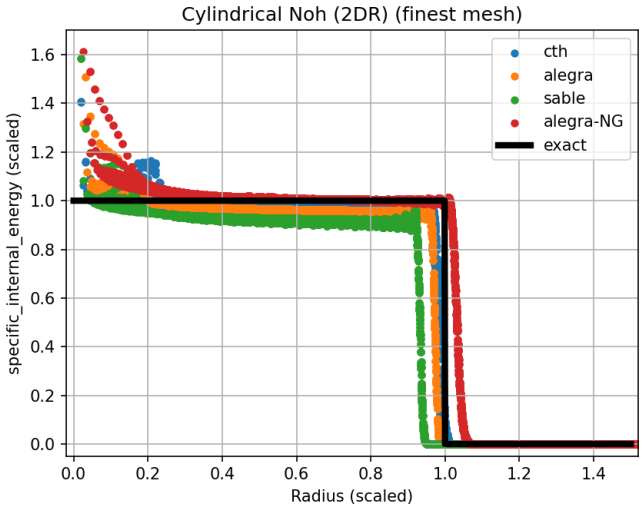

Figure 7-2. Cylindrical Noh 2DR: wall heating effect on specific internal energy

- errors in post-shock density and velocity for CTH, Alegra, and SABLE on Sedov; and
- post-shock overshoots and oscillations for SABLE and Alegra on Noh.

The author recommends future studies to identify the effect of energy conservation on mission relevant problems and to prioritize needed code improvements.

8. APPENDIX: SPHERICAL SEDOV INPUT FILES

8.1. CTH Spherical Sedov 1DS

```
*CTHid SPYPLT SPYHIS
*
*************************************************************************
*eor* cthin
*************************************************************************
*
Sedov Point Explosion Problem
*
*************************************************************************
*
*0.1
*2
*0.03
control
  mmp0
  tstop = 1.2
  VISCOSITY BL = 0.1 BQ = 2 BS = 0.03
endcontrol
*
*
mesh
  block 1 geom=1ds type=e
    x0 0.0
      x1 dxf=0.01 dxl=0.01 w=1.2
    endx
  endb
endmesh
*
*
*
spy
  Save("VOLM,P,M,PM,IE,VMAG,DENS,ARTV");
  SaveTime(0,0.1);

  SaveHis("DISCARD,GLOBAL,P,DENS,IE,T,VX,VMAG");
```

```
  SaveTracer(ALL);
  HisCycle(0,1);
endspy
*
*
*
* 8510.72
* * using fixed src, energy region radius = 0.02
** 3.351032164e-05
diatoms
  package 'Energetic Zone'
    material 1
    iter = 5
    lilvf = 0.5
    pwdiom = 1
    dens = 1.0
    t = 253973092
    insert box
      p1 0. p2 0.02
    endinsert
  endpackage
  package 'Ambient Air'
    material 1
    iter = 5
    lilvf = 0.5
    pwdiom = 1
    dens = 1.0
    t = 2.54e-4
    insert box
      p1 0. p2 1e3
    endinsert
  endpackage
enddiatoms
*
*
*
tracer
  add 1 fix=x
endt
*
*
*
eos
  mat1 idgas user gm1=0.4 cv=1.0e-4
endeos
```

```
*
*
*
convct
  convection = 0
  interface = smyra
endc
*
*
*
edit
  shortt
    tim = 0.0 , dt = 1.0
  ends
  longt
    tim = 0.0 , dt = 1.0
  endl
  plott
    tim = 0.0 , dt = 10e-3
  endp
ende
*
*
*
boundary
  bhy
    bxb = 0 , bxt = 0
  endh
endb
************************************************
```

8.2. CTH Spherical Sedov 2DC

```
*CTHid SPYPLT SPYHIS
*
*******************************************************************************
*eor* cthin
*******************************************************************************
*
Sedov Point Explosion Problem
*
*******************************************************************************
*
```

```
*0.1
*2
*0.03
control
  mmp0
  tstop = 1.3
  VISCOSITY BL = 0.1 BQ = 2 BS = 0.03
endcontrol
*
*
mesh
  block 1 geom=2dc type=e
    x0 0.0
      x1 dxf=0.01 dxl=0.01 w=1.2
    endx
    y0 0.0
      y1 dyf=0.01 dyl=0.01 w=1.2
    endy
  endb
endmesh
*
*
*
spy
  Save("VOLM,P,M,PM,IE,VMAG,DENS,ARTV");
  SaveTime(0,0.1);

  SaveHis("DISCARD,GLOBAL,P,DENS,IE,T,VX,VY,VMAG");
  SaveTracer(ALL);
  HisCycle(0,1);
endspy
*
*
*
* 0.000254
* 8510.72
* * using fixed src, energy region radius = 0.02
** 3.351032164e-05
diatoms
  package 'Energetic Zone'
    material 1
    iter = 5
    lilvf = 0.5
    pwdiom = 1
    dens = 1.0
```

```
    t = 253973092
    insert circle
       center 0 0
       radius 0.02
    endinsert
  endpackage
  package 'Ambient Air'
    material 1
    iter = 5
    lilvf = 0.5
    pwdiom = 1
    dens = 1.0
    t = 0.000254
    insert box
      p1 0. 0. p2 1e3 1e3
    endinsert
  endpackage
enddiatoms
*
*
*
tracer
  add 0.7071067812 0.7071067812 fix=xy
  add 1 0 fix=xy
  add 0 1 fix=xy
endt
*
*
*
eos
  mat1 idgas user gm1=0.4 cv=1.0e-4
endeos
*
*
*
convct
  convection = 0
  interface = smyra
endc
*
*
*
edit
  shortt
    tim = 0.0 , dt = 1.0
```

```
  ends
  longt
    tim = 0.0 , dt = 1.0
  endl
  plott
    tim = 0.0 , dt = 10e-3
  endp
ende
*
*
*
boundary
  bhy
    bxb = 0 , bxt = 0
    byb = 0 , byt = 0
  endh
endb
************************************************
```

8.3. Alegra Spherical Sedov 2DC

```
$ vim: set syntax=alegra:

units, cgs

title: Spherical Sedov in 2D cylindrical coordinates

exact termination time 1.3

solid dynamics

  cylindrical     $ R-Z

  dynamics time integrator, central difference
  end

  domain
  end

$ --- MESH ---
  mesh, inline
    brick
     xmin 0.0
```

```
     ymin 0.0
     numx 1
      xblock 1 1.2 first size 0.01 last size 0.01
     numy 1
      yblock 1 1.2 first size 0.01 last size 0.01
    end

    set assign
      nodeset,ilo,10
      nodeset,ihi,11
      nodeset,jlo,20
      nodeset,jhi,21
      sideset,ilo,10
      sideset,ihi,11
      sideset,jlo,20
      sideset,jhi,21
    end
  end

  no displacement, nodeset 10,r $ R = 0
  no displacement, nodeset 20,z $ Z = 0

  no displacement, nodeset 11,r $
  no displacement, nodeset 21,z $

$ 8510.72
$ $ using fixed src, energy region radius = 0.02
$$ 3.351032164e-05
  diatom
    package source
      material 1
      iter = 5
      pwdiom = 1
      density 1.0
      temperature 253973092
      insert circle
         center 0 0
         radius 0.02
      endinsert
    endp
    package 'Ambient Air'
      material 1
      iter = 5
      pwdiom = 1
      density = 1.0
```

```
      temperature = 2.54e-4
      insert box
        p1 -1e3 -1e3 p2 1e3 1e3
      endinsert
    endpackage
  enddiatom

  block 1
    eulerian mesh
    add diatom input
    material 1
  end

tracer points
  eulerian tracer 1 x 0.7071067812 y  0.7071067812
  eulerian tracer 2 x 1 y 0
  eulerian tracer 3 x 0 y 1
end

end

$$$$$$$$$$$$$$$$$$$$$$$$$$$$$$$$$$$$$$$ EXECUTION CONTROL

emit screen: cycle interval = 200
emit plot: time interval = 0.1
emit hisplt: cycle interval = 1
emit restart: time interval = 0.1
ascii history format

history plot variables
  velocity, magnitude
  pressure, avg
end

Plot variable
  density
  density, avg
  velocity
  temperature
  temperature, avg
  sound speed
  min dt
  mass
  el mass
  pressure
```

```
  pressure, avg
  energy
  energy, avg
end

$$$$$$$$$$$$$$$$$$$$$$$$$$$$$$$$$$$$$$$$ MATERIAL DEFINITION

material 1 gas
  model 10
  density 1.0
  temperature 1.0e-10
end

model 10 ideal gas
  rho ref = 0.0
  tref = 0.0
  cv = 1.0e-4
  gamma = 1.4
end

$$#########################

exit
```

8.4. SABLE Spherical Sedov 2DC

```
SABLE2D
$ control: hack for submit.sh
$-----------------------------------BEGIN_QA-----------------------------------
$ ID:         sedov
$ Title:      Test for remap, structured hydro
$ Category:   Regression
$ Physics:    comprehensive
$ Dimension:  3D
$ Owner:      Mark Christon
$
$ Description:This test problem covers diatoms (dioms), remap and
$             structured hydro
$
$ References:
$
$
```

```
$ Directory:  Benchmarks/Regression/3D/comprehensive
$ Tags:       ?
$ CVS: ?
$-----------------------------------END_QA-----------------------------------

TITLE
  ideal gas sod problem

  units, cgs

  cylindrical

$120
  mesh, inline
    rectilinear
      ncells = 120
      bx =  1
      by =  1
      cellsize = 0.01
      gmin = 0 0
    end
    set assign
      nodeset,ilo,1
      nodeset,jlo,2
    end
  end

  no displacement, nodeset 1, x
  no displacement, nodeset 2, y

$  time step scale 1.0
$  GRADUAL STARTUP FACTOR 1.0

$ 8510.72
$ $ using fixed src, energy region radius = 0.02
$$ 3.351032164e-05
  diatom
    package source
      material 1
      iter = 5
      pwdiom = 1
      density 1.0
      temperature 253973092
      insert circle
         center 0 0
```

```
        radius 0.02
      endi
    endp
    package background
      material 1
      iter = 5
      pwdiom = 1
      density 1.0
      temperature 2.54E-04
      insert box
        p1 -1e3 -1e3 p2 1e3 1e3
      endi
    endp
  enddiatom

  BLOCK 1
    eulerian mesh
    remesh frequency 1
    add diom input
  END

tracer points
  eulerian tracer 1 x 0.7071067812 y  0.7071067812
  eulerian tracer 2 x 1 y 0
  eulerian tracer 3 x 0 y 1
end

termination time 1.3

#
#-------------------------------------------------------------------------
#                           P L O T T I N G
#-------------------------------------------------------------------------
#
EMIT SCREEN,CYCLE INTERVAL = 10

plot,exodus
emit, time interval = 0.1
PLOT VARIABLE
  no material globals
  no underscores
  pressure
  energy
  temperature, as "TEMP"
  velocity
```

```
  velocity,magnitude, as "VMAG"
  density
  density, avg
  pressure, avg
  energy, avg
END
END

plot,history
emit, cycle interval = 1
end

$
$-----------------------------------------------------------------------
$                            M A T E R I A L S
$-----------------------------------------------------------------------
$

MATERIAL 1
  model, IDEAL GAS
    GAMMA 1.4
    RHO REF 0.0
    CV 1.e-4
    TREF 0.
  END
END


EXIT
```

9. APPENDIX: CYLINDRICAL SEDOV 2DR INPUT FILES

9.1. CTH Cylindrical Sedov 2DR

```
*CTHid SPYPLT SPYHIS
*
*********************************************************************
*eor* cthin
*********************************************************************
*
Sedov Point Explosion Problem
*
*********************************************************************
*
*0.1
*2
*0.03
control
  mmp0
  tstop = 1.2
  VISCOSITY BL = 0.1 BQ = 2 BS = 0.03
endcontrol
*
*
mesh
  block 1 geom=2dr type=e
    x0 0.0
      x1 dxf=0.01 dxl=0.01 w=1
    endx
    y0 0.0
      y1 dyf=0.01 dyl=0.01 w=1
    endy
  endb
endmesh
*
*
*
spy
  Save("VOLM,P,M,PM,IE,VMAG,DENS");
```

```
  SaveTime(0,0.1);

  SaveHis("DISCARD,GLOBAL,P,DENS,IE,T,VX,VY,VMAG");
  SaveTracer(ALL);
  HisCycle(0,1);
endspy
*
*
*
*3113.57
*0.001256637061
diatoms
  package 'Energetic Zone'
    material 1
    iter = 5
    lilvf = 0.5
    pwdiom = 1
    dens = 1.0
    t = 2477700.281
    insert circle
       center 0 0
       radius 0.02
    endinsert
  endpackage
  package 'Ambient Air'
    material 1
    iter = 5
    lilvf = 0.5
    pwdiom = 1
    dens = 1.0
    t = 2.54e-4
    insert box
      p1 -1e3 -1e3 p2 1e3 1e3
    endinsert
  endpackage
enddiatoms
*
*
*
tracer
  add 0.5303300859 0.5303300859 fix=xy
  add 0.75 0 fix=xy
  add 0 0.75 fix=xy
endt
*
```

```
*
*
eos
  mat1 idgas user gm1=0.4 cv=1.0e-4
endeos
*
*
*
convct
  convection = 0
  interface = smyra
endc
*
*
*
edit
  shortt
    tim = 0.0 , dt = 1.0
  ends
  longt
    tim = 0.0 , dt = 1.0
  endl
  plott
    tim = 0.0 , dt = 10e-3
  endp
ende
*
*
*
boundary
  bhy
    bxb = 0 , bxt = 0
    byb = 0 , byt = 0
  endh
endb
************************************************
```

9.2. SABLE Cylindrical Sedov 2DR

```
SABLE2D
$ control: hack for submit.sh
$----------------------------------BEGIN_QA-----------------------------------
$ ID:         sedov
```

```
$ Title:      Test for remap, structured hydro
$ Category:   Regression
$ Physics:    comprehensive
$ Dimension:  3D
$ Owner:      Mark Christon
$
$ Description:This test problem covers diatoms (dioms), remap and
$             structured hydro
$
$ References:
$
$
$ Directory:  Benchmarks/Regression/3D/comprehensive
$ Tags:       ?
$ CVS: ?
$-------------------------------------END_QA-----------------------------------

TITLE
  ideal gas sod problem

  units, cgs

$100
  mesh, inline
    rectilinear
      ncells = 100
      bx =  1
      by =  1
      cellsize = 0.01
      gmin = 0 0
    end
    set assign
      nodeset,ilo,1
      nodeset,jlo,2
    end
  end

  no displacement, nodeset 1, x
  no displacement, nodeset 2, y

$  time step scale 1.0
$  GRADUAL STARTUP FACTOR 1.0

$ 3113.57
$ 0.001256637061
```

```
  diatom
    package source
      material 1
      iter = 5
      pwdiom = 1
      density 1.0
      temperature 2477700.281
    insert circle
       center 0 0
       radius 0.02
    endinsert
    endp
    package background
      material 1
      iter = 5
      pwdiom = 1
      density 1.0
      temperature 2.54E-04
      insert box
        p1 -1e3 -1e3 p2 1e3 1e3
      endi
    endp
  enddiatom

  BLOCK 1
    eulerian mesh
    remesh frequency 1
    add diom input
  END

tracer points
  eulerian tracer 1 x 0.5303300859 y 0.5303300859
  eulerian tracer 2 x 0.75 y 0
  eulerian tracer 3 x 0 y 0.75
end

termination time 1.2

#
#-----------------------------------------------------------------------
#                          P L O T T I N G
#-----------------------------------------------------------------------
#
EMIT SCREEN,CYCLE INTERVAL = 10
```

```
plot,exodus
emit, time interval = 0.1
PLOT VARIABLE
  no material globals
  no underscores
  pressure
  energy
  temperature, as "TEMP"
  velocity
  velocity,magnitude, as "VMAG"
  density
  density, avg
  pressure, avg
  energy, avg
END
END

plot,history
emit, cycle interval = 1
end

$
$-----------------------------------------------------------------------
$                            M A T E R I A L S
$-----------------------------------------------------------------------
$

MATERIAL 1
  model, IDEAL GAS
    GAMMA 1.4
    RHO REF 0.0
    CV 1.e-4
    TREF 0.
  END
END


EXIT
```

9.3. Alegra Cylindrical Sedov 2DR

```
$ vim: set syntax=alegra:

units, cgs

title: Cylindrical Sedov in 2D cartesian coordinates

exact termination time 1.2

solid dynamics

  dynamics time integrator, central difference
  end

  domain
  end

$ --- MESH ---
  mesh, inline
    brick
     xmin 0.0
     ymin 0.0
     numx 1
      xblock 1 1 first size 0.01 last size 0.01
     numy 1
      yblock 1 1 first size 0.01 last size 0.01
    end

    set assign
      nodeset,ilo,10
      nodeset,ihi,11
      nodeset,jlo,20
      nodeset,jhi,21
      sideset,ilo,10
      sideset,ihi,11
      sideset,jlo,20
      sideset,jhi,21
    end
  end

  no displacement, nodeset 10,x $ R = 0
  no displacement, nodeset 20,y $ Z = 0
```

```
  no displacement, nodeset 11,x $
  no displacement, nodeset 21,y $

$ 3113.57
$ 0.001256637061
  diatom

    package source
      material 1
      iter = 5
      pwdiom = 1
      density 1.0
      temperature 2477700.281
    insert circle
       center 0 0
       radius 0.02
    endinsert
    endp

    package 'Ambient Air'
      material 1
      iter = 5
      pwdiom = 1
      density = 1.0
      temperature = 2.54e-4
      insert box
        p1 -1e3 -1e3 p2 1e3 1e3
      endinsert
    endpackage
  enddiatom

  block 1
    eulerian mesh
    add diatom input
    material 1
  end


tracer points
  eulerian tracer 1 x 0.5303300859 y 0.5303300859
  eulerian tracer 2 x 0.75 y 0
  eulerian tracer 3 x 0 y 0.75
end

end
```

```
$$$$$$$$$$$$$$$$$$$$$$$$$$$$$$$$$$$$$$$$ EXECUTION CONTROL

emit screen: cycle interval = 200
emit plot: time interval = 0.1
emit hisplt: cycle interval = 1
emit restart: time interval = 0.1
ascii history format

history plot variables
  velocity, magnitude
  pressure, avg
end

Plot variable
  density
  density, avg
  velocity
  temperature
  temperature, avg
  sound speed
  min dt
  mass
  el mass
  pressure
  pressure, avg
  energy
  energy, avg
end

$$$$$$$$$$$$$$$$$$$$$$$$$$$$$$$$$$$$$$$$ MATERIAL DEFINITION

material 1 gas
  model 10
  density 1.0
  temperature 1.0e-10
end

model 10 ideal gas
  rho ref = 0.0
  tref = 0.0
  cv = 1.0e-4
  gamma = 1.4
end
```

```
$$#########################

exit
```

9.4. Alegra-NG Cylindrical Sedov 2DR

```
name = "alegraNG_sedov_cyl_2DR"

analyst = require("analyst")

local units = require("units")
local erg = units.erg
local cm = units.centimeter
local gram = units.gram

local E0 = 0.311357 * erg
local R0 = 0.02 * cm
local w = 1.0 * cm
local cv = 1e-4
local domain_depth = 1.0 * cm

local source_type = "circle"

local dx = 0.01 * cm
local tstop = 1.0 + 0.2

local sedov_initial_volumes = {
    ["circle"] = math.pi * R0^2 * domain_depth,
    ["square"] = 4 * R0^2 * domain_depth
    }

local initial_volume = sedov_initial_volumes[source_type]
local density = 1 * gram / cm^3
local initial_mass = density * initial_volume

local high_specific_internal_energy = E0 / initial_mass
local low_specific_internal_energy = 2.54e-12

local high_temperature = high_specific_internal_energy / cv
local low_temperature = low_specific_internal_energy / cv

tracer_pos=0.75 * cm
```

```
local circle_geometry = {
        {
          type = "cylinder",
          material = 1,
          radius = R0,
          iterations = 5,
          state = {
            density = density,
            temperature = high_temperature
          },
          ce1 = {
            0.0,
            0.0,
            -0.5*domain_depth
          },
          ce2 = {
            0.0,
            0.0,
            0.5*domain_depth
          }
        },
        {
          state = {
            density = density,
            temperature = low_temperature
          },
          type = "everywhere",
          material = 1
        }
    }

local square_geometry = {
        {
          type = "box",
          material = 1,
          iterations = 5,
          state = {
            density = density,
            temperature = high_temperature
          },
          p1 = {
            -R0,
            -R0,
            -0.5*domain_depth
```

```
          },
          p2 = {
            R0,
            R0,
            0.5*domain_depth
          }
        },
        {
          state = {
            density = density,
            temperature = low_temperature
          },
          type = "everywhere",
          material = 1
        }
    }

local sedov_geometries = {
    ["circle"] = circle_geometry,
    ["square"] = square_geometry
    }

local geometries = sedov_geometries[source_type]

input = {
  time_controls = {
    plot = {{type = "time periodic", interval = 0.1}},
    screen = {{type = "cycle periodic", interval = 10}},
    termination = {{type = "at time", time = tstop}},
    history = {{type = "time periodic", interval = 0.0001}}
  },
  domains = {
    {
      save_history = true,
      name = "alegra",
      volumetric_scale_factor = domain_depth / dx,
      mesh = {
        xmin = 0.0,
        ymin = 0.0,
        zmin = -dx/2.0,
        zblocks = {
          {
            size = dx,
            cell_size = dx
          }
```

```
  },
  yblocks = {
    {
      size = w,
      cell_size = dx
    }
  },
  xblocks = {
    {
      size = w,
      cell_size = dx
    }
  }
},
plot_variables = {
  {
    name = "density",
    materials = "average",
    component = "none"
  },
  {
    name = "pressure",
    materials = "average",
    component = "none"
  },
  {
    name = "temperature",
    materials = "average",
    component = "none"
  },
  {
    name = "energy",
    materials = "all",
    component = "none"
  },
  {
    name = "velocity",
    materials = "none",
    component = "all"
  }
},
final_solution_variables = {
  {
    name = "density",
    materials = "average",
```

```
    component = "none"
  },
  {
    name = "pressure",
    materials = "average",
    component = "none"
  },
  {
    name = "temperature",
    materials = "average",
    component = "none"
  },
  {
    name = "energy",
    materials = "all",
    component = "none"
  },
  {
    name = "velocity",
    materials = "none",
    component = "all"
  }
},
save_final_solution = true,
geometries = geometries,
tracers = {
    {id = 1, kind = "eulerian", position = {tracer_pos/math.sqrt(2.), tracer_pos
    {id = 2, kind = "eulerian", position = {tracer_pos, 0, 0}},
    {id = 3, kind = "eulerian", position = {0, tracer_pos, 0}},
},
tracer_variables = {
    {name = "pressure", component = "none", material = "average"},
    {name = "velocity", component = "all", material = "none"},
},
materials = {
  {
    model = {
      eos = {
        gamma = 1.4,
        type = "ideal gas",
        cv = cv
      }
    },
    id = 1
  }
```

```
      }
    }
  }
}

analyst.write_json("input_file.json", input)

alegra.run(input)
```

This page intentionally left blank.

10. APPENDIX: CYLINDRICAL NOH 2DR INPUT FILES

10.1. CTH Cylindrical Noh 2DR

```
*CTHid SPYPLT SPYHIS
*******************************************************************************
* CTH input deck for 1DS Noh calculation
*
* *Parameter values for this input deck match LA-UR-06-6444
*
*******************************************************************************
*eor* cthin
*******************************************************************************
*
Noh Problem
*
*******************************************************************************
*
control
  mmp0
  tstop = 0.8
  hashs = 1000000
  tbad = 5e8
endcontrol
*
*
mesh
  block 1 geom=2dr type=e
    x0 0.0
      x1 dxf=0.02 dxl=0.02 w=1.2
    endx
    y0 0.0
      y1 dyf=0.02 dyl=0.02 w=1.2
    endy
  endb
endmesh
*
*
*
```

```
spy
  Save("VOLM,P,M,PM,IE,VMAG,DENS");
  SaveTime(0,0.06);

  SaveHis("DISCARD,GLOBAL,MAT_GLOBAL,P,DENS,IE,VX,VY,VMAG");
  SaveTracer(ALL);
  HisTime(0,1e-6);
endspy
*
*
*
diatoms
  package 'Inner Uniform Flow'
    material 1
    iteration 4
    dens = 1.0
    rgr p1 = 0. 0.
    rmv = t1
    t = 1.e-22
    insert circle
      center 0 0
      radius 1.0
    endinsert
  endpackage
  package 'Outer Uniform Flow'
    material 2
    iteration 4
    dens = 1.0
    rgr p1 = 0. 0.
    rmv = t1
    t = 1.e-22
    insert box
      p1 0. 0. p2 1e3 1e3
    endinsert
  endpackage
enddiatoms

deftable=1
  int=L
  0 -1
  400 -1
enddeftable
*
*
*
```

```
tracer
  add 0.1414213562 0.1414213562 fix=xy
endt
*
*
*
eos
  mat1 idgas user gm1=0.6666667 cv=1.0e12
  mat2 idgas user gm1=0.6666667 cv=1.0e12
endeos
*
*
*
convct
  convection = 0
  interface = smyra
endc
*
*
*
celthermo
  mmp0
endc
*
*
*
edit
  shortt
    tim = 0.0 , dt = 1.0
  ends
  longt
    tim = 0.0 , dt = 1.0
  endl
  plott
    tim = 0.0 , dt = 10e-3
  endp
ende
*
*
*
*fracts
* pfracl =
*endf
*
*
```

```
*
boundary
  bhy
    bxb = 0 , bxt = 3
    byb = 0 , byt = 3
  endh
endb
*

*discard
*   material=-1
*   denl 0 dens 1.0e90 prel -1.0e90 pres 1.0e90 teml -1.0e90 tmp 0
*endd
************************************************
```

10.2. SABLE Cylindrical Noh 2DR

```
SABLE2D
$ control: hack for submit.sh
$-----------------------------------BEGIN_QA---------------------------------
$ ID:          sedov
$ Title:       Test for remap, structured hydro
$ Category:    Regression
$ Physics:     comprehensive
$ Dimension:   3D
$ Owner:       Mark Christon
$
$ Description:This test problem covers diatoms (dioms), remap and
$              structured hydro
$
$ References:
$
$
$ Directory:   Benchmarks/Regression/3D/comprehensive
$ Tags:        ?
$ CVS: ?
$-------------------------------------END_QA---------------------------------

debug mode:performancetimers
debug mode: performance
debug mode: performancetimers_flat
debug mode: profiletime
```

```
TITLE
  ideal gas sod problem

  units, cgs

$60
  mesh, inline
    rectilinear
      ncells = 60
      bx =  1
      by =  1
      cellsize = 0.02
      gmin = 0 0
    end
    set assign
      nodeset,ilo,1
      nodeset,jlo,2
    end
  end

  no displacement, nodeset 1, x
  no displacement, nodeset 2, y

$  time step scale 1.0
$  GRADUAL STARTUP FACTOR 1.0

diatoms
  package 'Inner Uniform Flow'
    material 1
    iteration 4
    dens = 1.0
    rgr p1 = 0. 0.
    rmv = -1
    t = 1.e-22
    insert circle
      center 0 0
      radius 1.0
    endinsert
  endpackage
  package 'Outer Uniform Flow'
    material 2
    iteration 4
    dens = 1.0
    rgr p1 = 0. 0.
```

```
    rmv = -1
    t = 1.e-22
    insert box
      p1 0. 0. p2 1e3 1e3
    endinsert
  endpackage
enddiatoms

  BLOCK 1
    eulerian mesh
    remesh frequency 1
    add diom input
  END

USER DEFINED INITIAL CONDITION, velocity
  "
   double theta = atan2(coord[1],coord[0]);
   field[0] = -1.0*cos(theta);
   field[1] = -1.0*sin(theta);
  "
END

tracer points
  eulerian tracer 1 x 0.1414213562 y 0.1414213562
end

termination time 0.8

#
#-------------------------------------------------------------------------
#                            P L O T T I N G
#-------------------------------------------------------------------------
#
EMIT SCREEN,CYCLE INTERVAL = 10

plot,exodus
emit, time interval = 0.06
PLOT VARIABLE
  no material globals
  no underscores
  pressure
  energy
  temperature, as "TEMP"
  velocity
  velocity,magnitude, as "VMAG"
```

```
  density
  density, avg
  pressure, avg
  energy, avg
END
END

plot,history
emit, cycle interval = 1
end

$
$-----------------------------------------------------------------------
$                            M A T E R I A L S
$-----------------------------------------------------------------------
$

MATERIAL 1
  model, IDEAL GAS
    GAMMA 1.6666667
    RHO REF 0.0
    CV 1.e12
    TREF 0.
  END
END
MATERIAL 2
  model, IDEAL GAS
    GAMMA 1.6666667
    RHO REF 0.0
    CV 1.e12
    TREF 0.
  END
END


EXIT
```

10.3. Alegra Cylindrical Noh 2DR

```
$ vim: set syntax=alegra:
```

```
$ gamma = 1.4

units, cgs

title: Cylindrical Sedov in 2D cartesian coordinates

exact termination time 0.8

solid dynamics

  dynamics time integrator, central difference
  end

  domain
  end

$ --- MESH ---
  mesh, inline
    brick
     xmin 0.0
     ymin 0.0
     numx 1
      xblock 1 1.2 first size 0.02 last size 0.02
     numy 1
      yblock 1 1.2 first size 0.02 last size 0.02
    end

    set assign
      nodeset,ilo,10
      nodeset,ihi,11
      nodeset,jlo,20
      nodeset,jhi,21
      sideset,ilo,10
      sideset,ihi,11
      sideset,jlo,20
      sideset,jhi,21
    end
  end

  no displacement, nodeset 10,x $ R = 0
  no displacement, nodeset 20,y $ Z = 0

  no displacement, nodeset 11,x $
  no displacement, nodeset 21,y $
```

```
  diatom
    package 'Inner Uniform Flow'
      material 1
      iteration 4
      dens = 1.0
      rgr p1 = 0. 0.
      rmv = -1
      t = 1.e-22
      insert circle
        center 0 0
        radius 1.0
      endinsert
    endpackage
    package 'Outer Uniform Flow'
      material 2
      iteration 4
      dens = 1.0
      rgr p1 = 0. 0.
      rmv = -1
      t = 1.e-22
      insert box
        p1 0. 0. p2 1e3 1e3
      endinsert
    endpackage
  enddiatom

  block 1
    eulerian mesh
    add diatom input
    material 2
  end

USER DEFINED INITIAL CONDITION, velocity
  "
   double theta = atan2(coord[1],coord[0]);
   field[0] = -1.0*cos(theta);
   field[1] = -1.0*sin(theta);
  "
END

function 1
  0 -1
  400 -1
end
```

```
tracer points
  eulerian tracer 1 x 0.1414213562 y 0.1414213562
end

end

$$$$$$$$$$$$$$$$$$$$$$$$$$$$$$$$$$$$$$$$$$$$ EXECUTION CONTROL

emit screen: cycle interval = 200
emit plot: time interval = 0.06
emit hisplt: time interval = 1e-6
emit restart: time interval = 0.1
ascii history format

history plot variables
  velocity, magnitude
  pressure, avg
  density, avg
  energy, avg
end

Plot variable
  density
  density, avg
  velocity
  temperature
  temperature, avg
  sound speed
  min dt
  mass
  el mass
  pressure
  pressure, avg
  energy
  energy, avg
end

$$$$$$$$$$$$$$$$$$$$$$$$$$$$$$$$$$$$$$$$$$$$ MATERIAL DEFINITION

material 1 gas
  model 10
  density 1.0
  temperature 1.0e-10
end
```

```
model 10 ideal gas
  rho ref = 0.0
  tref = 0.0
  cv = 1.0e12
  gamma = 1.6666667
end

material 2 gas
  model 20
  density 1.0
  temperature 1.0e-10
end

model 20 ideal gas
  rho ref = 0.0
  tref = 0.0
  cv = 1.0e12
  gamma = 1.6666667
end

$$#########################

exit
```

10.4. Alegra-NG Cylindrical Noh 2DR

```
name = "alegraNG_sedov_cyl_2DR"

analyst = require("analyst")

--custom parser for aprepro output from SAW
parameters = {}
local file = 'params.in'
for line in io.lines(file) do
  local arr = {}
  for s in string.gmatch(line, "%S+") do
    arr[#arr+1]=s
  end
  parameters[arr[2]]=arr[1]
end

local units = require("units")
```

```
local erg = units.erg
local cm = units.centimeter
local gram = units.gram
local eV = 11604.0

initial_radius = 1.0 * cm
local w = parameters.w * cm
local cv = 1e12 * erg / eV
local domain_depth = 1.0 * cm

local dx = parameters.dx * cm
local tstop = parameters.tstop + 0.2

local density = 1 * gram / cm^3
local temperature = 1.0e-22 * eV
local speed = -1 * cm

local function radial_velocity(x,y)
  r = math.sqrt(x*x+y*y)
  vx = speed * x/r
  vy = speed * y/r
  return vx,vy
end

input = {
  time_controls = {
    plot = {{type = "time periodic", interval = 0.06}},
    screen = {{type = "cycle periodic", interval = 10}},
    termination = {{type = "at time", time = tstop}},
    history = {{type = "time periodic", interval = 0.0001}}
  },
  domains = {
    {
      save_history = true,
      name = "alegra",
      volumetric_scale_factor = domain_depth / dx,
      mesh = {
        xmin = 0.0,
        ymin = 0.0,
        zmin = -dx/2.0,
        zblocks = {
          {
            size = dx,
            cell_size = dx
          }
```

```
  },
  yblocks = {
    {
      size = w,
      cell_size = dx
    }
  },
  xblocks = {
    {
      size = w,
      cell_size = dx
    }
  }
},
plot_variables = {
  {
    name = "density",
    materials = "average",
    component = "none"
  },
  {
    name = "pressure",
    materials = "average",
    component = "none"
  },
  {
    name = "temperature",
    materials = "average",
    component = "none"
  },
  {
    name = "energy",
    materials = "all",
    component = "none"
  },
  {
    name = "velocity",
    materials = "none",
    component = "all"
  }
},
final_solution_variables = {
  {
    name = "density",
    materials = "average",
```

```
    component = "none"
  },
  {
    name = "pressure",
    materials = "average",
    component = "none"
  },
  {
    name = "temperature",
    materials = "average",
    component = "none"
  },
  {
    name = "energy",
    materials = "all",
    component = "none"
  },
  {
    name = "velocity",
    materials = "none",
    component = "all"
  }
},
save_final_solution = true,
geometries = {
  {
    type = "cylinder",
    material = 1,
    radius = initial_radius,
    state = {
      density = density,
      temperature = temperature
    },
    ce1 = {
      0.0,
      0.0,
      -0.5*domain_depth
    },
    ce2 = {
      0.0,
      0.0,
      0.5*domain_depth
    },
    velocity = radial_velocity
  },
```

```
        {
          state = {
            density = density,
            temperature = temperature
          },
          type = "everywhere",
          material = 2,
          velocity = radial_velocity
        }
      },
      tracers = {
          {id = 1, kind = "eulerian", position = {0.2/math.sqrt(2.0), 0.2/math.sqrt(2.
      },
      tracer_variables = {
          {name = "pressure", component = "none", material = "average"},
          {name = "velocity", component = "all", material = "none"},
          {name = "density", component = "all", material = "average"},
          {name = "energy", component = "all", material = "average"}
      },
      materials = {
        {
          model = {
            eos = {
              gamma = 5./3.,
              type = "ideal gas",
              cv = cv
            }
          },
          id = 1
        },
        {
          model = {
            eos = {
              gamma = 5./3.,
              type = "ideal gas",
              cv = cv
            }
          },
          id = 2
        }
      }
    }
  }
}
```

```
analyst.write_json("input_file.json", input)

alegra.run(input)
```

REFERENCES

[1] J. S. Brock, J. R. Kamm, W. J. Rider, S. Brandon, C. Woodward, P. Knupp, and T. G. Trucano. Verification test suite for physics simulation codes. Technical report, Lawrence Livermore National Laboratories, Livermore, CA, 2006.

[2] M. Gehmeyr, B. Cheng, and D. Mihalas. Noh's constant-velocity shock problem revisited. *Shock Waves*, 7:255–274, 1997.

[3] L. I. Sedov. *Similarity and Dimensional Methods in Mechanics*. Academic Press, New York, 1959.

[4] W. F. Noh. Errors for calculations of strong shocks using an artificial viscosity and an artificial heat flux. *J. Comp. Phys.*, 72:78–120, 1978.

[5] James R. Kamm and F. X. Timmes. On efficient generation of numerically robust sedov solutions. Technical Report LA-UR-07-2849, Los Alamos National Laboratory, Los Alamos, NM 87545, 2007.

[6] Scott W. Doebling. Standardized definitions for code verification test problems. Technical Report LA-UR-17-28269, Los Alamos National Laboratory, Los Alamos, NM 87545, 2007.

[7] Scott W. Doebling and et al. Code verification capabilities and assessments in support of asc v&v level 2 milestone #6035. Technical Report LA-UR-17-28532, Los Alamos National Laboratory, Los Alamos, NM 87545, 2007.

[8] S. R. Anderson, B. L. Bihari, and C. S. Woodward K. Salari. Code verification results of an llnl asc code on some tri-lab verification test suite problems. Technical report, Lawrence Livermore National Laboratories, Livermore, CA, 2006.

[9] Gabrielle C. Duncan and Christopher T. Key. Progress towards a new CTH code verification & validation test suite. Technical Report SAND2019-12020, Sandia National Laboratories, Albuquerque, New Mexico 87185, September 2019.

[10] Kevin Ruggirello and CTH Team. Cth user's manual: Version 13.0. Technical report, Sandia National Laboratories, Albuquerque, New Mexico 87185, 2023.

[11] E. S. Hertel, Jr., R. L. Bell, M. G. Elrick, A. V. Farnsworth, G. I. Kerley, J. M. McGlaun, S. V. Petney, S. A. Silling, P. A. Taylor, and L. Yarrington. Cth: A software family for multi-dimensional shock physics analysis. In R. Brun and L. D. Dumitrescu, editors, *Proceedings of the 19th International Symposium on Shock Waves*, volume 1, pages 377–382, Marseille, France, July 1993.

[12] John H.J. Niederhaus, Steven W. Bova, James B. Carleton, John H. Carpenter, Kyle R. Cochrane, Michael M. Crockatt, Wen Dong, Timothy J. Fuller, Brian N. Granzow, Daniel A. Ibanez, Stephen R. Kennon, Christopher B. Luchini, Ramón J. Moral, Christopher J. O'Brien, Michael J. Powell, Allen C. Robinson, Angel E. Rodriguez, Jason J. Sanchez, W. Alan Scott, Christopher M. Siefert, Alan K. Stagg, Irina K. Tezaur, Thomas E. Voth, and John R. Wilkes. Alegra: Finite element modeling for shock hydrodynamics and multiphysics. *International Journal of Impact Engineering*, 180:104693, 2023.

[13] D. M. Hensinger, M. A. Christon, C. T. Key, R. K. Nylen, and A. M. Agelastos. Sable user manual. Technical report, Sandia National Laboratories, Albuquerque, New Mexico 87185, 2023.

[14] David H. Hensinger, Anthony M. Agelastos, and Mark A. Christon. Investigation of the compatible energy conservation method in sable. Technical Report SAND2025-14594, Sandia National Laboratories, Albuquerque, New Mexico 87185, 2025.

[15] James J. Quirk. A contribution to the great riemann solver debate. *International Journal for Numerical Methods in Fluids*, 18(6):555–574, 1994.

[16] ExactPack: An Open-Source Software Package for Code Verification. [Online; accessed 15-October-2024].

DISTRIBUTION

Email—Internal

Name	Org.	Sandia Email Address
Marissa Adams	1443	mbadams@sandia.gov
Anthony Agelastos	1555	amagela@sandia.gov
Aaron Brundage	1555	albrund@sandia.gov
Brian Demaske	8752	bjdemas@sandia.gov
Gabrielle Duncan-Reynolds	1555	gcmille@sandia.gov
Dave Hensinger	1555	dmhensi@sandia.gov
Dan Ibanez	1443	daibane@sandia.gov
Rebecca Nylen	1555	rnylen@sandia.gov
Nathan Peterson	5417	njpeter@sandia.gov
Michael Powell	1443	micpowe@sandia.gov
Bill Rider	1544	wjrider@sandia.gov
Kevin Ruggirello	1555	kruggir@sandia.gov
Maher Salloum	8751	mnsallo@sandia.gov
Erik Strack	1540	oestrac@sandia.gov
Tracy Vogler	6632	tjvogle@sandia.gov
Travis Voorhees	8363	tjvoorh@sandia.gov
Justin Winokur	1544	jgwinok@sandia.gov
Technical Library	1911	sanddocs@sandia.gov

Sandia National Laboratories is a multimission laboratory managed and operated by National Technology & Engineering Solutions of Sandia LLC, a wholly owned subsidiary of Honeywell International Inc., for the U.S. Department of Energy's National Nuclear Security Administration under contract DE-NA0003525.